GEOLOGY OF THE VERMICULITE DEPOSITS, GOLD BUTTE MINING DISTRICT

SOUTHERN VIRGIN MOUNTAINS, NEVADA

Major

Thesis by

Freeman Beach Leighton

In Partial Fulfillment of the Requirements

For the Degree of

Doctor of Philosophy

California Institute of Technology

Pasadena, California

1952

ACKNOWLEDGMENTS

The writer is indebted to Dr. Ian Campbell under whose supervision the work was done. Dr. Isaac Barshad generously made X-ray, cation-exchange, and differential thermal studies. With the kind permission of John B. Myers, exfoliation tests were made in the laboratories of Zonolite Co. by R. J. Kujawa. Bill Oke rendered valuable assistance in some X-ray work. Rudolf von Huene aided in the preparation of microphotographs and made the thin sections. A critical review of the manuscript by Dr. Ian Campbell, Dr. A. E. J. Engel, Dr. R. H. Jahns, and Dr. J. A. Noble is much appreciated.

Chemical and spectrographic analyses were supported by a grant from the Geological Society of America. J. B. Vincent and the Permalite Co., Las Vegas, subsidized a portion of the field work and cooperated in many ways.

ABSTRACT

Vermiculite deposits lie within a one mile square area in the Gold Butte mining district, Southern Virgin Mountains, Nevada. An integrated field and laboratory study of the deposits was undertaken in an attempt to determine their origin. Particular attention was devoted to the mineralogy of the vermiculite and associated minerals and the geochemistry of vermiculitization.

The deposits occur in ultramafic sheets and lenses of probable pre-Cambrian age. Peridotites and perknites have intruded pre-Cambrian migmatites, granulites, and quartzites, and now crop out in the interior of an elliptical dome. Diverse ages of ultramafic intrusives, demonstrated by crosscutting relations, suggest multiple intrusion. Intrusion and formation of the domical structure are believed essentially coincident in time, with intrusion outlasting the severe deformation associated with the forceful injection of an ultramafic crystal-mush.

During an early Cenozoic(?) orogeny the Gold Butte granite porphyry was emplaced. This granite was the probable source of most granitic pegmatites which are abundant in the area. Hydrothermal solutions supplied from the granitic magmas circulated through the ultramafic rocks, profoundly altering them.

Vermiculite is widely distributed in altered ultramafic rocks, occurring in veins, stringers, pockets, and as scattered flakes.

A study of X-ray, chemical, differential thermal, and heat exfoliation data indicate two distinct types of vermiculite mixtures are present. All vermiculites examined were one of these two types or gradations between them. All must be considered varieties of hydrobiotite, for K_2O is present in every case and represents a contamination by biotite layers. One type is a vermiculite-biotite mixture with the approximate ratio of 2:1, respectively. The second type is essentially biotite, containing approximately four per cent vermiculite. Both types show a marked degree of heat exfoliation, the second type to a lesser degree.

Considerable variation between the ratio of vermiculite and biotite exists in a single vein. This heterogeneity is believed due to the high cation-exchange capacity of vermiculite.

The fact that all samples showed either biotite interleaved with vermiculite, or non-expandable biotite along with hydrobiotite is one of the best evidences that ~~the~~ vermiculite has altered from biotite, which in most cases, is an intermediate product in the alteration of other ultramafic minerals.

Vermiculitization of biotite involved (1) progressive subtraction of the alkalies, (2) hydration and formation of loosely-bound interlayered water, and (3) progressive oxidation of ferrous to ferric iron. The process was largely accomplished by hydrothermal solutions. Zoning relations of vermiculite and other minerals in serpentine veins are especially indicative of hydrothermal activity. Still, other facts are suggestive of a meteoric origin. Hence it is believed that meteoric solutions continued the process of vermiculitization after hydrothermal activity ceased, and perhaps, in some cases initiated it.

TABLE OF CONTENTS

TABLE OF CONTENTS (cont.)

TABLE OF CONTENTS (cont.)

ILLUSTRATIONS

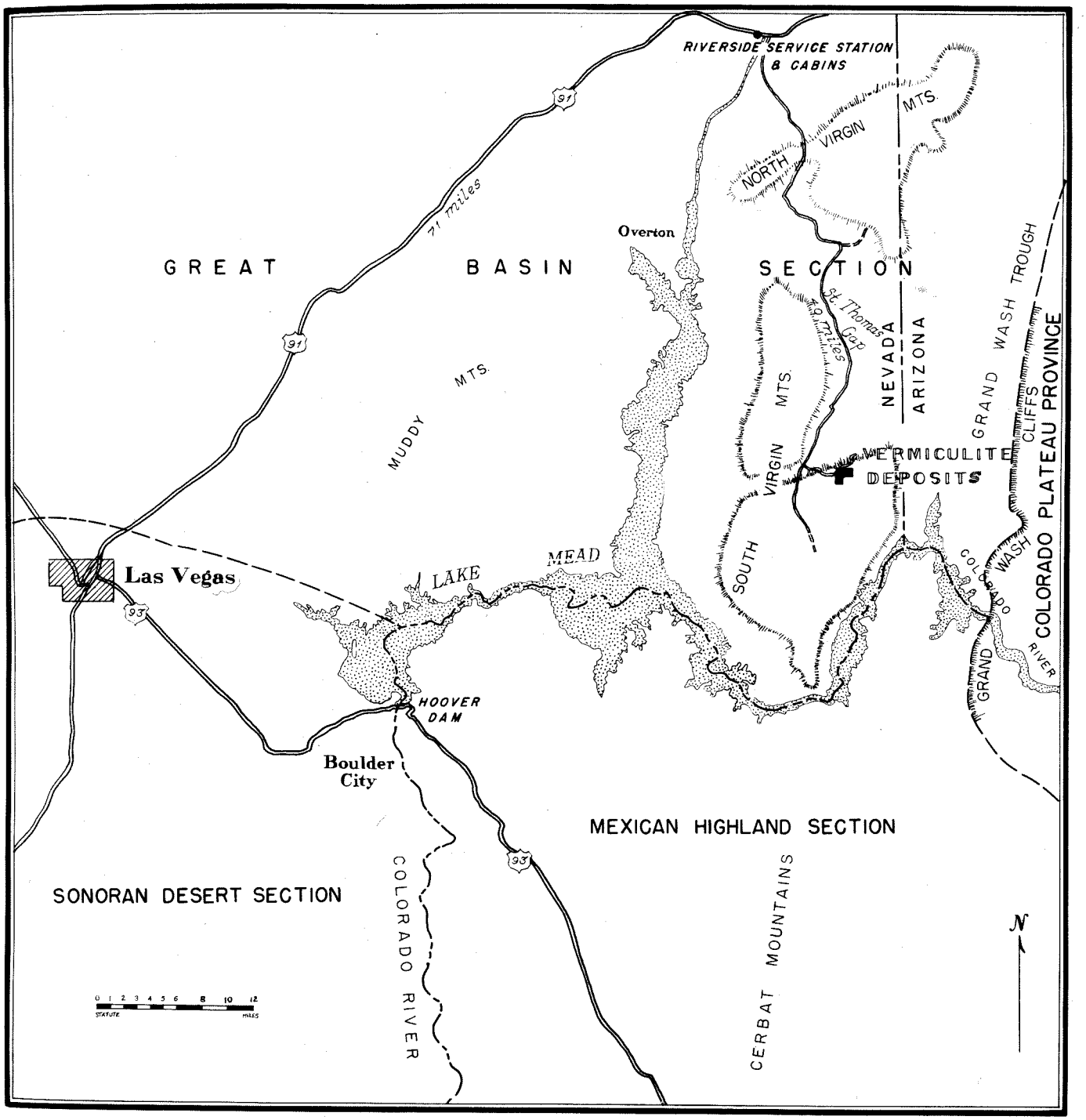

Fig. 1. Index map showing location of vermiculite deposits.

INTRODUCTION

Purpose of the study

The main goal of this work has been to map and describe the geology of the vermiculite deposits in the Gold Butte mining district, Southern Virgin Mountains, Nevada, and to determine their origin.

Vermiculite is one of the comparatively rare industrial minerals whose commercial uses are many and are still being developed. In view of the growing economic importance of vermiculite products and the possibility that the deposits herein described may become a commercial source of vermiculite, certain aspects of the potential exploitation of these deposits have also received attention.

Location of the area

The vermiculite deposits are in the central portion of the Southern Virgin Mountains, in the extreme southeastern portion of Nevada (fig. 1). They lie within a one mile square area in the Gold Butte mining district and are herein called the Gold Butte

vermiculite deposits. Once the site of a small gold mining village, the district is now almost deserted. It can be reached by an unsurfaced county road from federal highway 91, at a point 40 miles to the northwest. The nearest large city is Las Vegas, 111 miles away by present roads.

Regional setting

The Southern Virgin Mountains lie just within the southeast corner of the Great Basin section, Basin and Range province (Fenneman, 1930, map). They extend from the Colorado River north for 32 miles to St. Thomas Gap, beyond which lie the Northern Virgin Mountains which curve to the northeast and cross the Nevada line into the northwestern corner of Arizona.

Physical features

The advance topographic sheet of the Bonelli Quadrangle, 1926, prepared by the City of Los Angeles (pl. 1), shows that some peaks of the Southern Virgin Mountains exceed 5500 feet in altitude. Virgin River, which parallels the mountains on the west, is now ponded by Lake Mead to a point upstream opposite Overton, Nevada, where the altitude is 1255 feet A.T. The maximum relief is about 4300 feet.

The climate is sufficiently arid that no permanent streams exist in the mountains, and vegetation is sparse except on shaded slopes and around seepage. Cedar, scrub oak, juniper, yucca, and pinon are common varieties of trees, and mesquite, sagebrush, cacti, and creosote are characteristic of the smaller shrubs and plants.

The Southern Virgin Mountains are divided into two topographically dissimilar parts by an unnamed col, 3700 to 3800 feet A.T. (see pl. 1). The southern part is an irregular, rugged massif with scattered conical summit-peaks and sub-radial drainage. The northern part is a less rugged and more regular section with sub-parallel, north to northeast trending ridges and sub-trellis drainage. All named peaks appearing in plate 1 are located in the southern part. They are Mica Peak (5300- feet A.T.), Gold Butte (5,600- feet A.T.), and Bonelli Peak (4,800- feet A.T.).

Vermiculite deposits

The vermiculite deposits occur in an area of relatively low ridges and hills about 1½ miles north of Mica Peak. This tract is slightly over one mile in length in an east-west direction and about three-fifths of a mile in maximum width (pl. 1). The main ridges of the tract reach to Mica Peak.

The topographic map which serves as a base for plate 3 was prepared with the aid of stadia equipment. It shows a maximum relief for this local area of about 450 feet. With no government established bench-mark at hand, precise altitudes could not be determined, but from the Bonelli topographic map it is estimated that the 700-foot contour of the writer's map is roughly equivalent to an altitude of 4000 feet. Thus ridges of the vermiculite localities have an approximate altitude of 3700 to 3800 feet in the western part and 3900 to 4000 feet in the eastern part. Valleys are open in character, generally with sandy washes along their bottoms. Divides rarely reach more than 200 feet above the washes. Valleys in general trend northwestward and lead to the col nearby that divides the Southern Virgin Mountains into two parts.

The most conspicuous topographic feature is the basin in the eastern part of the area. Its long direction, 1200 feet in length, trends northeast, the direction of drainage escape.

A cabin and an idle mill, the only structures at present (1952), are situated in this basin. In a well nearby the mill the water-level has stood within 20 feet of the surface even in summer. A surface mine pit, almost 300 feet long, and waste dumps also occur near the mill (fig. 2). Elsewhere shallow test pits and exploration trenches dot the area.

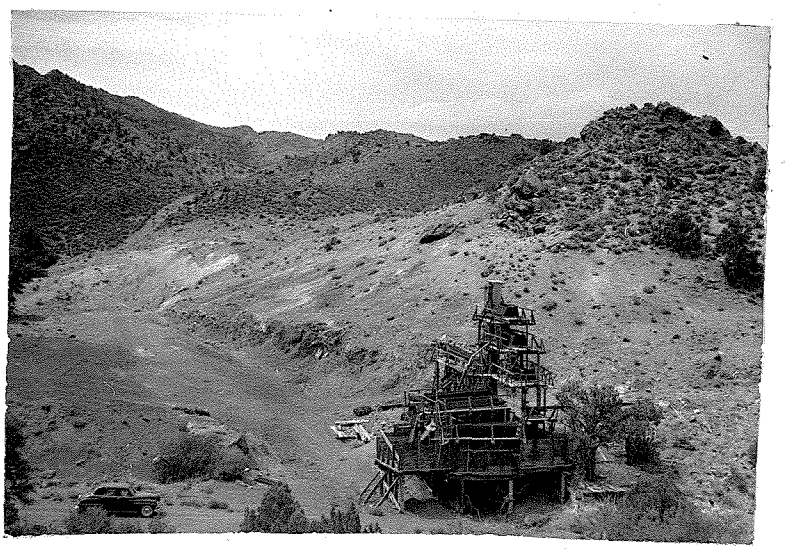

Fig. 2. Vermiculite surface mine pit and idle mill, looking south. Shoulder of Mica Peak to left. (July, 1951).

Brush was removed from the slopes by burning in 1941, and regrowth has been partial.

Midsummer temperatures of 110° F or higher are common. Fall and spring seasons are enjoyable. Some snow falls in winter. Strong winds are not uncommon in the fall, winter, and spring.

Summary of geology of Southern Virgin Mountains

Stratigraphy.-Longwell (1928, p. 1-152) mapped a part of the Southern Virgin Mountains in connection with his more detailed geologic work in the Muddy Mountains west of the Virgin River. His generalized geologic map of this part of the Southern Virgin Mountains appears herein as plate 2. It may be noted that sedimentary rocks crop out mainly in the northern portion of the mountains and crystalline rocks crop out mainly in the southern portion. A summary of the stratigraphy worked out by Longwell, applying principally but not exclusively to the northern portion, is presented in the geologic section below.

Summary of exposed rock formations in the Southern Virgin Mountains
(From C. R. Longwell, 1928, p. 20-103)

Age	Formation	Character	Thickness (feet)
Pleistocene		Alluvial fan deposits	Not stated
	Unconformity		
Cenozoic (Pliocene?)	Muddy Creek formation	Silt, clay, and sandstone Some salty and gypsiferous material. Lacustrine.	Not stated
	Unconformity		

(continued next page)

Summary of exposed rock formations in the Southern Virgin Mountains
(Continued from page 5)

Age	Formation	Character	Thickness (feet)
Cenozoic (Miocene?)	Horse Spring formation Overton fanglomerate	Mainly limestone, some sandstone, conglomerate, sandy shale, and fanglomerate. Continental.	60-396 (In Horse Spring Va
	Unconformity		
Jurassic(?)		Cross-bedded sandstone, typically red. Probably continental eolian and fluvial deposits.	Not state
	Unconformity		
Upper Triassic	Chinle formation (underlain by Shinarump conglomerate)	Red gypsiferous shales in upper part, variegated shales and sandstones in lower part. Arid, continental environment.	741 (In H Spring Val
Lower Triassic	Moenkopi formation	Sandstone, clay, and gypsum beds above marine limestones and gypsum beds below. Continental.	1,634 (In Horse Spring V
	Unconformity		
Permian	Kaibab limestone (Some Coconino sandstone at base in Grand Wash area	Gray cherty limestone with some gypsum, clay, and sandstone. Marine.	553 (South o Mud Well
Pennsylvanian(?)	Supai formation	Red sandstone, some gray and yellow in upper part. Largely continental.	Several hundred
Pennsylvanian	Callville limestone	Dark gray limestone, regularly bedded. Marine.	Several hundred
	Unconformity		

(continued next page)

Summary of exposed rock formations in the Southern Virgin Mountains
(continued from page 6)

Age	Formation	Character	Thickness (feet)
Cambrian (?) and younger	Paleozoic undifferentiated	Largely dolomite. Some limestone and shale	2585-
Cambrian	Muav (?) limestone	Dark-gray compact limestone. Marine.	775
Cambrian	Bright Angel(?) shale	Olive-green to maroon shale, some limestone. Marine.	311
Cambrian	Tapeats(?) sandstone	Sandstone and quartzite, reddish brown to gray, thick-bedded below to thin-bedded above. Marine.	295
Pre-Cambrian	METAMORPHIC ROCKS Gneiss, schist		
Pleistocene	IGNEOUS ROCKS Basaltic flows		
Cenozoic (?)	Gold Butte granite porphyry (not dated by Longwell)		

Structure.- Though the geologic section above relates mainly to the northern portion of the Southern Virgin Mountains, the formations now present there formerly extended into and probably across the southern portion. A steeply-dipping fault (pl. 2), trending N70°E, divides the

Southern Virgin Mountains into two parts at the low col already mentioned (p. 3). Uplift of the southern portion and resultant greater erosion of it are responsible for the widespread exposure of the pre-Cambrian basement complex. Judging from the eastward-dipping Paleozoic formations on the eastern flank of the Southern Virgin Mountains, Longwell (1937, p. 434) concluded that the mountain block as a whole has been rotated strongly eastward between two great north-south fault zones now concealed by alluvial fan deposits. The mechanism by which the mountain block was rotated about a longitudinal axis was not considered by Longwell.

With reservations, Longwell (1928, p. 121-126) summarizes the possible sequence of structural events as follows:

1. Intense folding and thrusting of all formations up to and including the Jurassic (?) cross-bedded sandstone in pre-Miocene(?) time.

2. Earliest normal faulting, probably concurrently with the deposition of Miocene(?) formations.

3. Reoccurrence of compressive deformation, with less intensity than in (1), at the end of the Miocene, or in early Pliocene time.

4. Extensive and profound normal faulting, blocking out the Southern Virgin Mountains probably during Pliocene time. A precipitous fault scarp was formed on the west side of the mountains and was maintained for some time by repeated movements in spite of extremely

active erosion of the range and filling of the adjacent basin.

5. Pleistocene warping and faulting.

It is evident that the origin of the vermiculite deposits herein considered must be related to the active orogenic history of the Southern Virgin Mountains.

Method of investigation

The only topographic base available of the region is the advance Bonelli Quadrangle sheet published on the scale of 1:96,000 (pl. 1). This preliminary edition is too generalized for detailed geologic mapping. Therefore, the topography of the one square mile surrounding the deposits was mapped with stadia equipment on a scale of 200 feet to the inch. Because of the rough terrain horizontal control was established by two means, triangulation to claim corners established by transit survey, and triangulation to a base line measured parallel to the long direction of the area with a steel tape. A topographic map with a contour interval of 20 feet was prepared from an assumed datum plane. This map provided the base for the geology (pl. 3).

No previous geologic mapping had been done in this area. It was geologically mapped by the writer in as much detail as possible. Emphasis was placed upon field delineation of rock units and their spatial relations. The general pattern of rock units achieved, petrographic studies were made of 38 thin sections and numerous samples of crushed material. This microscopic work permitted some subdivision of rock units; however, most of these proved unmappable because of their similar appearance, poor outcrops, or small size.

In addition to the field mapping and petrographic work, detailed mineralogic studies were undertaken to gain more information on the properties of vermiculite and to understand better the paragenesis and geochemistry of vermiculitization. Optical, chemical, X-ray, exfoliation, and spectrographic examinations plus an intensive literature research were made. Detailed procedures involved in some of these examinations are discussed later under their respective titles.

Survey of vermiculite

The name vermiculite originates from the Latin, vermiculari, meaning "to breed worms". It was first applied by Webb (1824, p.55) to a mineral from Millbury, near Worcester, Massachusetts, because of the mineral's odd behavior of expanding into long wormlike columns when heated.

Chemically, vermiculite is a hydrated magnesium aluminum silicate with variable amounts of iron, titanium, chromium, sodium, nickel, manganese, calcium, and potassium. Prior to 1934, whenever one of these variable elements was present in abnormally large amounts, the vermiculite received a subspecies name. Numerous varieties from various localities were described, the name vermiculite being applied to any mica-like material that expanded upon heating. Dana (1945, p. 674) lists the following as members of the vermiculite group: jeffersite, vermiculite, culsagieite, kerrite, lennilite, hallite, philadelphite, vaalite, maconite, dudleyite, pyrosclerite.

The question whether vermiculites were distinct minerals puzzled mineralogists for a long time. Finally Gruner (1934, p. 557-575) and Kazantzev (1934, p. 464), working independently and using X-ray methods, showed that vermiculite exists as a definite mineral species with a distinctive crystal structure. Further investigations by Gruner revealed that many of the materials, earlier classed as vermiculites, were really biotite-vermiculite mixtures.

Vermiculite may occur as a clay mineral (MacEwan, 1951, p. 306) in particles of microscopic size or in crystals as large as several inches in diameter. It is micaceous in habit, but unlike biotite the individual flakes lack elasticity. Large flakes are soapy to the touch. The mineral ranges in color from black to brownish-yellow to green. Its hardness is 1.5, which is intermediate between talc and biotite. Before expansion the specific gravity averages 2.35, less than that of biotite (2.7-3.2). After expansion the specific gravity is approximately 0.9. Pure biotite will not expand when heated.

The economically important property of vermiculite is its ability to expand when heated. This property, known as exfoliation, may cause flakes to expand to twenty or even thirty times their original length normal to the basal cleavage. Exfoliated vermiculite has many industrial applications. Because of its lightness, low thermal conductivity, high sound absorption coefficient, and rot-resistance, it is used chiefly as a lightweight aggregate, as a sound and heat insulator, and lately as a soil conditioner.

It is interesting to note that all commercial "vermiculites" are essentially biotite-vermiculite mixtures whose structure as well as composition is intermediate between true vermiculite and biotite. The mixtures are known as hydrobiotites. Walker (1951, p. 213) states that of eleven specimens labelled vermiculite, he found eight of them to be actually hydrobiotites. Like pure vermiculites, hydrobiotites exfoliate when heated and if the ratio of biotite to vermiculite is not high, the extent of the exfoliation is not markedly decreased.

FIELD RELATIONSHIPS

Rock units and their distribution

The following rock units were delineated in the course of the study and are shown below.

Summary of rock units recognized in area near Gold Butte vermiculite deposits

Age	Rock units	Character	Economic Val
Early Cenozoic(?)	Pegmatites	Two types: small concordant and large crudely zoned discordant; largely granitic.	Sheet mica from one pegmatite
Early Cenozoic(?)	Intermediate mixed facies	augen gneiss in an altered ultramafic rock border zone.	
Early Cenozoic(?)	Gold Butte granite porphyry	massive, extremely coarse-grained pluton with potash feldspar phenocrysts	

(continued next page)

Summary of rock units recognized in area near Gold Butte vermiculite deposits
(continued from page 13)

Age	Rock units	Character	Economic value
Pre-Cambrian(?)	Ultramafic rocks	largely altered peridotites and perknites	vermiculite
Pre-Cambrian	Gneiss complex	migmatites, granulites, and quartzites	

Gneiss complex.- This complex comprises rocks of predominantly migmatites, quartzites, and granulites. It is mapped as one unit, because all degrees of transition exist between these rock types.

Outcrops are widespread. The rocks are resistant and occupy the crests of ridges, in some places as residual boulders. Pyramidal bouldery outcrops stand 30 feet above some ridge crests. Outcrop surfaces are generally brown from weathering.

This unit is considered pre-Cambrian in age because of its high degree of metamorphism and its stratigraphic position below Cambrian sedimentary rocks (see pl. 2).

Ultramafic rocks.- This unit consists of peridotites and perknites which intrude the gneiss complex. They are the host rocks for the vermiculite deposits.

Ultramafic rocks underlie much of the area. They are highly susceptible to weathering. Subdued weathered outcrops and relatively smooth slopes contrast with the craggy outcrops and boulder-strewn slopes of the gneiss complex. In most places rubble from the gneiss complex coats and protects slopes of the ultramafic rocks. In an

unaltered condition the ultramafic rocks are tenaceous, hard, and dense, but exposure to weathering renders them friable, soft, and of lower density. Fresh masses are sparsely distributed, for the major surficial portions of the ultramafic bodies have been converted into weathered products. A few bold outcrops mark the sites of relatively unaltered masses. On a smaller scale remnants of unaltered rock as large as several feet in width and unaltered nodules an inch or two in diameter are like "plums in a pudding" within the weathered portions.

The ultramafic rocks are dated tentatively as pre-Cambrian(?), because of lack of evidence that they are genetically related to younger plutons nearby, and because foliation of ultramafic rocks in the western part of the area is concordant to foliation of the gneiss complex. Foliation of these rock units is discussed under the section, Structural Interpretation.

Gold Butte granite porphyry.- This rock unit does not crop out in the area mapped and, therefore, is not described in detail in sections to follow. However, its general features are summarized, because it is the probable source of at least the larger pegmatite bodies and the hydrothermal solutions that so profoundly influenced the history of the area.

The Gold Butte granite porphyry is a massive, extremely coarse-grained pluton with abundant potash feldspar phenocrysts as much as several inches in diameter. Its intrusive contact with the gneiss complex lies one mile south of the area mapped. Much of the Southern

Virgin Mountains south of this contact is composed of the Gold Butte granite porphyry, which forms giant bouldery outcrops and tor-strewn slopes.

Without doubt this granite porphyry postdates the gneiss complex, because it intrudes the gneiss complex, contains inclusions of it, is devoid of foliation, and contrasts in degree of metamorphism with the gneiss complex. An early Cenozoic age is favored, because the intense folding of Mesozoic and Paleozoic rocks of the Virgin Mountains probably occurred at this time according to Longwell (1928, p. 126). In addition the Gold Butte granite porphyry has the same appearance and general lithology as the Ithaca Peak granite porphyry of the Cerbat Mountains to the south, which Thomas (1949, p. 109) has tentatively dated as Cenozoic.

Intermediate Mixed Facies.- In many places between the ultramafic rocks and the gneiss complex, or within the ultramafic rocks is an augen gneiss which appears to be dominantly altered ultramafic rock. The width of this zone ranges from a knife edge to about 300 feet. In some outcrops a perfect gradation from the intermediate into the ultramafic rocks and from the intermediate into the gneiss complex is well-shown.

Because this rock unit is of secondary origin, its age is dependent upon the nature of the alteration, to be discussed in part VII.

Pegmatites.- Pegmatites are largely granitic. Two principal structural types are present, concordant and discordant. Concordant pegmatites consist of numerous small sills, rarely attaining a width of two or three feet. They predominantly parallel the foliation of the gneiss complex and intermediate facies, transecting it only locally and usually at a small angle. Discordant pegmatites are large dikes, comparatively few in number, which crosscut all rock types in the area.

Large pegmatites are restricted to the southeastern part of the area, whereas small pegmatites occur in every sector.

Most pegmatites are believed to be genetically related to the Gold Butte granite porphyry for reasons considered in part VIII. In view of this kindred an early Cenozoic(?) age has been assigned.

Structural Interpretation

Secondary foliation and lineation in gneiss complex.- In the gneiss complex varying degrees of secondary foliation are expressed as gneissic layering, schistosity, and fracture cleavage. This lithologic unit is characterized by irregularity of structure. Single gneissic layers can seldom be traced for any considerable distance. They either die out, grade into schistosity, are contorted into small open folds, or are interrupted and obliterated here and there by invasion of igneous material.

In other places where rocks of original simple composition such as quartzites are present, the only change has been recrystallization of the quartz and development of closely spaced joints, i.e., fracture cleavage. What appears to be original bedding in some of these quartzites is concordant with the foliation in nearby outcrops.

All foliation is conformable with the structural grain of the area through varying degrees of transition between schistose and gneissic facies. This suggests that most of the present foliation has been inherited from pre-existing foliation. Transection of earlier foliation, except by a few pegmatite injections, was not observed. Ptygmatic folding, a common feature where host rocks lack schistosity (Turner and Verhoogen, 1951, p. 295), is generally lacking.

The foliation records the disposition of pre-Cambrian rocks in an elliptical dome, elongated northwest-southeast. In the northeast side, foliation attitudes have an average strike of N. 65° W. and an average dip of 75° N. In the southwest side the strike averages N. 35° W., the dip 80° N. The foliation sequence as it appears in the southwest part of the area is therefore inverted. In the nose of the dome, located in the northwest portion of the area, the foliation is nearly vertical, exhibiting an impressive arcuate pattern. A corresponding southwest nose, if present, would lie outside of the area mapped.

Overall, the gneissic layering is most distinct on the margins of the dome. This is consistent with the fact that magmatic intrusion, soaking, and recrystallization have been more active near the center

of the dome and have destroyed pre-existing structures.

It is not conclusive whether we are dealing with a deformed foliation or a foliation formed with that attitude as a result of igneous intrusion. Because introduction of granitic material into migmatites (described in part V) was probably guided by pre-existing foliation, the former is favored. If this be the case, foliation of the metasediments is probably parallel to original bedding, for it wraps around the nose of the dome, is concordant to apparent bedding lines in quartzites, and is conformable to lithologic changes that are unrelated to intrusion. It is believed that the foliation existing before introduction of granitic material was developed from the original bedding by plastic flowage in the solid state under regional orogenic stress. In any case it reflects considerable deformation and gives every indication of having been deeply buried.

In some outcrops the gneiss complex shows an ill-defined parallel arrangement of individual mineral grains or aggregates referred to herein as lineation. It is best developed where the gneiss contains minerals of fibrous or platy habit. Such lineation is oriented parallel to the long direction of these minerals. It may also be indicated by streaks and strung-out clots of mafic minerals and garnets.

Lineation is always within the foliation plane and is usually parallel to its strike. This is true even in the nose of the dome. Recorded differences in attitude of lineation are considered significant even though only three outcrops revealed marked deviations. These outcrops were distributed on both sides of the dome. In them the pitch

of the lineation ranged from 20°-27° NW. Local buckling and tilting by an underlying intrusive apophysis would be a reasonable hypothesis if the deviations were not so widely scattered and regular in degree. Perhaps the rise of intrusions was less forceful in these places and the lineations represent earlier stages of formation. Failure to observe a greater number of deviations may have been due to the lack of favorable exposures.

Jointing in gneiss complex.- An arbitrary system of distinguishing joint sets was adopted. They are divided into major and minor types on the basis of uniformity and strength of development. Major joint sets are well-defined and more or less uniform in attitude within an outcrop. Minor joint sets are less conspicuous and lack uniformity within an outcrop. The terms are relative, but nevertheless useful as a means of distinguishing the master sets and eliminating the "chance" fractures.

Point diagrams of major and minor joint sets are shown in fig. 3 and fig. 4, respectively. Two distinct and two less distinct master sets are revealed in fig. 3. This is demonstrated by the concentration of points in four different clusters. The most distinct joints are steeply-dipping north-south and east-west sets. Less distinct sets strike roughly northwest and northeast and are both steeply-dipping. The minor joint sets of fig. 4 show no preferred orientation.

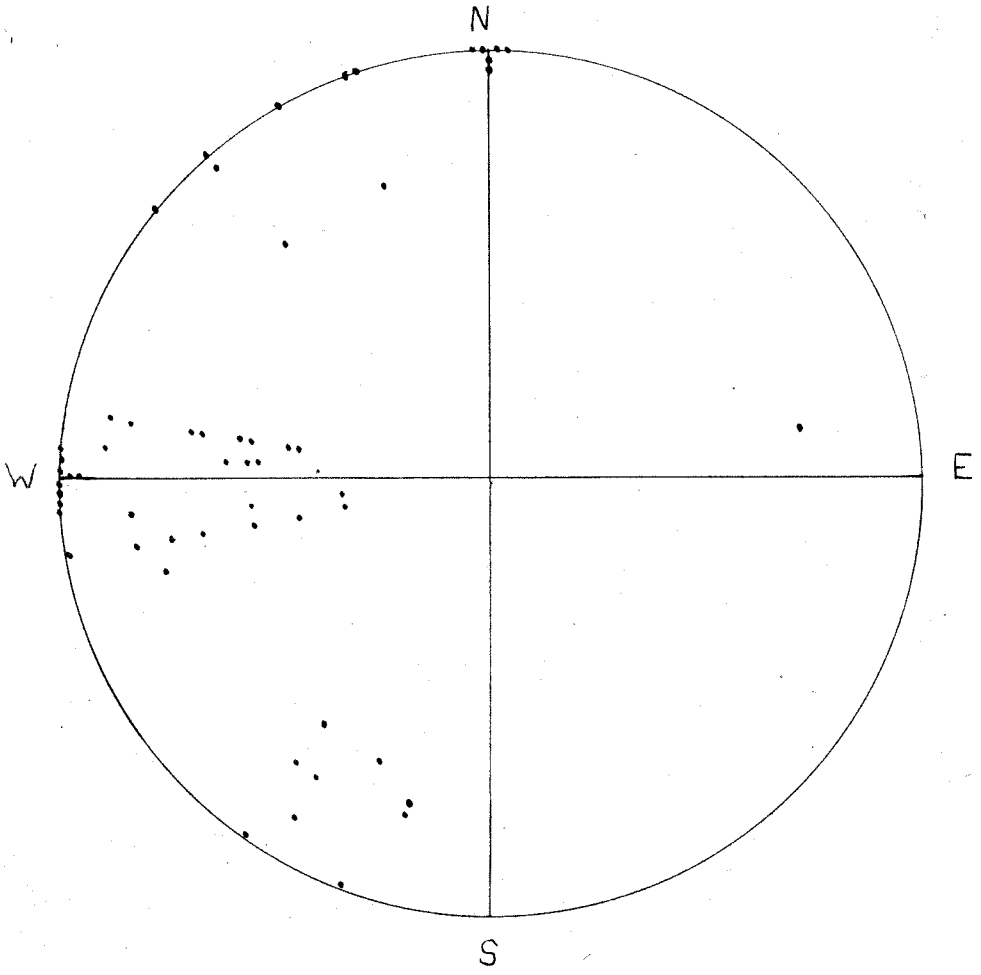

Fig. 3. Point diagram of 57 major joints in gneiss complex plotted on upper hemisphere. Equal area projection.

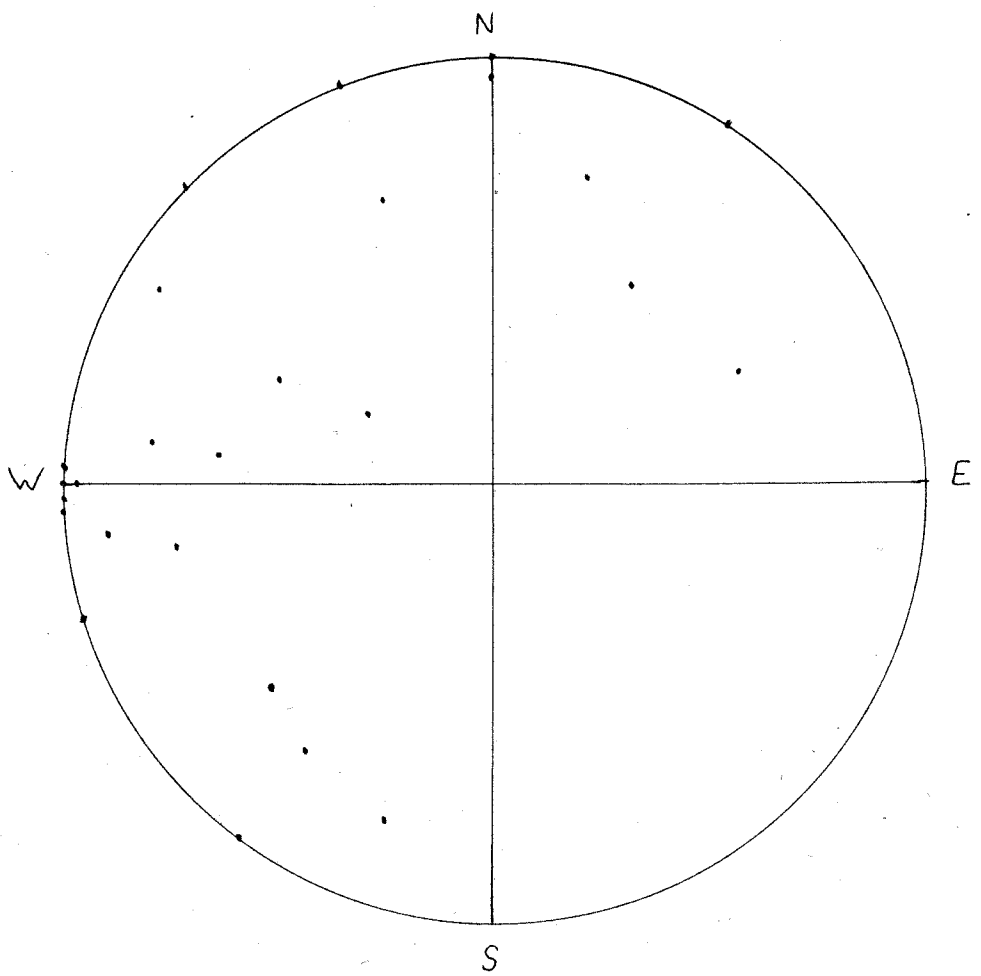

Fig. 4. Point diagram of 24 minor joints in gneiss complex plotted on upper hemisphere. Equal area projection.

It is difficult to offer a systematic interpretation of the dynamics of jointing, because (1) varied and complex stresses have been active since pre-Cambrian time and have superposed many joint sets, (2) such a small area was studied that at least part of the joint pattern may have no relationship to local structure and (3) the disposition of joints may be unrelated to the direction of greatest relief if that direction differs from the direction in which stresses initially accumulated faster than they could be accomodated by plastic flow. Bearing in mind these inherent limitations it still seems advisable to attempt to relate tentatively the jointing to the structure of the area with the evidence at hand.

The two distinct north-south and east-west joint sets form a conjugate joint system which could be interpreted as shear fractures, because the joints are symmetrically disposed about the strain axes of the dome and simulate the circular sections of the strain ellipsoid. Such a relationship implies that the greatest extension during deformation was in a northwest-southeast direction and not vertically. Available evidence does not substantiate this possibility. First, the greatest extension would be upward if upwardly-directed intrusion were the motivating force behind deformation (a hypothesis to be advanced). Secondly, the joint pattern is not an important factor in controlling intrusions in the area. Thirdly, the joint pattern is not controlled by foliation. Lastly and most conclusively, the jointing postdates the pegmatite bodies which are believed

to be associated in time with the Gold Butte granite porphyry of early Cenozoic(?) age.

Therefore, the two distinct joint sets, whether comprising a conjugate joint system or not, were formed probably by regional compressive forces during a Cenozoic(?) orogeny.

If doming is due to upwardly-directed forcible intrusion, then by deductive reasoning radial or ring jointing patterns should be present. The absence of these tensional patterns is believed no problem, because the intrusions we now observe were made at great depth where tensional stresses could be accommodated by plastic flowage.

The master set with a northeast-southwest trend is almost perpendicular to the long axis of the dome and could represent an extension joint set, resulting from elongation parallel to this axis. Because of the aforementioned evidence against tensional adjustments during intrusion, this tensional set is believed unrelated to intrusion.

Structure of ultramafic rocks.- The structure of the ultramafic rocks concerns both their shape and their tectonic structures. From these features and from facts dealing with the adjacent country rocks, certain deductions can be made concerning the mechanics and dating of intrusion.

The shape of the intrusive masses must be determined by the size and pattern of their outcrops and projected dips of their contacts.

To begin with one must consider whether there is more than one intrusive body or just one intrusive body cropping out in different sectors. If there are several or more intrusive masses, they must have the form of sheets or lenses that are essentially conformable with the domical structure. None is over one-eighth square mile in surface area. If the intrusive masses are parts of the same large body, it would underlie at least two-thirds of the one square mile area. Diverse ages of ultramafic intrusives, which are demonstrated in a later discussion, suggest multiple intrusion.

In the eastern portion of the area it appears that erosion has progressed almost to the roots of the gneiss complex. The ridges surrounding the basin which is underlain by softer ultramafic rocks are capped in many places by residual boulders of gneiss which are underlain by ultramafic rocks. In other places screens of the gneissic complex form the ridges, with outcrops of ultramafic rocks extending almost to the ridge crests on either side. Thus we are probably near the top of the intrusive. The structural trends of the invaded roof rocks conform closely to the detailed intrusive contacts, indicating considerable depth and plasticity at the time of intrusion. By analogy to occurrences of forcible intrusion in the Black Hills (Noble, 1952, p. 37-47) wall-rock screens are more easily explained by injection than by assimilation.

Because the ultramafic rocks have so fully controlled the erosion, it is difficult to infer how ultramafic contacts would change in strike where they cross divides. Hence it is uncertain whether the

contacts are steep or gentle. A clue that the contacts are steeply-dipping outward is afforded by the domical structure of the country rocks and the screens of metasedimentaries on the ridge crests that surround the eastern basin. Therefore, the bodies could be either stocks or laccoliths.

It is believed that these bodies were forcibly intruded into the gneiss complex and were not emplaced in their present positions either as gravity separations in a magmatic chamber or by permissive replacement processes. Probably these masses were forcibly injected in a solid state on the grounds that evidence of stoping is lacking, that the ultramafic rocks could not have formed by magmatic reaction with wall-rocks, and that ultramafic magma presumably cannot exist in a molten condition (Bowen and Tuttle, 1949, p. 439-460). However, the size and pattern of the ultramafic bodies are suggestive of a crystal mush intrusion sufficiently lubricated to impart a measurable degree of mobility. The masses made room for themselves by pushing rocks ahead of them and to a lesser extent by pushing aside their walls. The rocks that were pushed ahead have been removed by erosion, exposing the intrusives.

Joints are generally more closely-spaced in the ultramafic rocks than in the gneiss complex. In fact the intrusives are traversed by such a bewildering array of fractures that no definite orientation was determinable. This is not surprising in view of the multitude of different stresses that must have affected these rocks since pre-Cambrian time.

Foliation is well-developed in the eastern basin near the ultramafic borders in a few places, but it is lacking in the interior of this intrusive body. In general the foliation of the borders is a schistosity which strikes essentially parallel to the contacts and dips steeply, usually vertically.

This foliation is not characteristic of viscous molten magma, and it cannot be due to shear, inasmuch as evidence of rupturing or strain in these rocks is generally absent and the interiors of the ultramafic bodies display either a decussate or typical "igneous" texture. All of this points toward a primary origin during forceful intrusion. A suggestion is that it is due to frictional adjustment during movement of the masses against country rock walls.

Departures from this primary type of foliation occur in the nose of the dome. Paradoxically, most of the schistosity here is believed to be secondary, because it wraps around the nose of the dome and is concordant to metasedimentary foliation. Intrusion in the solid state precludes the idea of development of textures by soaking and replacement. This foliation is attributable to the doming.

The question arises concerning the relative age of ultramafic intrusion and regional deformation which formed the domical structure. The following facts are especially pertinent:

(1) Foliation of the ultramafic bodies is generally parallel to the wall-rock contacts.

(2) The interiors of the ultramafic bodies display either a decussate texture or typical "igneous" textures.

(3) Foliation in the nose of the dome is concordant to metasedimentary foliation.

The first two facts favor the concept of regional deformation antedating intrusion. Otherwise the foliation in the ultramafic mass would be continuous into the wall-rocks and the igneous textures would have been modified by the severe deformation. However, in the nose of the dome, foliation in the ultramafic rocks is parallel to that in the wall-rocks. The first hypothesis is suggestive that igneous activity is the result of deformation, whereas the latter is suggestive that igneous activity is the cause of deformation.

With these conflicting data in mind it is well to examine the hypothesis that the two events, intrusion and deformation, were essentially coincident in time, but that igneous activity was the driving force and that the domical structure was formed under conditions imposed by pulses of the intrusion itself. Even though the ultramafic rocks show crosscutting relations to the deformed country rocks, it is entirely possible that the deformation was the effect and not the cause of the intrusion and that what we observe is largely the last surge of a forceful injection. In this event one would assume that the intrusion and the orogeny began at the same time. The invasion of the crust by magma may have been well under way before the older, bedded rocks were severely deformed. To that earlier

stage much of the introduction of migmatite granite can be referred, although it may be related to a still earlier period. It is clear to the writer that the ultramafic rocks were emplaced in the nose before the foliation was superposed upon them. Here the deformation followed the intrusion. Intrusion elsewhere by the same or other ultramafic masses must have occurred at a later date, after the dome had been formed. If they had been earlier they should have had a foliation imposed upon them. Instead, either a decussate or "igneous" texture is present. Also, wall-rock contacts have been deformed and crumpled indicating the wall-rock structure formed first. The data at hand indicate all situations from ultramafic masses deformed after intrusion, through ultramafic masses intruded after deformation.

The sequence of major events concerned with the domal structure and ultramafic intrusion is pre-Cambrian(?) in age. Of course it would be remarkable if the general structure of the area has been approximately the same from pre-Cambrian(?) to present. No evidence of the eastward tilting of the South Virgin block as shown by Longwell was found within the area.

Secondary foliation in the intermediate mixed facies.- The rock possesses a gneissic structure formed by the crude alignment of mafic segregations. In the centers of large intermediate bodies the attitude of the gneissic structure is not constant and is less well-defined than elsewhere. Gneissic structure is more conspicuous near the ultramafic contacts and grades into the schistosity of the ultramafic contact zones. Outcrops showing contacts with the gneissic

complex are poor, but suggest the same type of gradation with the foliation of the gneisses. Wherever noted, lineation is within the foliation plane and parallel to its strike.

Faulting.- Faulting is subordinate to folding. Only two faults of sufficient size to map have been observed. One is located in the nose of the dome, its trace being essentially at right angles to the long axis. Visible discontinuity of structures can be recognized, but the separation involved cannot be measured. However, it cannot be of considerable magnitude. The trace of the other fault lies within the northeast side of the dome and trends N. 10° W. Gouge within a zone one to two feet wide marks this trace.

The manner in which both fault traces cross changes in relief without change in trend indicates that the faults must be steeply-dipping. A steep dip is, of course, suggestive of normal rather than of thrust faults.

It seems likely that the faulting is related in time to the master joint sets. Noteworthy is the possibility that bedding faults and faults within the ultramafic intrusives may be of fairly large magnitude and yet give no evidence of their existence.

Shear zones were observed at scattered points but were not large enough to appear on the map. In all cases these zones were conformable with the foliation. They seem to represent the rock's ability to adjust along the foliation planes. Because intrusion, in the writer's view, outlasted the formation of the dome, these shear zones, he believes, postdate this early period of deformation.

GNEISS COMPLEX

Migmatites

The most widespread and diversified members of the gneiss complex are migmatites. The term was first applied in 1907 by J. H. Sederholm to hybrid gneisses occurring in southwest Finland. Since then migmatite has been variously defined. Following the usage of Turner and Verhoogen (1951, p. 294) the writer has classified as migmatite those mixed rocks in which a granitic component is clearly recognizable.

Description.- Throughout most of the area schists contain numerous stringers, lenses, knots, and sills of aplitic or pegmatitic granite (fig. 5). These sills of granite follow the foliation closely. Lenses and knots are consistently elongated in the foliation plane. In most cases dark schistose bands that contain wisps of lighter granitic rock alternate with light granitic bands streaked with septa of schist. Dark and light bands range in width from a knife edge to several feet. Commonly they are a fraction of an inch to two inches in width. Both dark and light bands are interrupted or fade out in places. Some continue after an interval. Folia are rarely extremely contorted, but are quite consistently weakly plicated or warped.

All gradations from schist into granite occur. In many places it is impossible to tell where the schist stops and the granitic rock begins. Locally, concordant migmatites are cut by younger granitic

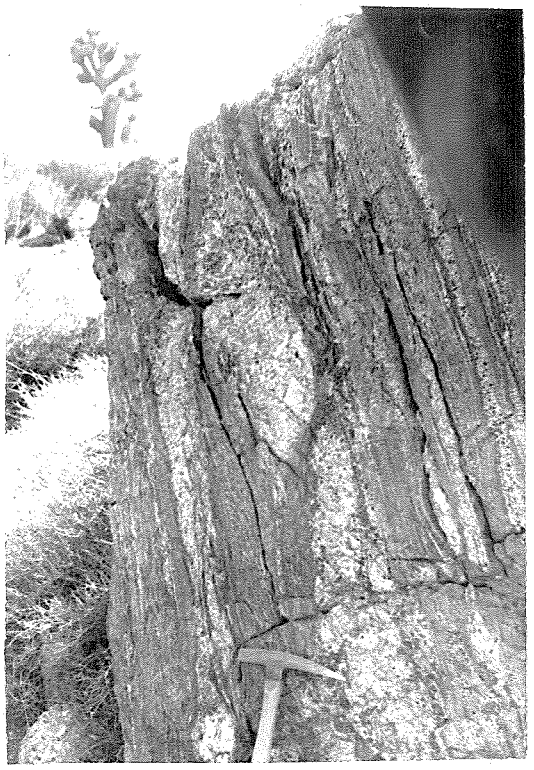

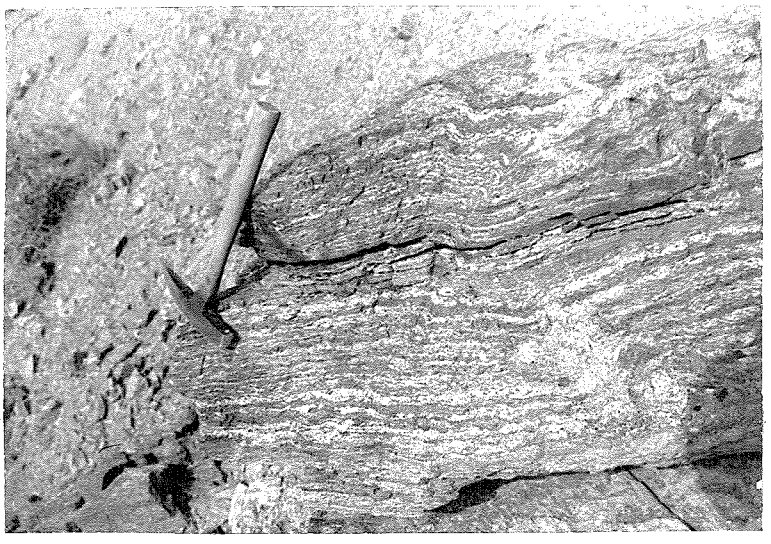

Fig. 5. Two typical migmatite exposures showing dark schist bands intimately mixed with light stringers, lenses, knots, or sills of granite.

dikes (fig. 6). This younger generation of intrusive granite approximates the composition of granitic folia in the pegmatites and may be genetically related. Graphic intergrowths of quartz and perthite are common in granitic portions. All gradations from irregular to well-defined textures are present.

Where enrichment of granitic material is most pronounced, gneissic and schistose layers are more or less obliterated by complete soaking and recrystallization (fig. 7). The product is a garnet aplite or garnet pegmatite which contains only vestiges of the original schistosity. These soaked areas range in width from a fraction of a foot to tens of feet. Most of the zones are crowded with garnet masses which reach a maximum diameter of 2½ to 3 inches near the center of the dome. More commonly the garnet masses are a fraction of an inch in diameter and their size in general decreases away from the dome. Many are elongated in the plane of foliation. Regardless of size and shape, each garnet mass appears to be a single crystalline unit and not a granular aggregate. Dodecahedral faces on a few of the larger masses and small fractures with conchoidal surfaces extending across most masses support such a view. Some large garnets clearly transgress the residual streaks of schist and other structures within the granite bodies, indicating a porphyroblastic origin. The majority of porphyroblasts are xenoblastic, but some are idioblastic with characteristic dodecahedral habit. A noteworthy feature is that the idioblasts decrease in size and abundance away from the ultramafic rocks.

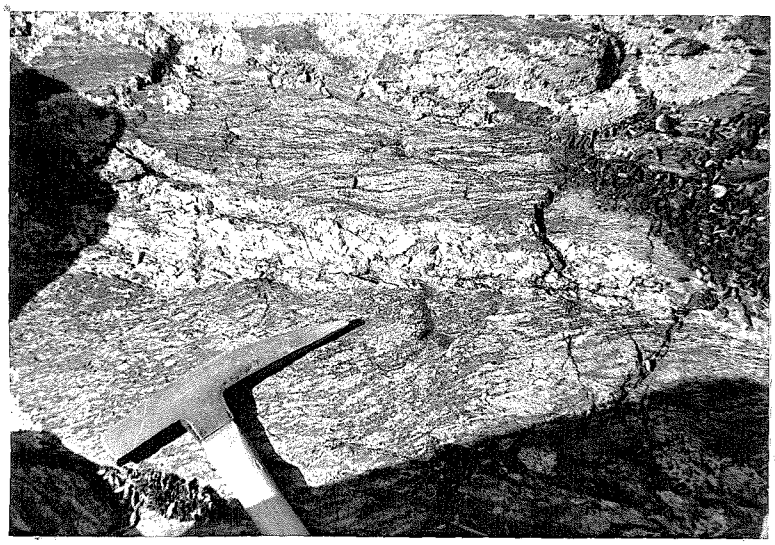

Fig. 6. Migmatite cut by pegmatitic granite dike.

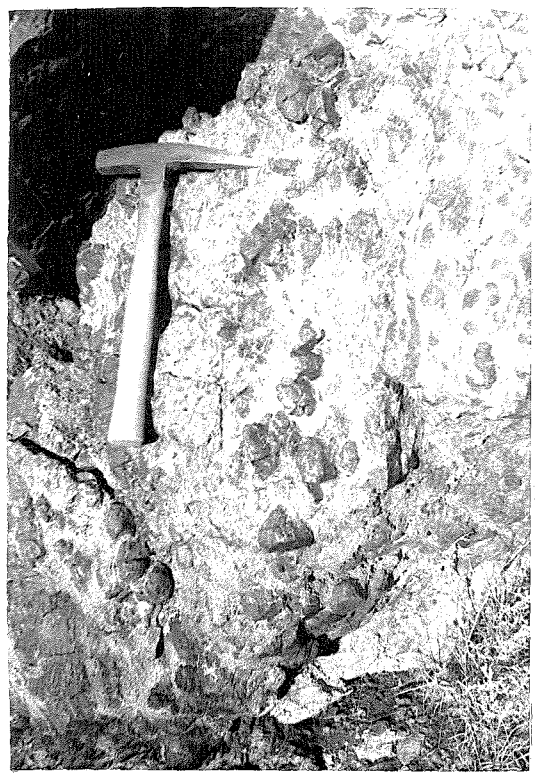

Fig. 7. Garnet porphyroblasts in migmatite enriched in granitic material.

In other outcrops recrystallization has progressed without the introduction of much granitic material and has obscured the foliation so that the former schist now resembles in texture either a normal melanocratic igneous rock or a hornfels of thoroughly massive habit.

Different facies of the migmatites may grade into each other. Their differences are due largely to effects of igneous intrusion and the action of granitic "juices", and also, to a lesser extent, to initial differences in composition of the schist.

Differential weathering has caused garnet-rich portions to stand out in relief, producing a rough outcrop surface. Weathering also tends to accentuate the color contrast between dark and light bands, the dark bands being further darkened by manganese and iron stains. This makes mineral identification of weathered hand specimens extremely difficult. Feldspar, quartz, and garnet are the most conspicuous minerals in hand specimen, the amount of each increasing where granitic juices have been most active.

The migmatites can be most effectively studied under the microscope, yet certain quantitative limitations are present. To evaluate the true mineralogic relations and associations, one must examine thin sections in which the entire assemblage is adequately shown. Some folia are thin enough that several of different compositions occur in a single thin section (fig. 8), but most folia are so wide and coarse in grain (fig. 5) that the proportion of minerals cannot be determined accurately from one thin section. Another difficulty is that folia contain not only sharply contrasted minerals characteristic

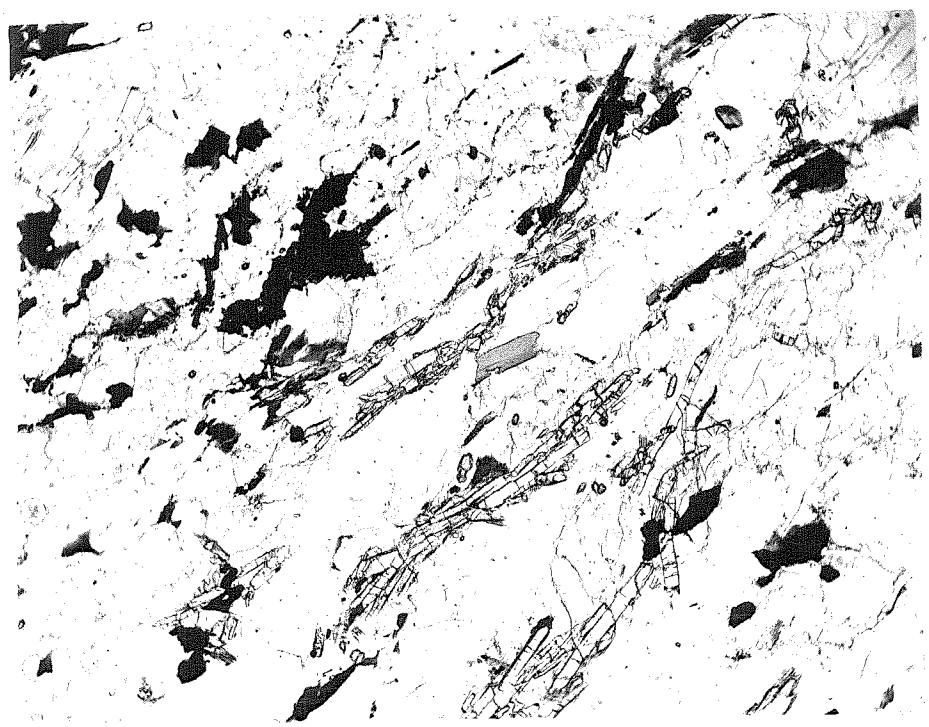

Fig. 6. Trains of prismatic sillimanite crystals surrounded by granitic material and oriented parallel to the foliation. Black mineral is spinel. Sample 0-2. X25. Plain light.

of metamorphic foliation, but also a mixing in varying proportions of the same minerals of a suite.

Microscopically, some boundaries between light and dark folia are sharp, but most boundaries are irregular, sutured, and gradational. Some dark bands have been reduced to strings of inclusions (fig. 8). Within the light bands and some dark bands a granulose texture prevails due to the predominance of equidimensional minerals. In most dark bands at least a semblance of schistosity is still present.

The light folia typically contain large amounts of oligoclase, perthite, or quartz. Percentages of these minerals are extremely variable, but combinations of the three always constitute the bulk of the light folia. Myrmekite is often present in accessory amounts. Mafites are generally lacking in the central portions of the wider folia. Spinel, biotite which exfoliates (hydrobiotite), muscovite, and chlorite are accessory. Hypersthene is locally prominent in border zones.

An average volumetric estimate of minerals in light folia from five representative thin sections is as follows:

Constituent	Per Cent
Perthite	60
Oligoclase	20
Quartz	10
Garnet	5
Muscovite	1
Hydrobiotite	1
Chlorite	1
Myrmekite	2

The dark schist bands are characterized by the presence of sillimanite, garnet, oligoclase, quartz, and hydrobiotite. Spinel and chlorite are locally abundant and are generally present in at least small quantities. Notable accessories are corundum, tourmaline, and clinozoisite. Where granitic material has invaded the dark bands, perthite and myrmekite increase in amount.

An average volumetric estimate of minerals in dark folia from three representative thin sections is as follows:

Constituent	Per Cent
Garnet	30
Oligoclase	25
Quartz	15
Hydrobiotite	10
Spinel	8
Sillimanite	5
Corundum, tourmaline, clinozoisite, chlorite, talc, perthite, myrmekite, apatite	6

Descriptions of the principal minerals in migmatites follows.

Garnet is essentially pyrope as determined by spectrographic examination. Megascopically, it is easily confused with hypersthene, because both appear red to reddish brown. However, both minerals consistently do not occur in the same thin section, and are therefore believed to form under different environmental conditions.

In thin section garnet is pink to colorless. Most porphyroblasts in thin section are badly fractured, embayed, and drawn out. The association of these xenoblasts with fresh-looking idioblasts, which were examined only in hand specimen, gives the impression that garnet

is an extremely persistent mineral and perhaps belongs to two or more epochs of formation. There is no evidence of more than one variety of garnet.

Within perthite crystals, fine-grained garnet is poikiloblastic. Garnet crystals containing cores of perthite, quartz, and hydrobiotite are common. A characteristic sieve texture is usually present.

The outer portions of some garnets contain many fine-grained inclusions, especially sillimanite needles. Because the inner portions of the porphyroblasts contain relatively few inclusions, it seems that either the garnet crystals started to form before sillimanite, or that they ejected the inclusions at an early stage. The orientation of most sillimanite needles in concentric fashion around the crystal boundaries appears to favor the latter alternative, namely forceful ejection. Needle-like inclusions of sillimanite in garnet would make any helicitic texture at once apparent. As this texture is not observed, no rotation has probably occurred, at least during later stages of porphyroblastic growth.

Quartz is present in seven out of eight slides in amounts from 6 to 60 per cent. It shows several modes of occurrence. Where associated with perthite it displays a typical quartz mosaic or graphic intergrowth. In dark folia it is generally interstitial and poikilitic. In places a thin quartz vein separates the schistose and pegmatitic folia, or crosscuts both. Quartz is seriate within the range fine-grained to medium-grained in all associations except in pegmatites, where large phenocrysts have grown. Most grains show wavy extinction, but are clear and unbroken.

At least three generations of quartz are believed to be present, one in the original schist, one in the pegmatitic additions, and another veining the other generations.

Perthite is present as mega- and microperthite in seven out of eight slides in the amount of 2 to 80 per cent. Two essential minerals are present, namely, albite and microcline(?). The grid structure of microcline is conspicuous in one section, and faint or absent in others. Faint traces of the grid structure occur near borders of crystals that otherwise appear to be orthoclase. Albite occurs as strings, rods, and veins, and displays interlocking, platy, and patch patterns. Thus, exsolution and replacement have both played a part. In some perthite grains albite rods are S-shaped. If the rods have formed by exsolution, perthite grains may have been rotated during growth.

Perthite grains are subhedral to anhedral. In most thin sections perthite is fairly fresh with only small amounts of sericite and kaolinite. Some perthite crystals show relic lamellar twinning of plagioclase. Simultaneous extinction of grains under crossed nicols in some slides signifies either a preferred orientation or remnants of one large crystal. The former alternative is favored because of spatial relations.

Oligoclase occurs in seven out of eight slides and ranges from 15 to 30 per cent in amount. Oligoclase forms sutured blebs in the dark schist bands. Some oligoclase grains are untwinned; in other grains the twin lamellae are extremely faint. Where twinned the

the lamellae are narrow. In some grains twin lamellae have been deformed. A little crushing between grains of oligoclase has produced a mortar structure within schist bands. The granulated material is traversed by quartz veinlets, indicating the granulation occurred before entry of the quartz. Oligoclase shows only slight kaolinization.

The oligoclase has the composition An_{30} as shown by the following optical properties: = 1.543- 0.003, = 1.547- 0.003, = 1.551- 0.003; 2V = 85°.

Sillimanite is present as matted needle bundles (fibrolite) within garnet and as larger prismatic blades. Crystal lengths range from 0.1 mm in the needles to 2.5 mm in the larger blades. The larger crystals show a preferred orientation parallel to the foliation in schist bands (fig. 8). Like the needles they occur in aggregates.

Sillimanite constitutes from 0 to 10 per cent of the schist folia. It is absent only where schist leaves have been largely assimilated by granitic material.

Crystals are colorless and free from inclusions. Transverse fractures cross the larger crystals, but are absent in the smaller needles.

Two generations of sillimanite are suggested by the differences in size, arrangement, and fracturing of the needles and blades. Sillimanite has suffered no visible alteration.

Spinel is both a varietal and accessory constituent in some thin sections. It occurs up to 20 per cent. Without chemical analysis,

it cannot be assigned to a definite spinel member. Because it appears both green and black, even within the same grain and is in places slightly magnetic, it is believed to approach the composition of chromohercynite.

Spinel is closely associated with garnet. Where one increases in amount so does the other. Some spinel is interstitial veinlet material and also fills fractures in garnet. Most grains are elongated and ragged. Some are rimmed by hydrobiotite and chlorite.

Hydrobiotite occurs in seven of eight slides in amounts ranging from 1 to 15 per cent. Although dark brown in hand specimen, it is pleochroic from pale tan to orange to orange-red in thin section. At extinction positions flakes have a curious speckled appearance, differing somewhat from the typical "curly maple" texture of biotite. Some large masses convey the impression that they are bundles of closely packed needles with a wavy arrangement. Others show curious strain shadows, mottling, or signs of regrowth (fig. 9).

Hydrobiotite is most abundant in schist bands, but is often found within granitic folia in a parallel and conformable arrangement, which probably marks the original lamination of the schist.

Flakes are in general medium-grained. However, trains of fine-grained inclusions of hydrobiotite are present in granitic folia. Also, along the contacts of the dark and light folia and in the presence of garnet, hydrobiotite is usually of large grain size and most abundant (fig. 9).

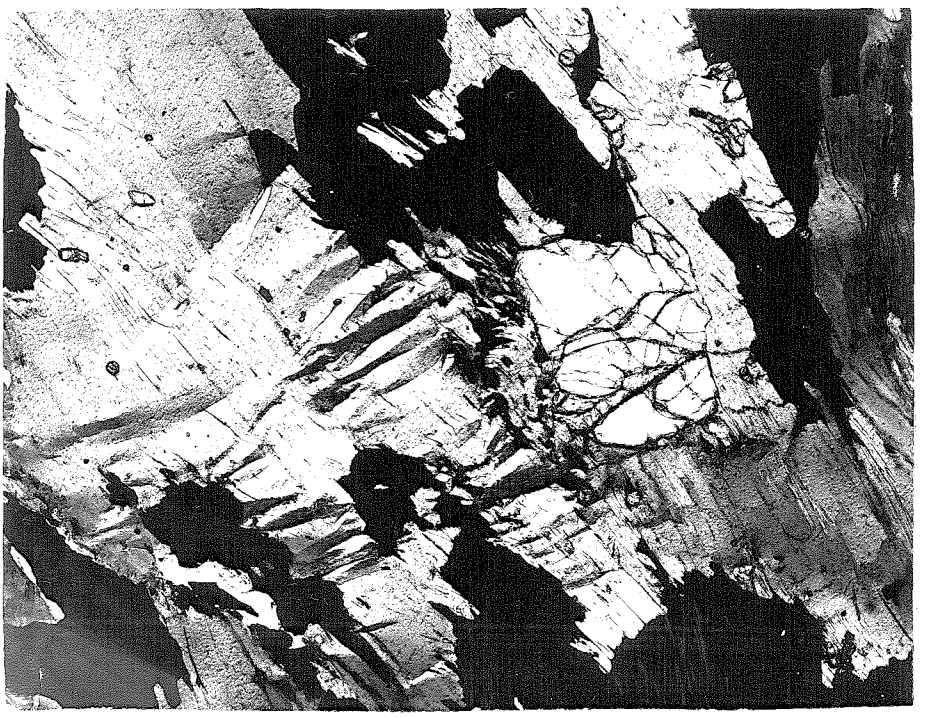

Fig. 9. Strained and mottled hydrobiotite replacing garnet (light grain with high relief). Black mineral is spinel. Sample 25-161. X25. Plain light.

Much evidence exists that hydrobiotite has replaced garnet (fig.9), both centrally and marginally. Pseudomorphs of hydrobiotite after garnet, and ragged, residual cores of garnet in hydrobiotite are not uncommon. Fine-grained euhedral blades are found along fractures in garnet. Overgrowths of hydrobiotite on garnet are also visible. In places, zones of chlorite and hydrobiotite are present as tertiary products that coat and vein garnet and spinel.

Accessories:

Myrmekite intergrowths and other implication textures involving quartz and alkali feldspar seldom exceed 2 per cent in any slide, but their presence in migmatized rocks seems significant. The myrmekitic textures show elongated blebs or worm-like patches of quartz in feldspar. Other textures include the cuneiform type of intergrowths of quartz in feldspar. A sharp distinction between graphic and myrmekitic intergrowths cannot always be made. Gilluly (1933, p. 72-73) also recognized a gradation in these texture types near Sparta, Oregon.

The intergrowths occur at the borders of perthite and oligoclase. In slides where oligoclase is absent, myrmekite is also absent. This association suggests that the intergrowth results from the replacement of oligoclase by the vermicular quartz.

Corundum is present in two thin sections in fine-grained twinned rhombic cross-sections. It is interstitial between sillimanite, garnet, oligoclase, and spinel in schist folia.

Tourmaline occurs as tiny blue-green scattered idioblasts in schist folia. Its fresh condition, euhedral form, and proximity to channels of supply seem to rule out the possibility of its being authigenic. The variety of tourmaline is probably schorl.

Clinozoisite occurs as tiny colorless aggregates of fibers. It is found in schist folia that have been invaded by granitic material.

Apatite is invariably present as small rounded scattered grains. It shows no sign of change, even in these highly metamorphosed rocks. Obviously, this is in keeping with the general principle that rock constituents yield to metamorphism in an order the reverse of that in which they originally formed from a magma.

Muscovite is present as clusters of small flakes in the granitic folia.

Chlorite is present in veinlets associated with hydrobiotite, spinel, and garnet. Its properties seem to vary, so more than one type of chlorite may occur. Some, or perhaps all, of the chlorite is probably penninite on the basis of ultra-blue interference color, pleochroism, and parallel extinction.

Talc is commonly associated with garnet, as an alteration product. Flakes of talc occupy fractures in garnet and are oriented perpendicularly to the length of the vein filling, simulating comb structure of cavity fillings.

Origin.- Whether the migmatites have been formed principally by injection, by magmatic soaking and replacement, or by segregation of magma newly formed by differential fusion in place is a question to be resolved only by extensive petrographic and chemical studies. Clearly, a blending of the first two factors is exhibited by field and petrographic relations.

The younger generation of pegmatite involved in the production of the migmatites has been injected in lit-par-lit fashion and appears related to the epoch of extensive pegmatitic intrusion. Perthitic and graphic textures, and local transgression and splitting of foliation by granitic material are believed significant here.

A certain amount of assimilation has also occurred. The reconstituted folia contain varying proportions of the same minerals as the igneous folia. Most boundaries between light and dark folia are irregular, sutured, and gradational. Where granitic folia are close together, the intervening material has been largely replaced, leaving parallel seams of residual nature.

The applicability of differential fusion (variously referred to as ultrametamorphism, anatexis, or palingenesis) is seriously questioned. Why were not the quartzites and granulites that are associated with the migmatites also affected by differential fusion? Surely in such a deep-seated zone as that imagined by Eskola (1933, p. 24) reactions would not be so local and selective.

The initial intrusions are believed to have been more replacive than displacive. Leaves of schist between granitic folia are in many

cases undeformed, showing that no exceptionally viscous material was forcefully injected. Had deformative stresses been active during migmatization, ptygmatic folding should be much more conspicuous.

Analyses of the evolution of migmatization by Fenner (1914, p. 701) and Thomas (1949, p. 32) are in accord with the views of this author concerning Gold Butte migmatites. Fenner and Thomas suggest that the invasion of magma is preceded by soaking of the host rocks. Working in a belt of migmatites, approximately 30 miles south of the Gold Butte district, Thomas reaches conclusions believed applicable to this area, to wit: "The magma entered among the layers of a foliated rock in a quiet manner, causing no violent disturbance of the attitude of the folia. The host rock was impregnated and somewhat softened by an 'advance dilute portion' (preceding phrase quoted by Thomas from Fenner) of the magma, which facilitated the injection process and initiated transformation of much of the invaded material."

It did not seem feasible in view of budgetary limitations to undertake many chemical analyses when the major aim of this work concerns the ultramafic rocks and not the gneissic complex. Also, in most cases, analyses of the migmatites now exposed would not afford a comparison of the composition of the original schist and the migmatite, but rather a comparison of rocks which have undergone varying degrees of migmatization. Nevertheless, in order to shed light on the chemical character of the initial schist, a specimen

representing schist that was relatively unaffected by granitic juices was selected for analysis. This analysis is shown below in wt. per cent.

Oxide	Schist
SiO_2	58.2
Al_2O_3	9.5
Fe_2O_3	1.5
FeO	4.8
MnO	0.5
MgO	20.1
CaO	1.1
Na_2O	3.1
K_2O	0.2
H_2O	0.6
Total	99.6

G. L. Cheney, analyst

That the schist portion has been influenced to a small extent by the injections is shown by the negligible amount of K_2O, a prime constituent of perthite in granitic portions. No perthite is present in the schist sample analysed. Because the mineral composition of the granitic folia corresponds to the mineral composition of the larger intrusive pegmatites (see part VIII), it seems safe to conclude that migmatization has resulted in an addition of alumina, alkalies, and silica. This was added in the form of feldspar and quartz.

As a result of the intimate association of the granitic folia with schist folia, the true nature of the original schist is difficult to perceive. Certainly, the primary textures of these schists have been largely or wholly obliterated by recrystallization, especially where mixing has occurred. In addition, the metamorphic minerals present in the schist folia represent such an advanced stage of metamorphism that they do not clearly reflect what early minerals might have been present.

The chemical classification of rocks by Osann (Johannsen, 1939, p. 68-82) is of great usefulness in separating para- from ortho-rocks. Differentiation is based upon a number of equations relating molecular proportions of oxides to one another, and plotting these resultant values upon triangular diagrams. Values have been calculated in table 1 from the chemical analysis of the schist folium. All fall within the inclosed field of sedimentary rocks in the S-Al-F and Al-C-Alk diagrams shown by Johannsen (1939, p. 79).

From the chemical composition and the presence of the mineral assemblage sillimanite-garnet-spinel it is believed that the original sediments were argillaceous in composition. The high magnesium content is not readily accounted for, because magnesium is not usually an abundant constituent of argillaceous sediments. It may be secondary and stem in part from diffusion of magnesium from pegmatitic solutions which became Mg-rich as a result of their circulation within the nearby ultramafic rocks. This is further suggested by the abundance of pyrope garnets in pegmatitic folia close to the ultramafic intrusives,

and their decrease in size and abundance farther away.

The pelitic schists are probably the best indicators of the rank attained by metamorphism. These rocks have an assemblage characterized by sillimanite-pyrope-spinel-oligoclase. According to Turner (1948, p. 85) this assemblage belongs to the sillimanite-almandine subfacies of the amphibolite facies. The assemblage is a product of highest-rank metamorphism, the type so prevalent in orogenic belts and in pre-Cambrian terranes. Evidences of earlier stages of progressive metamorphism are obscured by this high-rank assemblage. Inasmuch as the distribution of metamorphism within the area is on a regional scale, the term regional metamorphism is believed to be applicable here.

A question arises concerning whether the sillimanite assemblage is due to lit-par-lit injection or to an earlier epoch of metamorphism. Two more or less indirect lines of evidence suggest that sufficiently high temperatures were maintained during both epochs of metamorphism to produce such an assemblage.

(1) The sillimanite zone is known to be characteristic of pre-Cambrian orogenic regions. According to Turner (1948, p. 86) a sillimanite zone is often produced by the intrusion of granitic magma. Because the major epoch of visible pegmatitic intrusion is early Cenozoic(?), it seems likely that conditions favoring a sillimanite assemblage prevailed more than once.

Table 1. S-Al-F and Al-C-Alk proportions for migmatitic schist (from Osann)

Oxide	Mol. Wt.	Wt.%	Mol.	Mol%
SiO_2	60.06	58.22	.969	56.40
Al_2O_3	101.94	9.45	.093	5.41
Fe_2O_3	159.68	1.52	.010	0.58
FeO	71.84	4.80	.067	3.90
CaO	56.07	1.10	.020	1.16
MgO	40.32	20.10	.499	29.05
Na_2O	61.99	3.13	.050	2.91
K_2O	94.19	.18	.002	.12
MnO	70.93	.46	.006	.35
Cr_2O_3	152.02	.01	-	-
TiO_2	64.10	.15	.002	.12
P_2O_5	142.05	.017	-	-
CO_2	44.00	.07	-	-
		Totals-----	1.718	100.00%

(Sum of alkalies is less than Al_2O_3)

$S = SiO_2-TiO_2-ZrO_2-P_2O_5$

$= 56.40-0.12 = 56.52$

$Al = Al_2O_3 = 5.41$

$Alk = A = Mol\%$ of $Na_2O-K_2O = 3.03$

$C = CaO-BaO-SrO = 1.16$

$F = CaO-FeO-MnO-MgO-NiO-SrO-BaO = 1.16-3.90-0.35-29.05-34.46$

$S:Al:F = 56.52:5.41:34.46;\ \frac{96.39}{30} = \frac{S,Al,F}{S,Al,F}\ \underline{17.5:1.5:11.0}$

$Al:C:Alk = 5.41:1.16:3.03;\ \frac{9.60}{30} = \frac{Al,C,Alk}{Al,C,Alk}\ \underline{17.0:3.5:9.5}$

$NK = \frac{10Na_2O}{Na_2O-K_2O} = \frac{29.1}{3.03} = 9.60;\ MC = \frac{10-MgO}{MgO-CaO} = \frac{290.5}{30.21} = 9.62$

(2) At least two generations of garnet and sillimanite are clearly distinguished. The earlier stages of progressive change are obscured by this high-rank metamorphism.

A state of disequilibrium prevails in the pelitic schists as demonstrated by the heterogeneity of mineralogic composition and the obvious replacement of one mineral by another. These departures from the ideal assemblage by no means invalidate the classification of the ideal assemblage towards which regional metamorphism was progressing or had progressed (Turner and Verhoogen, 1951, p. 431), but are believed to have special significance.

The departures are at least of three types and result from (1) initial heterogeneity of the metamorphosed sediments, (2) metasomatism, and (3) retrograde metamorphism.

(1) The occurrence of corundum and spinel close to quartz, though not in contact with it, implies an original sediment consisting of silica-rich and silica-poor seams with a very narrow zone of free diffusion.

(2) Tourmalinization is evidence of boric pneumatolysis or boric high temperature hydrothermal activity; both are probably associated with lit-par-lit injection. In addition, potash feldspar and some quartz were added during lit-par-lit injection at the expense of minerals present in the schist.

(3) In high ranks of metamorphism, biotite and chlorite usually disappear (Harker, 1939, p. 57). Therefore, the replacement of garnet

and spinel by chlorite and biotite is clearly a retrograde change. Whether these and other retrograde transformations can be best correlated with the gradual decline of temperature following the zenith of regional metamorphism, or to uplift and resultant erosion, bringing these rocks to the surface, or to temperature decline following injection, or to hydrothermal metamorphism is conjectural.

The transformation of garnet to hydrobiotite is especially interesting in view of the similarity of the hydrobiotite to the vermiculite of the ultramafic rocks. As determined by spectrographic examination the garnet is a pyrope with minor amounts of iron and only a trace of alkalies, calcium, and manganese. Thus it approximates the composition of vermiculite minus water. In all probability the garnet has altered directly to a magnesium-rich hydrobiotite, or has reacted with introduced potash feldspar to produce a magnesium-rich biotite which has subsequently been hydrated to hydrobiotite.

Quartzites and granulites

Description and Origin.- Quartzites and granulites are interbedded with migmatites. Further regional work is needed to show whether they are distinct members of the gneiss complex, or part and parcel of the migmatite group. Lateral and vertical gradations abound, the quartzite in places being similar to the garnet aplite facies of the migmatites, and the granulite being gradational in texture, if not in composition to the migmatites. Quartzites are extremely resistant and form bold outcrops; granulites are less resistant and rarely

form distinct outcrops.

The granulites are dark brown in weathered hand specimen, dark gray in fresh hand specimen. They are uniformly fine-grained, granoblastic in texture, and strongly gneissic in structure. Segregations of amphibole and feldspar-quartz are responsible for the gneissic structure. In places the gneisses form border zones to large pegmatite intrusives and appear to be contact rocks. Commonly, pegmatitic stringers of implicated quartz and feldspar parallel the foliation.

In thin section the chief minerals are hornblende (20 to 30 per cent), plagioclase (20 to 35 per cent), quartz (10 to 15 per cent), magnetite (10 to 20 per cent). A fine-grained crystalloblastic texture is distinctive.

Hornblende is pale green to colorless and presents a blotchy appearance. Optical properties appear variable. Hornblende commonly makes poeciloblasts with their long direction parallel to the gneissic structure. These crystals are set in aggregates of quartz and feldspar. Magnetite and hornblende form kelyphite intergrowths which are at least in part controlled by the amphibole cleavage.

Surprisingly enough, the plagioclase is labradorite. Most twinning lamellae are extremely broad. Some plagioclase is untwinned. Most crystals are relatively clear; others contain inclusions or are covered with a highly birefringent flaky aggregate believed to be sericite and calcite. Reaction has produced symplektite intergrowths with quartz.

Quartz is widely distributed. It shows undulatory extinction. Because of its tendency to react with all other constituents it is believed to be a late introduction.

Magnetite not only forms intergrowths with hornblende, but also with quartz to a lesser degree. It appears relatively unaltered.

No positive evidence that these rocks are of contact origin or products of metasomatism of sediments could be found. There is no doubt, however, that they are thoroughly recrystallized rocks in a state of marked disequilibrium. All minerals appear to be secondary with the exception of labradorite.

The quartzite displays a tan weathered surface. The fresh surface may be lighter or darker than the weathered surface. Hand specimens appear dense and aphanitic. A faint lamination is apparent.

Under the microscope the quartzites present a typical quartz mosaic structure, in which all traces of the former clastic origin are obliterated. A slight schistosity can be seen. Quartz shows strain shadows characteristic of metamorphism. Some grains are crudely banded in lines closely parallel to the apparent schistosity.

These are impure arenaceous rocks as evidenced by the presence of small quantities of oligoclase, biotite, chlorite, magnetite, and garnet. In some quartzites large poeciloblastic crystals of garnet are evident. The presence of garnet in some facies reveals that the rocks have been completely recrystallized in at least a moderate-rank metamorphic zone.

ULTRAMAFIC ROCKS

General description

In hand specimen the ultramafic rocks are black or greenish gray and show a medium- to coarse-grained granitoid to gabbroid texture. Where fresh the rocks have a sparkling luster, but partly altered specimens present a dull speckled appearance. Weathered surfaces are commonly reddish-brown and usually exhibit a hackly surface.

Essentially, the ultramafic rocks are composed of various combinations of olivine and serpentine, pyroxenes, amphiboles, biotite, and vermiculite. Magnetite-chromite (a single isomorphous species) is a notable accessory. Under weathering conditions the olivine and rhombic pyroxene are indicated by reddish-brown spots. Some mineral grains are coated with pulverulent magnesite and calcite.

Vermiculite is widely distributed in altered ultramafic rocks, occurring in veins, stringers, pockets, and as scattered flakes. The width of the veins, stringers, and pockets ranges from a fraction of an inch to several feet. In pockets and at the intersections of vermiculite veins and stringers, flakes attain their largest size. Books 4 to 5 inches in their longest dimension have been measured. Those one-fourth to two inches in diameter are the rule here, however.

Vermiculite disseminated in loose small flakes constitutes the bulk of the mineral. No other megascopic micaceous mineral occurs in altered portions; all mica-like material exfoliates to some extent

under heat from an acetylene torch.

Pegmatitic dikes of diopside, an inch or two in width, cut the ultramafic rocks. Diopside crystals reach a maximum of three inches in length. Most are a quarter to a half inch long. The dikes are usually bounded by coarse hornblende crystals of about the same size. Vermiculite also increases in crystal size close to the dikes.

Small pegmatitic injections of labradorite (An_{65-70}) invade the ultramafic rocks. These range from a fraction of an inch to two inches in width. The labradorite is massive and dark gray. Coarse-grained diopside crystals as much as half an inch long are in places intergrown with the feldspar and in other places border the dikes. Here again vermiculite becomes coarser close to the dikes. No distinctive attitude nor apparent control is found in either sets of dikelets.

Large discordant felsic pegmatites also penetrate the ultramafic rocks. Their border relations are discussed in part VIII on pegmatites.

Two grayish-brown dike-like bodies of extremely fine-grained and altered ultramafic material occur in the worked face 300 feet south of the mill. The bodies bear some resemblance to sandstone dikes. In thickness they are 1 to 2½ inches and 6 to 13 inches, respectively. They trend roughly south and dip almost vertically. Thin sections indicate an intersertal and pseudomorphous texture. The chief minerals are clinozoisite and vermiculite; the varietals are serpentine, magnetite and hematite, and spherulitic chalcedony. A microcrystalline

groundmass includes undetermined isotropic brown aggregates. In places mesh and bastite texture can be seen, indicating derivation of serpentine from olivine and hypersthene.

The segregation of material in dike-like form was attributed at first to supergene action. This view was dismissed when further observations revealed microscopic mesh and bastite textures and showed megascopic veinlets of feldspathic material definitely crosscutting the dikes. The alteration products are believed to have been derived from ultramafic rock by intensive hydrothermal alteration.

The B-zone of soils, and fractures in the ultramafic rocks contain a caliche that consists of approximately 90 per cent calcium carbonate and 10 per cent magnesium carbonate. This represents a mixture ~~of fine-grained calcite and magnesite~~ that has been concentrated by weathering processes. The caliche and the highly alkaline character of soil solution reflect prolonged weathering in an arid climate that apparently has prevailed for a long time.

Caliche is most abundant in the highly weathered rocks. Here veinlets of caliche are extremely numerous and ramified. Some cracks now occupied by caliche were formerly occupied by serpentine, as indicated by the remnant coatings of brown serpentine on the sides of the cracks. Veinlets of caliche are usually a fraction of an inch in width, but some attain a width of 5 inches. Caliche also occurs in intimate association with vermiculite in veins, stringers, and pockets. Tree roots follow serpentine veins now calcified.

The relative proportion of minerals in the ultramafic rocks is variable. No essential or varietal mineral is ubiquitous. Table 2 shows the ultramafic rock varieties which have been recognized.

Peridotites predominate over other ultramafic types. Perknites, though widely distributed, typically take either the form of large, irregular-shaped foliated bodies which are present in the northwestern sector, or dikes which cut the foliated bodies and the dominant peridotite.

The peridotites are rich in iron, magnesium and water, whereas perknites are relatively rich in aluminum, calcium, and iron.

Peridotites

These lithologic types are characterized by the presence of olivine and other mafic minerals. Serpentine in at least an incipient stage of development is universally present.

Most of the peridotite has a granular appearance with little or no evidence of deformation in hand specimens. An appearance of homogeneity may be deceptive. Thin sections of the peridotites reveal greater variation in the proportion of minerals present, than would be expected from megascopic appraisal.

It has not been feasible to separate cortlandtites from hornblende peridotites in the present mapping, because they so nearly approximate each other in composition and texture, and outcrops are so few.

Cortlandtite.- This member crops out principally in the worked areas near the mill and cabin. It displays marked variations in the degree of alteration, more than any other unit in the area. Most of the

Table 2. Ultramafic rock varieties.

	Peridotite Suite					Perknite Suite	
	cortlandtite		hornblende peridotite			Hornblende perknite	
Essential components	olivine & amphibole & pyroxene		olivine & hornblende			hornblende, biotite-hydrobiotite, pyrox	
Chemical analyses in wt.%: (1) average composition from Daly (1933, p. 19-21) (2) = a composition from Gold Butte, Nev. Analyst: G.I. Cheney.	(1)	(2)	(1)	none available		(1)	(2)
SiO_2	44.5	43.0	40.9			42.8	43.3
Al_2O_3	6.4	3.7	5.0			10.6	15.0
FeO	7.9	1.3	8.0			9.2	1.1
Fe_2O_3	2.9	9.8	4.6			6.6	12.8
MgO	25.0	25.0	30.8			12.5	9.2
CaO	8.3	9.3	4.4			11.7	11.6
K_2O	0.9	0.1	0.4			1.0	1.3
Na_2O	0.5	0.7	0.6			1.9	2.4
Cr_2O_3	-	1.0	-			-	0.2
TiO_2	1.2	0.2	0.7			1.6	0.1
MnO_2	0.2	0.1	0.1			0.2	0.4
H_2O	1.8	5.9	4.6			1.7	2.2

cortlandtite is extremely friable, and as a result most of the hand-dug test pits are found in weathered cortlandtite. Within weathered portions residual boulders of relatively unaltered cortlandtite (fig. 10) as large as several feet in diameter and residual hypersthene-rich nodules an inch or two in diameter are irregularly distributed. On a larger scale patches of resistant cortlandtite boulders of exfoliation occur in the eastern basin area. In places they form bold pyramidal outcrops as much as eight feet in height. The boulders range in diameter from one to four feet. They are reddened by iron-stains, but this oxidized condition penetrates no more than a fraction of an inch into the boulder. The interiors of the boulders are the least altered and most tenacious of any rock material. Even the outer shells, if not already detached by weathering, ring when struck by a hammer and require an exceptionally heavy hammer to remove them.

In thin sections of fresh specimens a mosaic of interlocking grains is displayed as in any other igneous rock. The texture is medium-grained, poikilitic, and anhedral to subhedral; the structure is massive.

The characteristic minerals are serpentine and olivine, hornblende-pargasite, diopside, enstatite-hypersthene, biotite and vermiculite. Magnetite-chromite and apatite are accessory; talc, magnesite and calcite, and various hydrated iron oxides are alteration products. The most abundant mineral in fresh specimens is olivine; in rocks showing the highest degree of alteration vermiculite and serpentine are most

Fig. 10. Residual boulder of cortlandtite (below hammer) surrounded by highly altered cortlandtite that contains white calcified vermiculite veinlets. Exposure in test pit in eastern basin, looking south. (July, 1951).

abundant. Veins of serpentine bounded by zones of intercalated serpentine, vermiculite, and actinolite are not uncommon. These veins are believed to have a direct bearing on the origin of vermiculite and are described in greater detail in part XI.

The average volumetric estimate of minerals in five representative cohesive specimens, as displayed in thin section, is as follows:

Constituent	Per Cent
Serpentine	40
Olivine	20
Hornblende-pargasite	15
Diopside	10
Biotite	5
Enstatite-hypersthene	6
Magnetite-chromite	3
Talc	1
	100

The petrographic relationships of these minerals will now be considered. Optical properties and chemical analyses of the most important rock-forming minerals are discussed in part XI.

Serpentine.- The chief serpentine mineral is antigorite. Under the binocular microscope serpentine appears black, pale green, brown, or light yellow. In thin section it may be pale green, mottled olive green, pale yellow, tan or colorless. Several colors are often exhibited in the same slide. The reason for the variance in color is not apparent,

although it may be due to varying iron content of host minerals which are replaced by serpentine. Limonite superposed upon antigorite may cause the mottled olive green and tan appearance.

All peridotites reveal at least incipient replacement of olivine and rhombic pyroxene by serpentine. A mesh of antigorite veinlets that enclose cores of amorphous-looking serpentine (serpophite), and relicts of olivine and rhombic pyroxene crystals is not uncommon. The veinlets are controlled for the most part by fractures in the minerals. Two fracture sets at nearly right angles predominate. That no change in volume has been involved in the replacement, at least on a microscopic scale, is demonstrated clearly where the original texture is preserved. Faint polygonal outlines of pseudomorphs of serpentine after olivine persist in some instances. The most serpentine present in any one of the five thin sections studied was 55 per cent by volume; the least was 15 per cent. In these specimens the olivine was never wholly destroyed. Iron oxides invariably form haloes about olivine remnants and separate them from the serpentine (fig. 11).

Olivine.- The mineral ranges in abundance from 15 to 30 per cent by volume. It is colorless, medium-grained, and saccharoidal. Anhedral to subhedral grains predominate. In extremely serpentinized specimens few grains with polygonal outlines remain. Tiny olivine euhedra are found in poikilitic association with diopside and hypersthene. Evidences of shearing, such as translation lamellae and undulatory extinction, are generally absent. Primary reaction rims are absent.

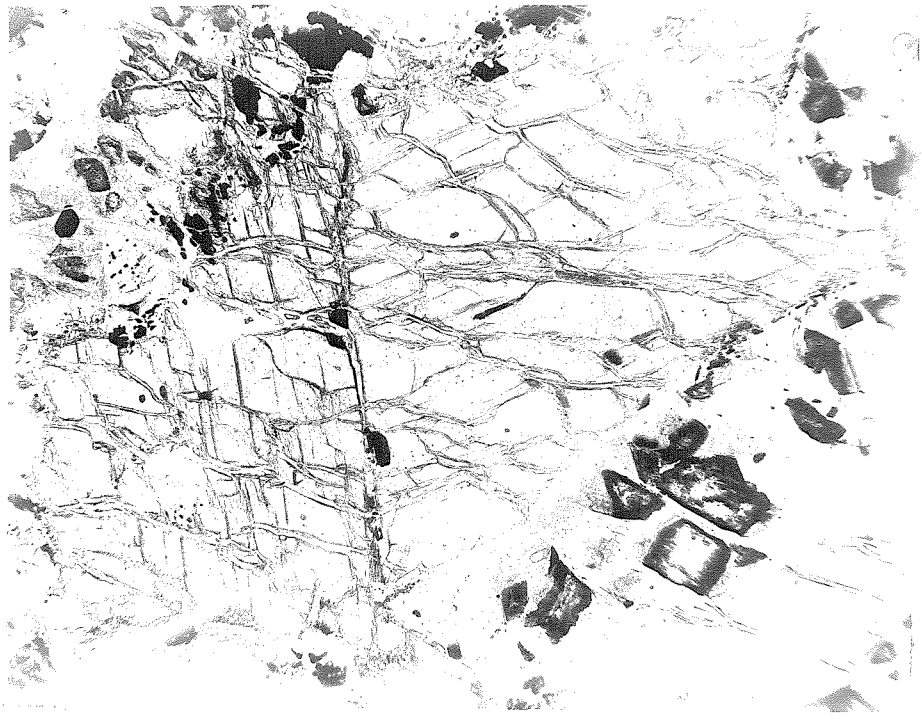

Fig. 11. Mesh of antigorite veinlets enclosing cores of serpophite and olivine remnants, a few of which are rimmed by iron oxide haloes. Sample 6-114a. X65. Plain light.

Hornblende-pargasite.- A green to colorless amphibole is always present. On the basis of optical properties and chemical analyses it varies between pargasite and hornblende proper. The amount present in thin section is between 10 and 20 per cent. Crystals are of bladed habit and medium-grained. Some euhedra are poikilitic in pyroxene. Larger grains range in crystal development from anhedral to euhedral. The large euhedra between 3 and 5 mm in diameter are not common and are scattered about irregularly. Many are ragged and show signs of resorption and corrosion. Antigorite veinlets often transect hornblende-pargasite grains in strongly serpentinized specimens. Most veinlets are controlled by the amphibole cleavage.

That most of the hornblende is primary is suggested by the high percentage present in relatively unaltered specimens. However, the variability in optical properties unrelated to zonal growth, and the increasing percentages in highly altered specimens are hardly suggestive of a primary origin. Therefore, some seem to have formed as a late alteration product, whereas most is believed to be primary.

Diopside.- In sections examined diopside ranges from 0 to 20 per cent by volume. Under the binocular microscope diopside is green. It may be colorless or have a faint greenish cast in thin section. Crystals are usually prismatic and anhedral to subhedral. All are medium-grained. Broad twinning lamellae are characteristic. In slightly altered specimens, hypersthene shows alteration to serpentine and uralite, whereas diopside remains unaltered.

An interesting feature is a number of lithophysae with hollow interspaces in the unaltered cortlandtite. They are less than 3 mm in diameter and are always formed by diopside grains. The reason for their formation is both baffling and intriguing.

Enstatite-hypersthene.- The two members of this series are differentiated by color and pleochroism in thin section. Both are pinkish brown under the binocular microscope, but in thin section enstatite is colorless, whereas hypersthene exhibits a pink to green to colorless pleochroism. Enstatite is present in place of hypersthene in unaltered rocks, constituting roughly 15 per cent by volume of the rock. Hypersthene is the rhombic pyroxene in altered rocks and reaches a maximum of 20 per cent. It is absent in intensely serpentinized rocks, where it probably has already altered to serpentine.

Enstatite-hypersthene and diopside form the largest crystals in cortlandtite. They are seriate, predominantly medium-grained, and anhedral. Several grains of enstatite exhibit schiller structure.

Biotite.- Fine-grained tan biotite is present in fresh specimens but is absent in those extremely serpentinized. It is not present in amounts greater than 10 per cent by volume. Subhedral flakes are plentiful and are distributed haphazardly in thin section. Some are poikilitic in hypersthene.

The biotite is not a vermiculite hybrid as shown by the substantial quantity of potassium and very small water content in the chemical analysis of unaltered peridotite (p.*88*). Nearly all of the 4.3 per cent of potassium oxide must belong to biotite, and nearly all of the

0.4 per cent of water must belong to the serpentine present.

Biotite is believed to be magmatic, because the rock is practically unaltered and no potassium is present in the formulas of other mineral constituents.

Magnetite-chromite.- Magnetite-chromite content ranges between 2 and 7 per cent. Most grains are opaque and are probably magnetite, but a few are translucent and green on the edges, and may be chromite. The absence of chromium oxide in chemical analyses of important rock-forming minerals is also evidence that it is present elsewhere, probably isomorphously with magnetite.

Magnetite-chromite occurs as rounded grains, as intergrowths with antigorite flakes (ophitic association), and as strings along the meshes of olivine and hypersthene. A patchwork of this oxide in serpentine retains the pattern of pyroxene cleavage and is thus probably produced either as an exsolution feature or, together with serpentine, as an alteration product of pyroxene. In fresh specimens magnetite borders biotite laths. Some of the magnetite has altered to hematite. "Opacite" is present in slide 6-114.

Talc.- The association of fine-grained, highly birefringent flakes with other magnesium minerals suggests the presence of talc rather than sericite. Talc is a scanty constituent, constituting less than one per cent by volume. Flakes are oriented on the edges of diopside grains and as small wisps elsewhere. They occur only in the most serpentinized specimens.

Hornblende peridotite.- This rock is actually a variation of cortlandtite, for it cannot be distinguished in hand specimen. However, in thin section two mineral relationships are distinctive. (1) Pyroxenes are absent or are minor constituents. (2) No biotite or vermiculite is present. In all other respects the mineralogy of the rock is similar to that of the cortlandtite.

Sections examined were serpentinized, though not over 55 per cent. Hornblende is universally present, averaging 20 per cent. Olivine is, of course, the other essential mineral.

It is recognized that this rock could be an altered product from a cortlandtite, in which case the pyroxene has gone to serpentine.

Perknites

Whereas peridotites are undersaturated, with considerable olivine appearing in the mode, perknites are saturated rocks without olivine. It is difficult to distinguish between these two ultramafic varieties in the field and consequently they have not been differentiated on the map (pl. 3). In thin section perknites are characterized by the predominance of amphibole (hornblende), pyroxene (hypersthene and diopside), and biotite-hydrobiotite. As much as eight per cent plagioclase is present in some specimens. Alteration products include talc, limonite, antigorite, iddingsite. Magnetite-chromite, apatite, and quartz are accessory. The higher percentages of aluminum, potassium, and calcium and the lower percentage of magnesium and water, as compared with those within peridotites, are chemical features worthy of note.

Texturally, perknites are of coarser grain than peridotites. A poikilitic, subhedral fabric is the general case (fig. 12). Some textures are notably decussate.

Perknites are associated in close proximity with peridotites. They exist usually as small isolated irregular-shaped masses which are chaotically distributed within the peridotites. They crop out principally in the northwest sector where deformation has superposed a foliation on most of the rock. At least one perknite body, dike-like in shape, was found to cut this foliation. It appears as though this latter intrusion took place following the formation of the foliation, though hydrothermal activity may have induced replacement and rearrangement at a later date. Post-magmatic alteration has not affected the perknites as much as the peridotites, probably because of the more stable mineralogic makeup of the former.

Contradictory indications of time of intrusion between perknites and peridotites are probably really due either to hydrothermal rearrangement, or to primary heterogeneity. At least perknites appear to be related to the peridotites genetically, differing only in being richer or poorer in certain mineral constituents.

Though only one variety of perknite, hornblende perknite, is listed in table 2, diopside perknites also exist near contacts with the migmatites and pegmatites. Because little, if any, vermiculite is associated with diopside perknites, they were not accorded as much attention as the hornblende perknites, the chief variety.

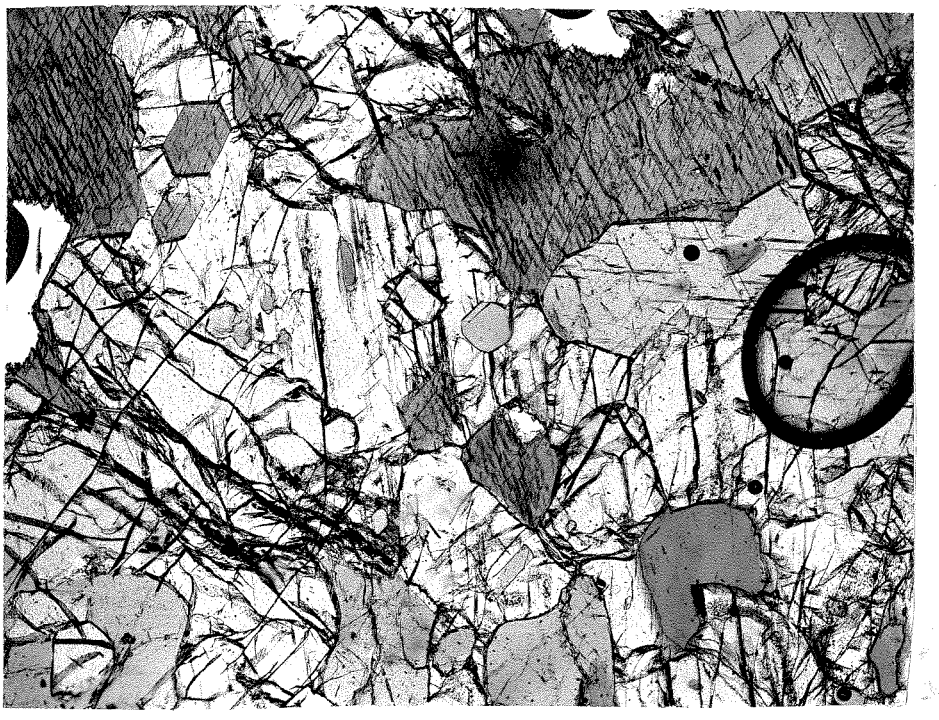

Fig. 12. Typical poikilitic subhedral fabric of perknite. Note tiny euhedra of hornblende in diopside. Hypersthene grain also present above bubble in upper right corner. Sample 6-123. X25. Plain light.

The average volumetric estimate of minerals in nine representative specimens for hornblende perknite, as shown in thin section, is as follows:

Constituent	Per Cent
Hornblende	40
Hypersthene	20
Diopside	15
Biotite-hydrobiotite	15
Plagioclase	4
Talc	3
Magnetite	2
Other accessories	1
	100

Individual descriptions and petrographic relationships of these minerals under the microscope follow.

Hornblende.- This is a universal constituent of perknites examined, and in seven out of nine specimens was the most abundant mineral. Its volume percentage ranges from 10 to 65.

Under the binocular microscope it is black or dark green. In thin section it is either bright green or light green. Pleochroism is extremely variable. Texture is medium-to coarse-grained, anhedral to euhedral, fibrous and in some cases nematoblastic. Small calcite inclusions occur in hornblende crystals and are more plentiful in the coarser variety of hornblende.

Hornblende is usually closely associated with diopside. Where intergrown, diopside is the host mineral. Blebs, patches, and lamellae of hornblende in diopside have a common orientation, and display an "ice cake", or "island and sea" texture (fig. 13). Hornblende islands

Fig. 13. "Island and sea" texture showing hornblende "islands" in diopside "sea". Sample 6-124. X25. Plain light.

show simultaneous extinction under crossed nicols. Small euhedra of hornblende in diopside are probably idioblasts (fig. 12). Intergrain replacement of diopside by hornblende and overgrowths of hornblende on diopside are quite common.

Alteration of hypersthene and biotite-hydrobiotite to hornblende, and hornblende to biotite-hydrobiotite is a common feature and will be discussed under the other mineral headings.

Hypersthene.- Hypersthene and diopside are almost equally distributed in two specimens. Overall, the quantity of hypersthene ranges from 0 to 45 per cent. The mineral is absent in only one specimen.

Hypersthene is pinkish brown under the binocular microscope and pink in thin section. Texture is medium-grained, anhedral, and equant. Many grains are fractured, others are veined by talc and iron oxides.

Some crystals show transformation to hornblende; disseminated hornblende grains in hypersthene show simultaneous extinction under crossed nicols.

A notable feature in slide 6-125 is hypersthene with a few garnet inclusions.

Diopside.- In quantity diopside ranges from 0 to 40 per cent. It is not found in two of the specimens examined.

Diopside is $\not$ faint greenish-yellow to colorless in thin section and green under the binocular microscope.

Many relict grains are poikilitic in hornblende. The large grains show signs of strain, i. e., they are stretched and fractured. A few garnet inclusions are in diopside in slide 6-125. In slide 7-116 diopside is altering to antigorite and quartz.

Biotite-hydrobiotite.- Under the binocular microscope biotite-hydrobiotite is dark brown or black, but in thin section it exhibits considerable variation in color, occurring in orange, yellow, tan, and dark brown shades. A seriate lepidoblastic texture is characteristic. The mineral ranges in amount from 6 to 40 per cent.

Most flakes do not show good extinction and instead show "curly maple" texture at the darkest positions. Generally, flakes are not intensely sheared, or broken. Biotite shows preferred orientation in folisted specimens. This is probably due to growth in a direction perpendicular to the greatest stress. A few pleochroic haloes, probably denoting the presence of xenotime or monazite, are noted.

Evidence of at least two generations of biotite is present. The mineral appears to have formed both earlier and later than hornblende. Where earlier, biotite flakes are bent and ragged. Hornblende pierces cleavage planes of these flakes (slide 7-116). Apatite is included within biotite flakes of only this generation. On the other hand, later crystals (fig. 14) reveal cores of remnant hornblende, replace hornblende along cleavage planes and rim hornblende blades. Biotite has grown across a fracture in a hornblende crystal (slide 9-131a). Biotite has formed in fractures of hyperathene (in slide 5-120) where talc and iron oxides are also present. Here one blade of biotite shows a central parting, indicating possible growth along a fracture. If these fractures form only at supergene levels as some believe, then presumably this biotite is very late. Another interesting

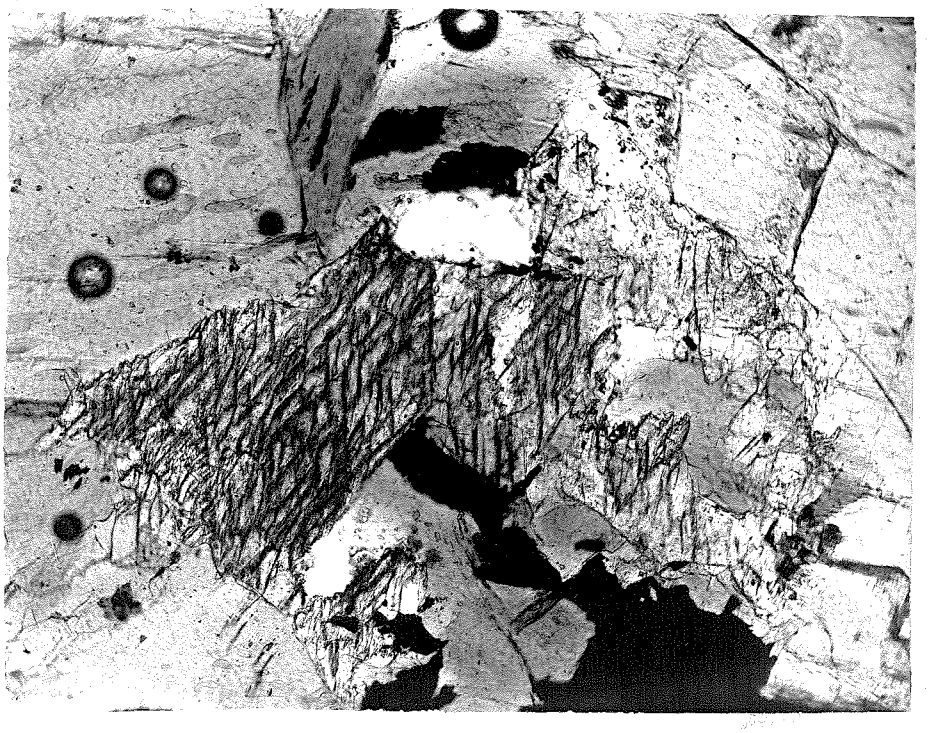

Fig. 14. Biotite-hydrobiotite replacing hornblende crystal.
Sample 4. X65. Plain light.

feature is the development of laths along fractures at points where the fractures parallel each other. These crystals seem to have a preferred orientation and have grown larger than crystals oriented in other positions.

Small biotite euhedra within hornblende crystals may have formed before the hornblende which encloses them, or may be idioblasts of the late biotite generation. Their fresh condition is suggestive of the latter.

Plagioclase.- The plagioclase is predominantly labradorite (An_{65-70}), but locally a little bytownite is present (in slide 3-156). Plagioclase occurs as small grains in or contiguous to hornblende and hypersthene in subophitic fashion. In a few places it has penetrated cleavage planes of biotite.

Plagioclase constitutes 8 to 10 per cent of one specimen, but is lacking in most, and in others does not exceed 5 per cent.

Talc.- Talc is present in amounts as great as 5 per cent but appears in only four of the nine specimens. It is concentrated as small flakes in veinlets along contacts of biotite and hypersthene and within hypersthene, and probably represents an alteration product of hypersthene.

Accessories.- Of all accessories magnetite is the most abundant, averaging three per cent in thin section. Many grains are opaque and are probably magnetite, but some are green and translucent and are probably chromite. No particular segregation of either was noted.

Magnetite-chromite occurs as coronas on hornblende, hypersthene, and diopside and as ragged small grains. An exceptionally large grain measured 4 mm across.

Apatite occurs as small grains, disseminated in hypersthene, diopside, and early biotite. In slide 3-109 apatite reaches its maximum of 1 to 2 per cent.

Quartz evidences itself as small grains associated with antigorite in slide 7-116, and as scattered small grains in slide 3-109.

INTERMEDIATE MIXED FACIES

Description

The intermediate mixed facies occurs in most places as a narrow zone between the ultramafic rocks and the gneissic complex. It ranges in width from a knife edge to roughly 300 feet, and grades into either one or both of the two other rock groups on all sides. No sharp contacts are observed. A few irregular masses of ultramafic rock five to six inches in diameter are observed within the intermediate facies.

In hand specimen the intermediate facies shows a gneissic structure with augen of dark mafites oriented in a relatively leucocratic feldspathic background. The augen average 5 mm in greatest diameter and vary in color from black to reddish-black to green. The typical specimen is fine- to medium-grained, consisting of 30 to 45 per cent mafites and the remainder feldspar. (fig. 15).

Fig. 15. Typical exposure of intermediate mixed facies (augen gneiss) grading into ultramafic rock in upper right corner of photo.

Pegmatitic andesine-labradorite dikelets one-fourth to two inches wide are present. They generally are linear and parallel the gneissic structure, but locally where they crosscut the gneissic structure they become contorted into pygmatic folds. Contacts are gradational over a fraction of an inch. Feldspar laths are gray and are as much as half an inch in length. Clusters of green diopside crystals of approximately the same size border the feldspar dikes.

In thin section the most unusual and interesting feature of the intermediate facies is the wide variety and range of feldspars present. Plagioclase from albite through labradorite, and perthite and a little antiperthite all occur.

The feldspar shows a characteristic crystalloblastic texture. Boundaries are sutured and recrystallized, inclusions are common, and chadacrysts occur in the mafites. Most of the feldspar is relatively unaltered, showing only slight kaolinization. A little of the basic feldspar has altered to calcite and epidote. Tiny veinlets and other anastomosing stringers containing yellow cryptocrystalline material and basic feldspar crosscut other feldspar grains. These veinlets are intensely kaolinized. Subhedral apatite needles and kernels are abundant as scattered inclusions in the feldspars.

Most of the twinned plagioclase ranges from Ca-andesine to Na-labradorite in composition. Some plagioclase grains show a peculiar embayed type of zoning. Sodic cores with calcic shells demonstrate reverse zoning. Zoned crystals are not present within the mafic augen

or as chadacrysts in the mafites. Andesine-labradorite inclusions are common in more albitic grains, the majority of which are untwinned.

Andesine-labradorite is the host in antiperthite. Both perthite and antiperthite contain rods and beads of albite and orthoclase, respectively. These are more abundant in the centers of grains than at the sides. Ghost remnants of plagioclase grains are indicated by faint lamellae extending across perthite grains.

The principal mafites are diopside, hypersthene, and hydrobiotite. Diopside and hypersthene have optical properties similar to diopside and hypersthene in the ultramafic rocks, but in the intermediate facies their oriented ragged remnants signify corrosive action and replacement by feldspar. Hydrobiotite is pleochroic from tan to dark brown. Larger grains are anhedral, crinkly, and bent. Small subhedral to euhedral laths that show a decussate arrangement are poikilitic in hypersthene and diopside (fig. 16). Accessories associated with the mafites are apatite, magnetite, and iddingsite.

Some evidence shows that hydrobiotite has grown at the expense of diopside and hypersthene. Rims and overgrowths of hydrobiotite are common. Uralite forms fringes on many pyroxene grains and grades into hydrobiotite. Magnetite in irregular small grains accompanies the uralitic alteration.

Plagioclase appears to replace the mafites. Cleavage lines of hydrobiotite have been forced apart by the entry and crystallization of plagioclase. Some shreds have been replaced. Ghost-like remnants of hydrobiotite appear in feldspar grains.

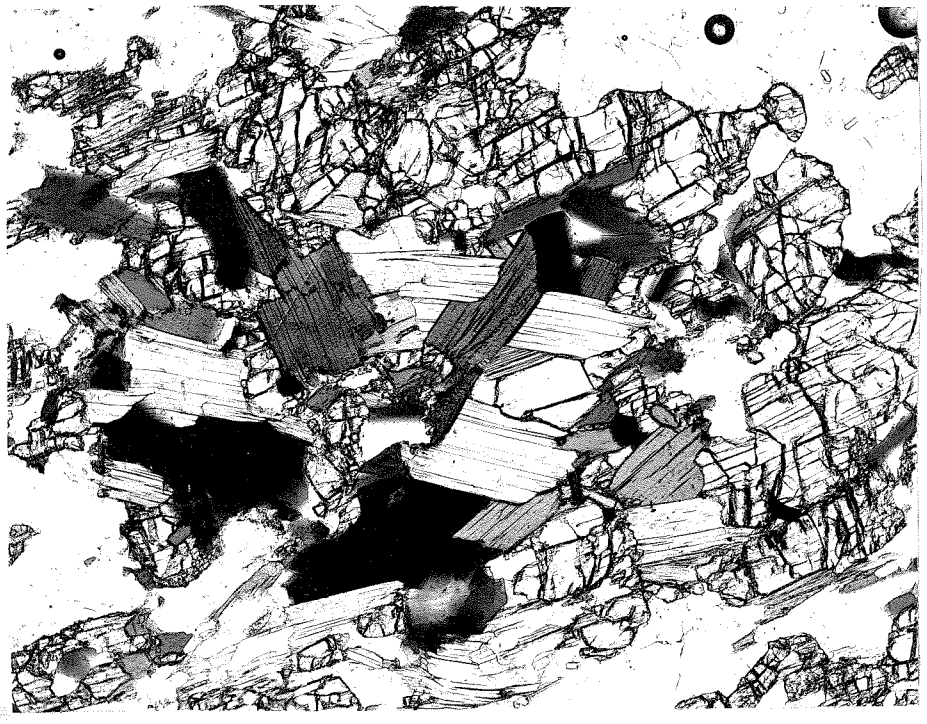

Fig. 16. Mafic segregation in felspathic background of intermediate facies. Hydrobiotite laths display a decussate arrangement in hypersthene and diopside remnants. Sample 10-189. X25. Plain light.

Table 3 shows the spatial mineralogical relationships of the ultramafic rocks, intermediate mixed facies, and gneiss complex.

Origin

Larsen (1928, p. 418) states that secondary transition zones are invariably associated with ultramafic rocks. Field relations suggest a secondary origin for the intermediate mixed facies. The position of the intermediate facies between the gneissic complex and ultramafic rocks in most places and the complete gradation between the three rock types favors a secondary origin.

At least six petrographic features also are in accord with a secondary origin. They are as follows:

1. As shown in table 3 minerals present in the transition zone are also present in either the gneiss complex or the ultramafic rocks.

2. The peculiar irregular type of plagioclase zoning is a product of reaction and does not resemble in amount, composition, or appearance the plagioclase of the gneissic complex or ultramafic rocks.

3. The presence of diverse types of plagioclase, especially basic feldspar veinlets cutting more acidic feldspar, and perthite replacing lamellar plagioclase, illustrates disequilibrium within the rock.

4. Ghost-like remnants of hydrobiotite in plagioclase, and plagioclase encroaching on the mafites is evidence of replacement by plagioclase.

5. Remnant grains of diopside and hypersthene, essential minerals of the ultramafic rocks, implies alteration of rocks that were once more basic.

Table 5. Mineralogical sequences from ultramafic rocks to gneiss complex

Mineral	Gneissic complex	Intermediate mixed facies	Ultramafic rocks
Plagioclase	Albite-Oligoclase (An_{30})	Albite-Labradorite	Labradorite-Bytownite (An_{65-80})
Feldspar intergrowths	Perthite Myrmekite Graphic	Perthite Antiperthite	Absent
Quartz	Quartz essential-varietal	Rare, if present	Rare
Garnet	Abundant	Absent	Absent
Biotite-Vermiculite	Hydrobiotite	Hydrobiotite	Biotite-Vermiculite
Ferromagnesian minerals	Hypersthene Hornblende rare	Diopside Hypersthene	Olivine Hornblende-pargasite Diopside Hypersthene Actinolite
Common accessories	Spinel Corundum Tourmaline Clinozoisite Piedmontite Monazite Apatite	Apatite Magnetite	Magnetite-Chromite Apatite

6. The abundance of apatite grains (1 to 2 per cent) seems indicative of alteration. Nockolds (1932, p. 442) describes the occurrence of abundant apatite needles in basic rocks intruded or included by acid magmas.

What is the origin and the chemical nature of this alteration? Two modes of origin seem possible. First, the replacement features may be the result of selective fusion of country rocks by the ultramafic intrusions. Secondly, they may be the result of metasomatic action.

At least three lines of evidence already advanced appear to rule out the possibility of selective fusion by ultramafic intrusions.

1. It may be argued that because ultramafic rocks were intruded in the solid state, they do not possess the necessary degree of superheat to assimilate large quantities of country rock.

2. As already noted, no xenoliths of country rock occur in ultramafic rocks.

3. In places contacts between ultramafic rocks and gneissic complex are exceptionally sharp.

Thus, the transition zone can be satisfactorily regarded as the result of metasomatism. Two mechanisms of metasomatism are likely.

1. Diffusion between the gneissic complex and ultramafic rocks.

2. Introduction of solutions from pegmatite intrusions.

Chemical investigations are necessary to reveal the true nature of the metasomatism. Chemical analyses and norms of the three principal rock groups are given in table 4, together with the estimated modes of samples analysed. Minor constituents of principal rock groups are listed in table 5. Fig. 17 shows a Harker plot of the chemical analyses in table 4. Table 6 gives the calculations of S-Al-F and Al-C-Alk proportions of the intermediate mixed facies according to the Osann system.

Obviously, pegmatitic intrusion was a late event, because it was controlled in the transition zone by the gneissic structure. Therefore, if diffusion between the gneissic complex and ultramafic rocks played a part in forming the transition zone, it occurred before pegmatitic alteration.

The driving forces of diffusion processes are differences in chemical activity (Ramberg, 1945, p. 99) or chemical potential (Bugge, 1945, p. 57), which in turn, are dependent upon such variables as temperature, pressure, concentration, and the gravitational field. Between the ultramafic rocks and gneissic complex large differences in composition exist. At the time of intrusion probably no great temperature gradient was present, but activation by elevated temperatures during intrusion must have exerted a great influence on chemical activity gradients. Pressure differences were probably negligible. The gravitational field may have had some effect, because the contact between ultramafic rocks and gneissic complex was not vertical.

Table 4. Norms[1]

Mineral	Gneiss complex	Intermediate facies	Ultramafic rock (peridotite)
Quartz	3.48	-	-
Orthoclase	-	8.34	13.34
Albite	26.70	24.65	-
Anorthite	5.56	3.89	-
Corundum	2.44	-	-
Olivine	-	Fa-2.65 Fo-2.80	Fa- — Fo-20.16
Pyroxene	Wo- — En-50.30 Fs- 8.32	Wo-14.73 En- 9.60 Fs- 4.09	Wo-10.09 En-21.90 Fs- —
Acmite	-	-	14.78
Magnetite	2.32	2.55	2.32
Hematite	-	-	12.80
Potassium Metasilicate	-	-	4.33
Nephelite	-	25.84	-
Plagioclase	Ab_{83} An_{17}	Ab_{83} An_{17}	

1. Normative pyroxene and olivine compositions were calculated according to the method proposed by Barth (1931, p. 1-7).

(continued next page)

Table 4. Analyses[2]
(continued from page 87)

Oxide	Gneiss complex	Intermediate facies	Ultramafic rocks (peridotite)
SiO_2	58.22	52.00	44.60
Al_2O_3	9.45	16.70	2.48
Fe_2O_3	1.52	1.76	19.60
FeO	4.80	4.90	0.79
MnO	0.46	0.09	0.05
MgO	20.10	5.43	20.33
CaO	1.10	7.92	4.88
Na_2O	3.13	8.59	2.01
K_2O	0.18	1.41	4.29
H_2O	0.57	0.58	0.39
	99.53	99.38	99.32

2. Analyst: G. L. Cheney

Approximate modes (estimated)					
Garnet	30	Feldspar (albite-labradorite, K-feldspar)	60	Olivine	30
Oligoclase	30			Enstatite	15
Quartz	10			Diopside	20
Hydrobiotite	10	Diopside	15	Hornblende	15
Spinel	8	Hypersthene	10	Biotite	10
Sillimanite	5	Hydrobiotite	10	Serpentine	5
Accessories including corundum	5	Accessories including quartz, apatite, magnetite	5	Magnetite-Chlorite	4
				Other accessories	1

Table 5. Minor constituents of principal rock groups*

	Gneiss complex	Intermediate facies	Ultramafic rocks (peridotite)
Cr	0.01*	0.05*	0.25*
Mn	0.46*	0.09*	0.05*
Ti	0.15*	0.10*	0.04*
Ba	0.01	0.01	Trace
V	0.005	0.005	0.05
Zr	0.05	0.01	-
Pb	0.001	0.001	-
Ga	0.005	0.005	Trace
Cu	0.005	0.005	0.005
Ni	0.001	0.005	0.05
Co	Trace	Trace	0.005

*Qualitative spectrographic analyses by T. C. McBurney. All quantities reported are approximately accurate to nearest factor of ten except those indicated with asterisk represent quantitative chemical analysis approximately accurate to - 0.03.

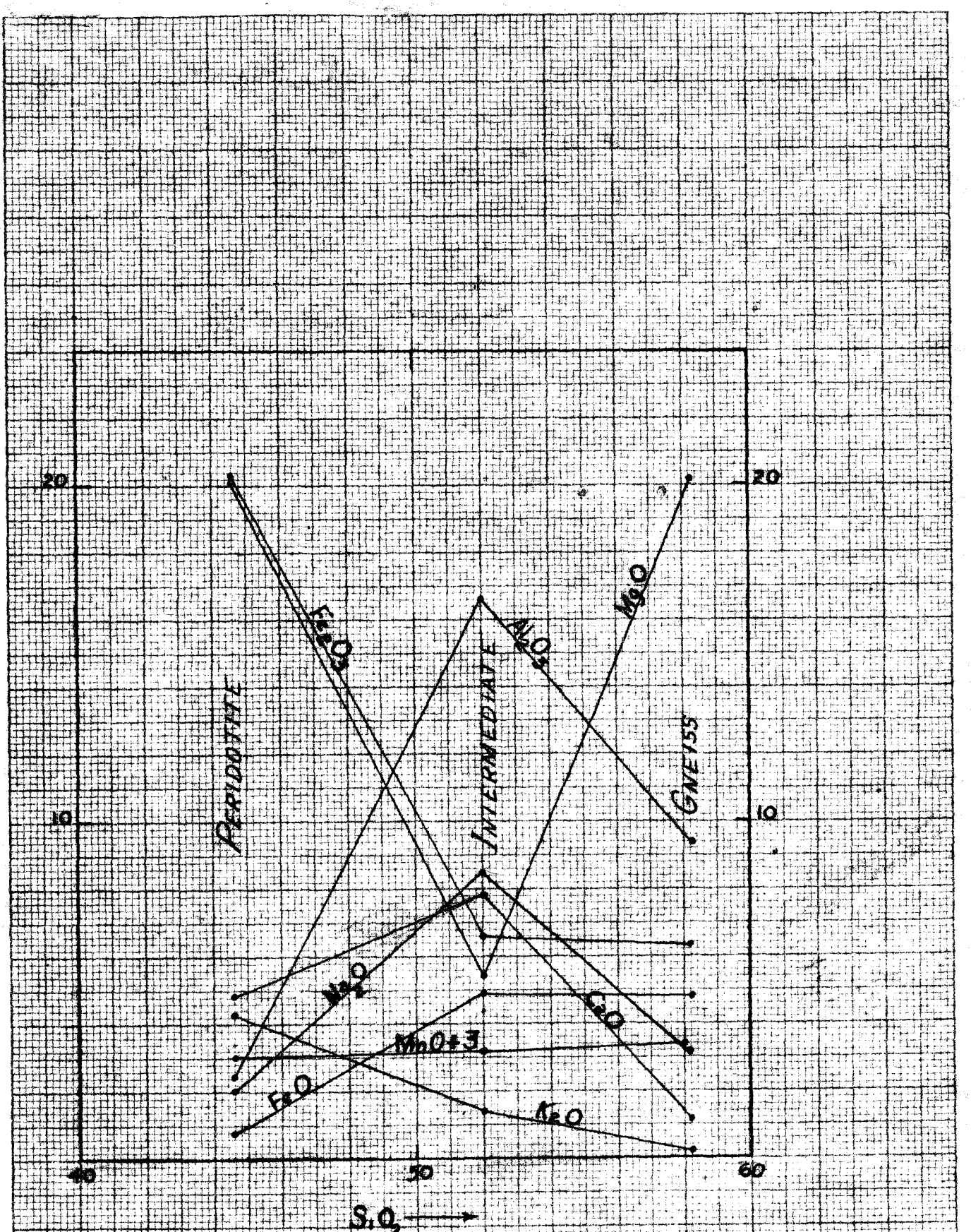

Fig. 17. Harker plot of chemical analyses in table 4.

Table 6 S-Al-F and Al-C-Alk proportions for intermediate mixed facies (from Osann)

Oxide	Mol. wt.	Wt.%	Mol	Mol%
SiO_2	60.06	52.00	.866	56.17
Al_2O_3	101.94	16.70	.164	10.65
Fe_2O_3	159.68	1.76	.011	.71
FeO	71.84	4.90	.068	4.41
CaO	56.07	7.92	.141	9.14
MgO	40.32	5.43	.135	8.75
Na_2O	61.99	8.59	.139	9.01
K_2O	94.19	1.41	.015	.97
MnO	70.93	.09	.001	.06
Cr_2O_3	152.02	.05	-	-
TiO_2	64.10	.10	.002	.13
P_2O_5	142.05	.012	-	-
CO_2	44.00	.08	-	-
		Totals--------	1.542	100.00%

(Sum of alkalies is less than Al_2O_3)

S = SiO_2-TiO_2-ZrO_2-P_2O_5 = 56.30

Al = Al_2O_3 = 10.65

Alk = A = Mol% of Na_2O-K_2O = 9.98

C = CaO-BaO-SrO = 9.14

F = CaO-FeO-MnO-MgO-NiO-SrO-BaO = 22.36

S:Al:F = 56.30:10.65:22.36; $\frac{89.31}{30}$ = $\frac{S,Al,F}{S,Al,F}$; 19.0-3.5:7.5

Al:C:Alk = 10.65:9.14:9.98; $\frac{29.77}{30}$ = $\frac{Al,C,Alk}{Al,C,Alk}$; 11.0:9.0:10.0

NK = $\frac{10Na_2O}{Na_2O-K_2O}$ = $\frac{90.1}{9.98}$ = 9.03; MC = $\frac{10MgO}{MgO-CaO}$ = $\frac{87.50}{17.89}$ = 4.89

Hence, the gradient for diffusion may have been present, if the principles established by Ramberg and Bugge hold for migration of ions through long distances in rock as well as migration through small distances. In view of the fact that these were deeply buried pre-Cambrian rocks in an orogenic belt, sources for pore solutions may have existed.

Strong evidence demonstrates that the present position of the transition zone was at one time essentially within the ultramafic rocks, i.e., that the zone has formed at the expense of these rocks. This evidence, cited below, stems from certain field and microscopic relations within the transition zone.

1. Relic ultramafic minerals and structures which have been partly replaced or recrystallized.

2. Lithologic similarity between the ultramafic rocks and inclusions in the transition zone.

3. S-Al-F and Al-C-Alk values (table 6) indicate that the transition zone is of igneous composition.

A comparison of the variations in rock analyses in tables 4 and 5 and figure 7 suggests that diffusion between the gneissic complex and ultramafic units will not account for most of the "geochemical culminations" (a term employed by Reynolds (1946, p. 389-446) for an increase of any constituent beyond the quantity present in the adjacent rock). A useful method of checking whether geochemical culminations signify diffusion is introduced by Chayes (1948, p. 413-425 by Wahlstrom, 1950, p. 256). He states that in rocks formed by replacement the amounts of residual

and introduced materials should vary inversely. If one variable (the introduced material) increases as the other variable (the residual material) decreases, it may be said that there is a "negative correlation" between the two. If the sequence of rocks under study does not show significant negative correlation between the variables, the diffusion hypothesis is untenable.

Certain negative correlations occur. For example there are negative correlations between Mg, Fe, and Ca, Na, Al. The transition zone appears deprived of Mg and Fe and enriched in Ca, Na, Al. Such a large increase in Na is not a likely contribution from the schistose portion of the gneiss which is believed to be a former argillaceous sediment. The average shale contains only 1.3 per cent Na. However, if the schist had been already partially migmatized, as seems probable, the gneiss would not be lacking in Na. It is noteworthy that minor constituents which reach their maximum in the gneissic complex (notably Mn, Ti, and Zr), are more abundant in the transition zone than in the ultramafic rocks.

Let us now consider the mechanism of metasomatism by the intrusion of pegmatites. Because pegmatitic activity occurred in the area later than ultramafic intrusion, it seems likely that the transition zone was either formed or affected by the entry of magmatic solutions. Moreover, some of the relations in the transition are such as would be expected from reaction with pegmatitic solutions. The heterogeneous nature of the gneiss, especially the zoned plagioclases, stringers of

albite, and the presence of both perthite and antiperthite cannot be explained by diffusion between the gneissic complex and ultramafic units. If this had been the only phenomenon influencing the transition zone, surely diffusion would have rendered these mixed plagioclases more uniform.

The concentration of apatite needles throughout the feldspars also opposes the diffusion hypothesis. Nockolds (1933, p. 561-589) cites eleven examples of an abundance of apatite in basic rocks intruded by acid magmas, and ascribed the concentration to the volatile action of the magmas.

The existence of numerous pegmatitic dikelets is evidence that magma has had access to the transition zone. In the southeast sector the intermediate facies borders a large pegmatite which has intruded the ultramafic rocks.

Several features of the dikelets indicate that they were relatively mobile and capable of producing considerable alteration in the wall rocks. Numerous stringers a fraction of an inch wide suggest highly attenuated solutions. Where contorted into ptygmatic folds, the dikelets evidence formation in a somewhat mobile host rock. Significant also are the contacts which are not sharp, but gradational over a fraction of an inch. The feldspar in the dikelets is andesine-labradorite. Because the dikelets are probably offshoots from the larger and more acidic pegmatites in the area, considerable chemical reaction between the ultramafic rocks and acidic solutions has taken place to render

the feldspar basic.

As pegmatitic solutions entered the ultramafic bodies, they were apparently desilicated in what is now the transition zone. To form the albite and perthite in the gneiss, leaving behind calcic plagioclase in the transition zone, a large amount of silica and sodium must be removed and also much K_2O and Al_2O_3 in molecular proportions. Increases of all these constituents (with the exception of K_2O) in the transition zone with respect to those in the gneiss complex and ultramafic rocks are shown by the chemical analyses. As the solutions became more basic, calcium could be added to the transition zone, and reversals in zoning could be formed. While lime and alkalies were added, Fe and Mg were apparently subtracted and carried into the gneiss complex.

Thus, the minerals and relations of the reaction zone are as would be expected from magmatic reaction with ultramafic rocks. According to Larsen (1928, p. 398-432) peripheral zones of altered ultramafic rock associated with pegmatites invariably have higher silica, alumina, and alkali contents than the unaltered ultramafic rock.

More chemical data from the gradational portions of the transition zone are needed before further extrapolation can be made. Available data are insufficient to warrant stoichiometric calculations which might disclose, among other things, whether the material removed is approximately equal to the material added. But the losses and gains mentioned are believed to be qualitatively reasonable and of the correct order of magnitude.

The role of metasomatism by diffusion between the gneissic complex and ultramafic rocks is not clear. Though present chemical evidence is far from conclusive and probably much oversimplified, it shows that such a diffusion process is a possibility. However, there is no strong evidence for its ability to produce the transition zone, and some evidence against its having done so.

Either pegmatitic solutions alone operated to form the zone, or their effects are merely superposed on earlier diffusion features. The former hypothesis is favored, because it raises less questions regarding the fundamental principles of diffusion in rocks, and because it is more consistent with the distinctive features of the transition zone.

PEGMATITES

Description

Types of pegmatites.- Pegmatites in the area may be divided into small concordant pegmatites and large discordant pegmatites.

Small concordant pegmatites in general parallel the rock or regional structure, only locally transgressing the foliation. Because of their small size most small pegmatites could not be shown on the geologic map. The presence of many is recognized by patches of white pegmatite float fragments. Lack of continuity of small pegmatites is characteristic and in sectors without outcrops is

demonstrated by isolated float patches. As a rule, outcrops are not very resistant and rise only slightly above the general surface level. The crumbly character of most outcrops reflects intensive weathering. Some outcrops are crudely aligned; others are disposed in an en echelon arrangement.

In contrast to large discordant pegmatites the small type is more abundant, more widespread, and more irregular in size and shape. A profusion of small pegmatites occur in all parts of the area. They range from stringers a fraction of an inch thick to bodies which average one to three feet in thickness. Some small pegmatites are tabular and vein-like, others form lenses, knots, and irregular protuberances.

In migmatites small pegmatites ordinarily form lit-par-lit injections. In both migmatites and intermediate mixed facies, vein-like pegmatites are locally thrown into ptygmatic folds. Relationships of these smaller pegmatites to the host rocks are discussed under host rock headings.

Compositionally, small concordant pegmatites are less complex than large pegmatites. They are essentially bi- or mono-mineralic. Most contain perthite with a variable quantity of intergrown quartz. Some thin pegmatites consist of pure quartz, plagioclase, or potash feldspar. In the migmatite phase, pegmatites contain appreciable amounts of garnet (pyrope) and minor amounts of muscovite and biotite.

Contacts of small pegmatites are gradational over a fraction of an inch to a foot, evidencing considerable soaking by pegmatitic solutions. This is in contrast to the contacts of large discordant pegmatites which are exceptionally clearcut. Certain smaller concordant pegmatites are undoubtedly offshoots from larger pegmatites, as they are intermingled with them locally.

Large discordant pegmatites occur only in the southeastern part of the area. Outcrops are ordinarily resistant to erosion and form rounded, hummocky outcrops above the host rock. For the most part, outcrops are discontinuous and persist for only a few feet to 150 feet laterally. Their lack of continuity makes it difficult to predict their plunge and lateral extent. Most of them weather pinkish-gray, but fresh exposures are brilliant white. In outcrop large pegmatites appear closely-fractured, but in fresh exposures are actually dominantly massive.

As a group, the large pegmatites crosscut other rock types in the area. None are concordant with foliation in older rock types. All strike roughly northeasterly and dip steeply. A secondary foliation has been induced in the gneissic complex along pegmatite contacts. This extends no more than a few feet from the contact. Contacts of main pegmatite bodies are in places of knife-edge sharpness.

Large pegmatites are characterized by a tabular to bulbous shape. Thicknesses range from 8 to 30 feet. One bulbous outcrop at the head

of the wash, 500 feet southeast of the cabin, attains a width of 40 feet. Variations in thickness within the same pegmatite reveal a pinching and swelling habit.

Perhaps the most striking feature of the large pegmatites is their extremely coarse- and irregular-grained texture. Subhedral blocks of quartz and perthite are as much as 3 to 4 feet in diameter. The cleavage of each block extends without interruption through its entirety, indicating that the block is all part of a single crystal. The average diameter of all crystals in a pegmatite may be measured in inches. No chilled margins were noted, but a conspicuous feature in the larger pegmatites is that they become increasingly coarser-grained toward the center.

Internal structure.- Three fundamental types of internal structure of pegmatites have been established (Cameron, et al., 1949, p. 14) as follows:

1. Fracture fillings
2. Replacement bodies
3. Zones

Only the latter type of internal structure, zones, has been distinguished with certainty by the writer in this area. Zones have been classified (Cameron, et al., 1949, p. 20) as follows:

1. Border zones
2. Wall zones
3. Intermediate zones
4. Cores

Three large pegmatite bodies show crudely-developed wall zones, intermediate zones, and cores. Border zones are missing. Wall zones are composed of perthite, with some muscovite and biotite. Intermediate zones consist of graphic granite, which typically consists of abundant cuneiform rods of quartz within crystals of perthite. Some mica and pink perthite are commonly associated. Cores of massive quartz are well-defined. Thus zones become more siliceous toward the center. Mica is distributed across the width of the wall and intermediate zones, but there is a tendency for main concentrations to lie near the walls. The black variety of tourmaline, schorl, occurs as a megascopic graphic intergrowth with quartz close to the pegmatite core. Coatings of green epidote are commonplace at contacts of wall zones with host rocks. A little apatite is found associated with perthite at margins of wall zones.

Contacts between zones vary greatly in distinctness. The cores are most distinct, but the wall and intermediate zones are somewhat gradational. The principal distinction between the wall and intermediate zones is that the intermediate zone is relatively quartz-free.

Description of two selected pegmatites.- Artifical cross-sectional exposures of two pegmatites permit three-dimensional analysis. These exposures occur on the north side of the road within 500 feet of its terminus to the southeast.

The largest pegmatite (fig. 18) has yielded some sheet mica. A drift has been driven 50 feet and some underground work accomplished. The exposed face of the pegmatite is 28 feet wide and 40 feet high.

It trends approximately N. 15° E. and dips 65° S. The lateral extent of the surface outcrop is 75 feet. Apparently the pegmatite plunges or pinches out to the north. Its tabular shape is clearly shown in figure 18.

Zones are present, but obscure in surface outcrop and somewhat poorly-defined in cross section. An irregular core of massive quartz is prominent approximately five feet west of the geometrical center. The usual intermediate zone of graphic granite becomes the wall zone and constitutes the bulk of the dike. Exceptionally rich concentrations of muscovite and biotite appear to be fracture-controlled close to the foot wall. Two sets of fractures cross at right angles and contain mica books with their cleavage parallel to the fractures. Many of the books are 5 to 12 inches in maximum dimension.

Of special interest are the country rock zones adjoining the pegmatite proper. Sodic andesine intermixed with highly pure vermiculite borders the pegmatite. Fine to medium-grained residual xenoliths of ultramafic composition occur below the foot-wall. They are especially rich in vermiculite and also contain admixed andesine and various ultramafic alteration products.

This first country rock zone gives way to granulites outward from the pegmatite. Labradorite replaces andesine as the plagioclase in this rock, which is described earlier as a member of the gneissic complex. The granulites are crosscut by a maze of irregular bulges, prongs, and dikelets of sodic andesine and minor vermiculite, and also

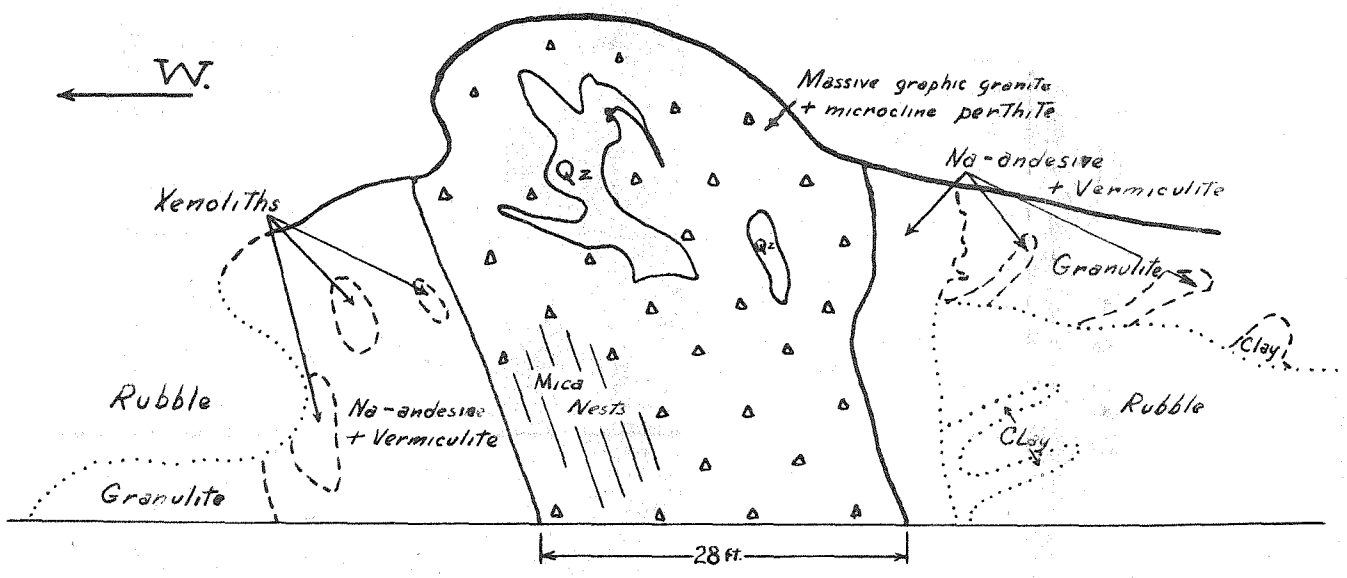

Fig. 18. Diagrammatic cross-section sketch of pegmatite (pictured above) in front of mine portal showing zoning within and without pegmatite body. (July, 1951)

by foot-wide clay dikes consisting of fine-grained ultramafic alteration products, namely, clinozoisite, vermiculite, serpentine, magnetite-hematite, and spherulitic chalcedony. The dikes are in turn threaded by andesine dikelets and serpentine-coated seams of caliche. Both andesine dikelets and caliche seams are less than four inches thick.

The second pegmatite roughly parallels the first at a distance of 500 feet to the west. A cross-section of this pegmatite (fig. 19) is bared by a road cut. The dike strikes N. 45° E. and dips 30° W. Its outcrops can be traced discontinuously for a distance of a quarter of a mile south of the road, but for less than 25 feet north of the road.

The pegmatite is tabular and 5 to 8 feet in breadth. It consists of a massive quartz core and an outer zone of graphic granite. Flakes and books of muscovite and biotite are scattered through the pegmatite, but occur mainly in the outer zone. The only notable concentration of tourmaline found in this area is the occurrence in this pegmatite. Rosettes and sunbursts of shiny, black schorl form intergrowths with quartz and perthite at the boundary of the quartz core.

A fine- to medium-grained vermiculite-rich zone 6 to 12 inches thick adjoins the pegmatite. Many graphic granite stringers extend into this zone from the pegmatite. This zone is bounded by granulites. Contacts between all zones within and without the pegmatite are sharp and clear-cut. Wall-rock contacts are coated with epidote.

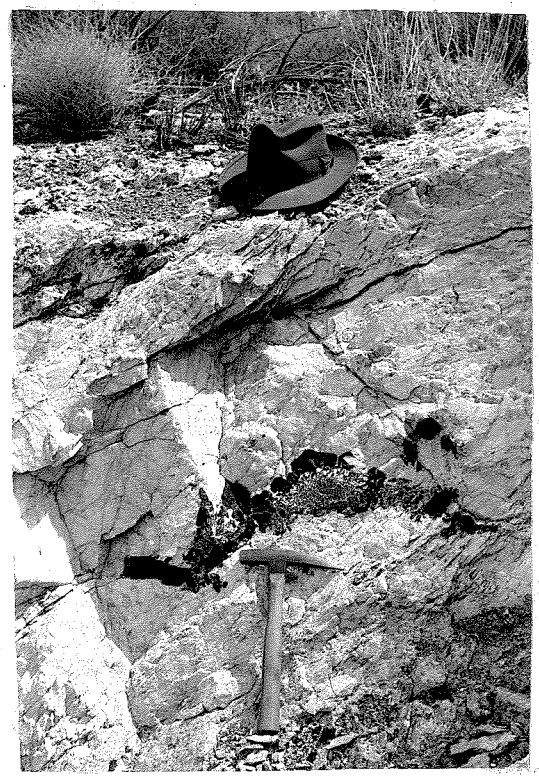

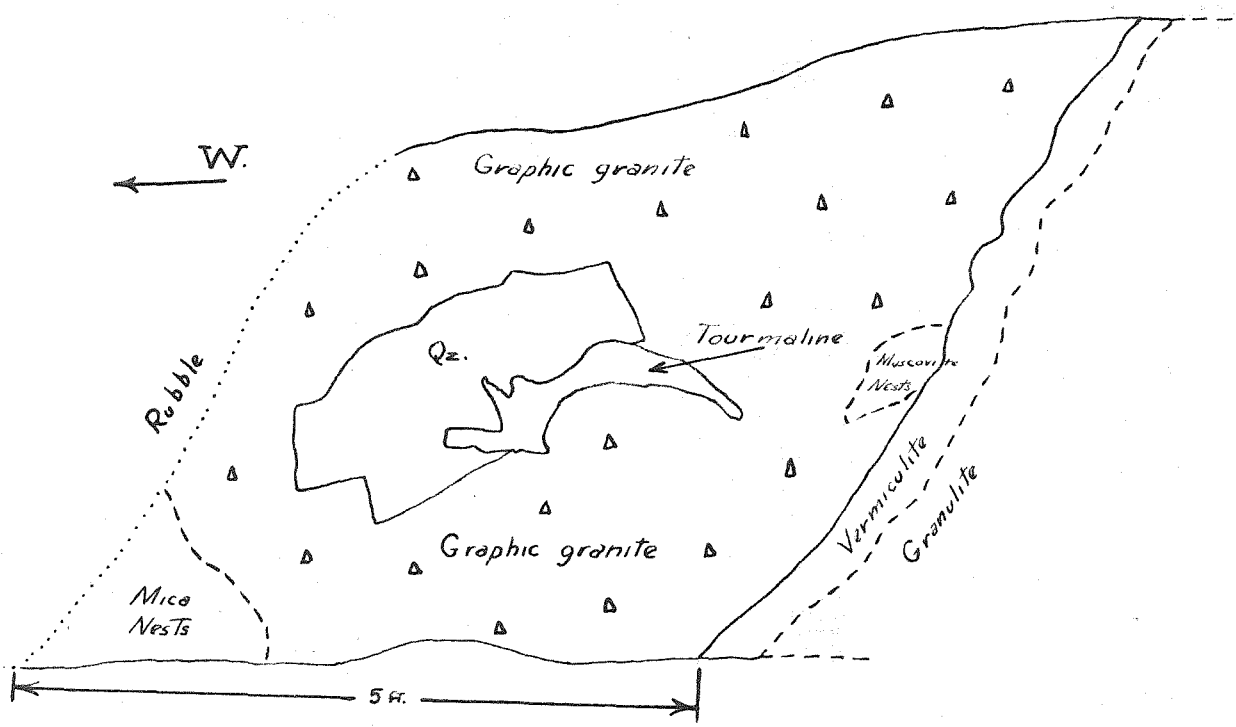

Fig. 19. Diagrammatic cross-section sketch of tourmaline pegmatite showing zonal relations. (July, 1951).

Origin

All pegmatites are believed to belong to one period of intrusion. They are younger than other rocks in the area and are probably genetically related to the Gold Butte granite porphyry which crops out almost one mile to the southwest. This is the only young granitic rock in the region. Large pegmatite dikes strike southwest and other pegmatites are observed trending towards and into the granite porphyry. The similar extremely coarse texture of the Gold Butte porphyry is another reason for considering it the source of the pegmatites.

A suggestion that the large pegmatites represent forcefully injected fluids is shown by the imposition of a secondary foliation in the wall-rock. Softened by heat and emanations, the wall-rock is believed to have behaved plastically.

The lithologic sequence of zones, inward coarsening of texture, and lack of replacement criteria favor the hypothesis suggested by Cameron, et al., (1949, p. 98-105) that the large bodies formed by fractional crystallization of relatively uncontaminated magmatic liquids from the walls of the pegmatite inward.

Prospectors have supplied the author with the following minerals from pegmatites within the Gold Butte porphyry: allanite, samarskite, monazite, uraninite, tantalite, and columbite. The absence of all these minerals from pegmatites in the area under study is puzzling. It may be due to the impoverishment of pegmatitic solutions upon reaching areas remote from their genetic source, to earlier crystallization of rare minerals under high temperature conditions, to localized

concentration of these constituents, or to the author's observations which were limited to a small area.

GENERAL MINERALOGY OF VERMICULITE

Crystal Structure

Investigations by Pauling (1930, p. 123-129; 1930, p. 578-582) demonstrated that a large number of alumino-silicates including the true micas, brittle micas, chlorites, vermiculites, pyrophyllite, talc, stilpnomelanes, and certain clay minerals have related layer, or sheet structures. Subsequent detailed structural studies of the micas by Jackson and West (1930, p. 211-227; 1933, p. 160-164) and Hendricks and Jefferson (1939, p. 729-771); the chlorites by McMurchy (1934, p. 420-432); pyrophyllite, talc, and vermiculites by Gruner (1934, p. 412-419; 1934, p. 557-575); the stilpnomelanes by Hutton and Fannkuchen (1938, p. 172-206); and the clay minerals by Ross and Kerr (1931, p. 55-64) and Gruner (1932, p. 75-88) confirm and extend Pauling's interpretation.

The sheet structure common to all these minerals consists of atomic groups arranged with hexagonal symmetry in superposed parallel layers. Within the layers the atomic groups are both tetrahedral and octahedral. Tetrahedral groups include four O atoms surrounding a Si, Al, or occasionally other atoms; octahedral groups consist of O and OH atoms surrounding Al, Fe, Mg, or occasionally other atoms.

Tetrahedra may be firmly superposed upon the octahedra to form a single sheet layer, or they may be firmly bound below as well as above the octahedra to form double sheet layers. In turn, the layers may be packed one upon another or may be separated by atoms which readily penetrate between them. These interlayer atoms serve to displace the layers, giving rise to new minerals. As a result there are four distinct types of layer structures:

1. single sheet structures (kaolinite, etc. fig. 20a)
2. single sheet structures with interlayer structure (halloysite, etc. fig. 20b)
3. double sheet structures (talc, etc. fig. 20c)
4. double sheet structures with interlayer structures (vermiculite, chlorite, biotite, etc., fig. 20d)

Because all these types have the same pattern of very similar lateral dimensions, there exist mixed structures containing interstratified layers of more than one type. Hendricks and Jefferson (1938, p. 861; 1939, p. 729-771) have shown that these different layers can be stacked in a variety of ways. They conclude, "..... any mixture of mica, vermiculite, chlorite, pyrophyllite, stilpnomelane (provided this is not a mixed structure) and talc layers would not be unreasonable. The list also might include kaolin and hydrated kaolin structures." Such mixtures result in no lateral displacement of the component layers, although the different layers may or may not be of equal thickness.

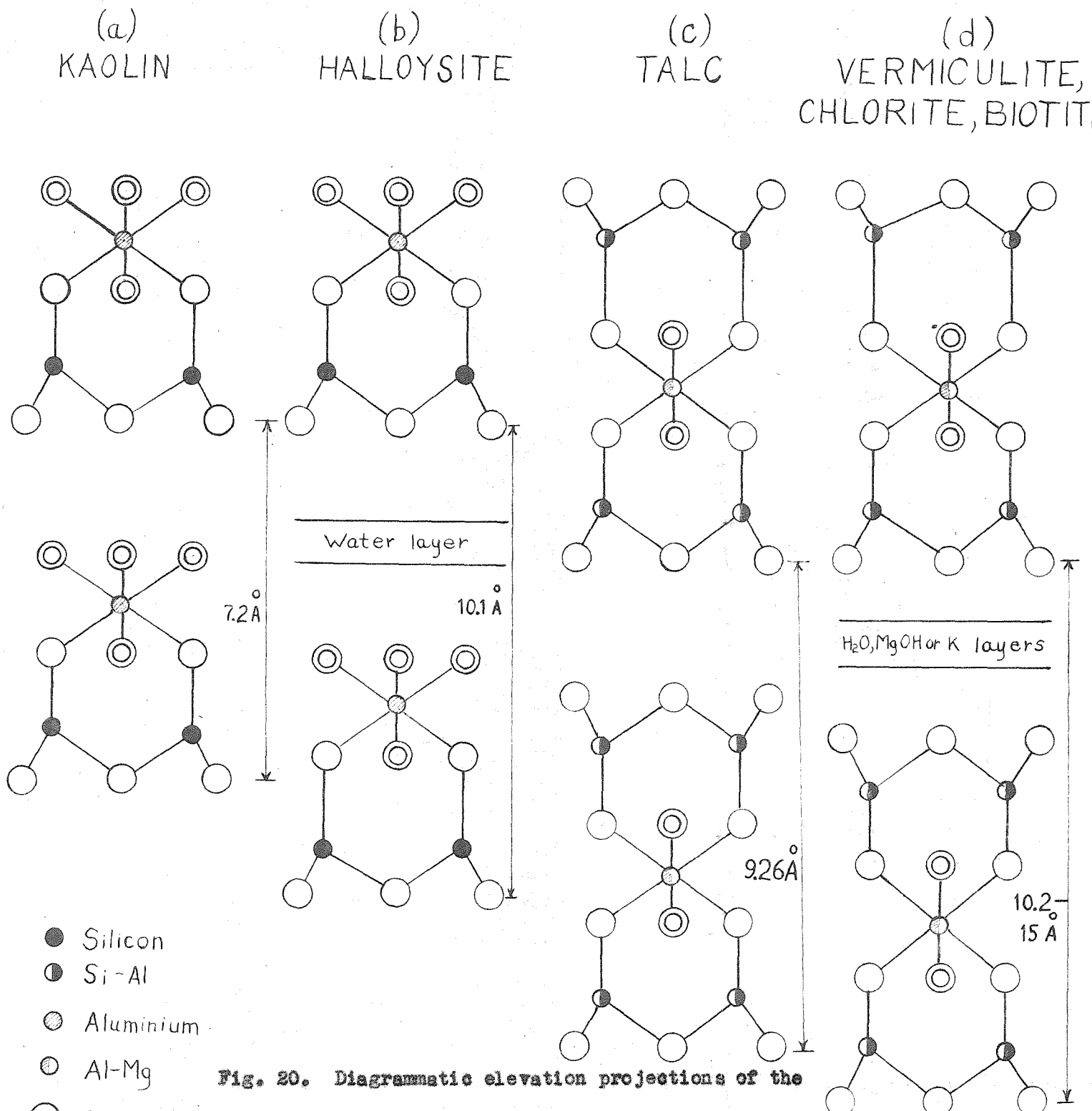

Fig. 20. Diagrammatic elevation projections of the four types of layer lattices. Each projection represents a group of minerals rather than a single structure. Ideas gained mainly from Brindley, also from Gruner and Barshad.

In view of the similar lateral dimensions within the sheet structures, it seems surprising that there is not greater multiplicity of layer structures within single crystals. Gruner (1948, p. 686) believes the reason, ".....may be found more likely in the relatively stationary or only slowly changing chemical environment in a system, than in any aversion on the part of the structures to change from layer to layer." In other words, if the composition of cation supply were changed at the same rate individual layers grew, a single crystal might contain more combinations of different layers.

Mineral types of the double sheet structure with interlayer arrangements exhibit the property of interleaving to the greatest extent. Layers may be distributed regularly, randomly, or a combination of both with the added possibility of segregation into zones (MacEwan, 1951, p. 266). A regular interleaving pattern is displayed by the well-known hydrobiotite from Libby, Montana. Samples of this hydrobiotite were studied by Barshad (1949, p. 682) and were shown to consist of vermiculite and biotite interleaved in the proportion of three biotite sheets to one vermiculite sheet. Most interleaved minerals, however, are merely mixed at random. According to Bradley (1950, personal communication) the concept of regular repetitive sequences is gradually being replaced by the concept of random intergrowth.

Results obtained by Barshad and Gruner indicate that there are four general classes of vermiculite-like minerals found in nature,

namely (1) true vermiculite, (2) vermiculite-biotite mixtures (hydrobiotites), (3) vermiculite-chlorite mixtures, (4) biotite-chlorite mixtures.

Structurally, the essential difference between biotite, vermiculite, and chlorite is that different interlayer structures are present, the main interlayer constituents being water molecules in vermiculite, potassium atoms in micas, and magnesium aluminum hydroxides in the chlorites. Each mineral has a characteristic unit cell, its size depending upon the thickness of the interlayer structure. Biotite consists of talc-like layers, 9.26A° high, alternating with potassium layers (1.07A°); chlorite consists of talc-like layers (9.26A°) alternating with magnesium hydroxide layers (4.86A°); vermiculite consists of talc-like layers (9.26A°), alternating with water layers 4.95A°-.

In an X-ray analysis of each of these minerals the basal spacing (d001) is not only the most important spacing for the purpose of identification, but is also essential in determining the height and structure of the unit cell. The height (c_0) of the unit cell measured normal to the base is twice this d001 spacing. Because the unit cell consists of two talc-like layers and two interlayers ("water layers"), the thickness of the interlayer may be found by subtracting 9.26A°, the thickness of a talc layer, from the basal spacing of the pure mineral (see fig. 20). The thickness (or height) of a "water layer" is thus defined as the distance between adjacent silicon-oxygen surfaces of successive talc layers.

All of the above four general classes of vermiculite-like minerals give characteristic diffraction patterns with the exception of vermiculite and vermiculite-chlorite hybrids. The similarity of unit cell layer spacings between chlorite and vermiculite partially accounts for the virtual impossibility of distinguishing vermiculite from a chlorite-vermiculite mixture by means of an X-ray powder pattern (Gruner, 1939, p. 430; Walker, 1941, p. 203). Differences are best brought out by chemical means. The combination of a low NH_4 capacity, the absence of K^+, and a low water content serve to distinguish the mixture from true vermiculite (Barshad, 1948, p. 676). Also, by heating a specimen to 500° C. all interlayer water will be driven off, and if, therefore, the characteristics of a random interstratification persist after this treatment, we may suppose that a chloritic component is present (MacEwen, 1951, p. 279).

Studies by Barshad (1948, p. 655) showed that vermiculite has a high cation-exchange capacity in the interlayer structure. The degree of displacement of the double sheet structures was found by Barshad (1950, p. 237) to depend upon the size, valency, and total number of interlayer cations as well as the kind of adsorbed cation, Li^+, K^+, Na^+, NH_4^+, Rb^+, Cs^+, Mg^{+2}, Ca^{+2}, or Ba^{+2}. Those adsorbed cations which produce contracted lattices were shown to be more or less fixed against replacement by a cation which itself produces a contracted lattice, but cations which produce an expanded lattice can replace a cation adsorbed in a contracted lattice, apparently by being able to expand the lattice gradually as it enters from the

edges. Barshad was able to convert biotite and hydrobiotite into vermiculite by cation-exchange of Mg^{+2} for K^{+}. It follows that vermiculite must be a biotite with either Mg ions, or Mg and Ca ions replacing the K ions in the interlayer positions.

Little, if any, experimental work to convert chlorite to vermiculite has been attempted. This appears impossible by cation-exchange, because Mg ions already occupy interlayer positions in the chlorite.

Although it has been demonstrated that theoretically any sheet structure may mix with another, it is particularly puzzling from a structural viewpoint why the interleaving of vermiculite and muscovite, and vermiculite and montmorillonite do not occur in nature. Muscovite has a similar lattice structure to biotite with Al_2 replaced by $(Mg, Fe)_3$. Montmorillonite contains the mica-type double sheet structure and has an expanded and hydrated lattice similar to vermiculite.

Winchell (1945, p. 267) shed some light on the mica problem by classifying micas into octo- and heptaphyllite groups. There is seldom isomorphous mixing between the octophyllite system, biotite, which has all or most of its three octahedral positions filled, and the heptaphyllite system, muscovite, which has only two or slightly more than two of these positions filled. Like biotite, vermiculite is "trioctahedral". Thus mixtures of biotite and vermiculite are common, mixtures of muscovite and vermiculite unknown.

No clear structural difference exists between microscopic vermiculite and montmorillonite (Grim and Bradley, 1950, personal communications). This is one reason why no mixtures of the two have been reported. Recent work by Barshad (1950, p. 237) reveals that the interlayer structure of air-dry vermiculite and montmorillonite is identical, whereas the interlayer structure of montmorillonite expands to a greater extent in glycerol or water. This phenomenon is not fully understood as yet.

Another problem deserving additional study is the manner of packing of water molecules in the interlayer space of vermiculite. Two major difficulties existed here. For a long time it was difficult to understand how almost half the water in vermiculite could be driven off at 110° C. without affecting the diffraction pattern (Gruner, 1934, p. 566; 1939, p. 433) (Bragg, 1937, p. 220). Recently Walker (1949, p. 726) showed that a change in the structure does actually occur, although it is obscured by rapid rehydration upon cooling. Another difficulty was presented by the variation in the height of the water layer in different crystals. Now it is known that the nature of the saturating interlayer cations determines the arrangement and amount of water present. According to Walker (1949, p. 726) when magnesium is the saturating cation the interlayer structure is surrounded by an octahedral group of water molecules. Barshad (1949, p. 683) believes that the water molecules in natural vermiculite form

tetrahedra with the bases of the linked silica tetrahedra of the lattice, giving rise to hexagonal rings of water molecules which are similar to hexagonal rings of oxygens at the vertices of the linked silica tetrahedra of the individual mica sheets.

Expansion of the crystal lattice of vermiculite is sometimes related to particle size. Although the common megascopic form of vermiculite differs from the microscopic form in size only (Grim, 1950, personal communication), the former does not seem to expand in organic liquids as does the latter (Bradley, 1945, p. 712). Recently, Barshad (1950, p. 233) has stated that the expansion of large vermiculite particles showed the same expansion as microscopic particles whether air-dry, immersed in water, or in glycol. This would be expected if mega- and micro-vermiculite were structurally identical. Perhaps under certain conditions vermiculite mixtures inhibit the introduction of liquids into large crystals even though the liquids may penetrate fine-grained vermiculite (Bradley, 1945, p. 712). It is interesting in this connection that the interlayer water is more easily removed from fine particles of vermiculite than larger particles (Walker, 1951, p. 209), suggesting that this is possibly due to different types of bonding or packing of atoms and molecules in the interlayer spaces.

Chemical mineralogy

Gruner (1934, p. 560) determined the formula of vermiculite, based on the average chemical analysis of seven true vermiculites, to be as follows:

$(OH)_2(Mg,Fe)_3(Si,Al,Fe)_4O_{10}.4H_2O$ or $22MgO.5Al_2O_3.Fe_2O_3.22SiO_2.40H_2O$

True vermiculite contains no potassium, and the formula is that of biotite with potassium being subtracted and water being added. The above formulas were later confirmed by Hendricks and Jefferson (1938, p. 851).

The old term "hydrobiotite", used for biotite-like material with a high water content, was revived by Gruner to designate an interleaving of biotite and vermiculite. For a biotite-vermiculite ratio of 1:1 Gruner set the formula as follows:

$$OH_4K(Mg,Fe)_6(Si,Al,Fe)_8O_{20}.4H_2O$$

Chemically, the essential difference between hydrobiotite and vermiculite is the presence of potassium in the former.

The first indication that these formulas were not satisfactory was Gruner's preparation of ammonium micas from vermiculites (1939, p. 428-433). How charged NH_4 groups could enter apparently neutral biotite or talc-like layers of vermiculite was not understood by Gruner. The existence of charged water particles which can be replaced by NH_4 groups was postulated by him but not substantiated.

Barshad (1948, p. 677) demonstrated that the cation-exchange capacity of vermiculite was approximately 50 per cent greater than that of montmorillonite, thus very pronounced. Experimental results

indicate that K ions in biotite can readily be exchanged for other cations and that this process is reversible between Na, Ca, Mg and K ions. By cation-exchange (Mg^{-2} for K^{-}) Barshad was able to convert biotite and hydrobiotite into vermiculite. He also accomplished the reverse process.

These results indicate that the old formula of vermiculite needs modification, because no provision had been made by Gruner for exchangeable cations. As a result the following formula for vermiculite was proposed by Barshad:

$$(H_2O)_x(Mg,Ca)_y(Al,Fe,Mg)_z(Si,Al,Fe)_4O_{10}(OH)_2$$

where x represents mols of H_2O, y, the exchangeable cations, and z, the octahedral ions. In hydrobiotite the exchangeable cations may be shown as $(K,Mg,Ca)_y$. The amount of hydrated water present in vermiculite and hydrobiotite is chiefly dependent on the kind of interlayer cation present and is directly proportional to the amount of K^{-} replaced by Mg^{-2} and Ca^{-2}.

Exfoliation

There are two means of exfoliating vermiculite, with heat and with chemicals. Both means are associated with the separation of individual lamellae and a change in color to silvery white. Heat exfoliation occurs with a loss in water and weight; chemical exfoliation may or may not result in a decrease in weight. Both exfoliated products have a lower specific gravity, but only sudden heat treatment causes the decrease necessary for commercial application.

Heat exfoliation.- There have been two theories explaining the mechanism of heat exfoliation.

(1) It depends at least partly upon the warping and buckling of the cleavage plates (Laschinger, 1946, p. 4; Byers from Davis and Johnson, 1936, p. 15; Goldstein, 1946, p. 22).

(2) It depends solely upon the rapid formation of water vapor between crystal plates (Barshad, 1948, p. 668; Walker, 1951, p. 208).

Laschinger explains the warping and buckling by the abrupt change in cell dimensions of contiguous layers upon dehydration. According to Byers, "The reason vermiculite expands is because the bonding of the planes of cleavage is weaker than the warping and twisting force and the plates are pressed apart, while in micas the bonds between the planes of cleavage are stronger than the twisting force which results in the same warping and twisting of the whole sheet, with some spreading thereof or a trace of swelling, but with no such expansion as occurs on heating a vermiculite in which the crystals are less tightly bound due to the natural solvent action along cleavages before the subsequent heat treatment". Both Laschinger and Byers believe the evolution of water vapor is also important.

Barshad found that vermiculite loses the property of exfoliation if the water is driven off slowly by gradually heating to 250° C. After being slowly dehydrated vermiculite was then suddenly heated to high temperatures, but it did not exhibit exfoliation. Thus, warping

and buckling cannot be the prime cause of heat exfoliation. Instead, Barshad's experiment favors the necessity of an explosive release of water between layers. That a rapid release is needed is also suggested when heat from a match causes cleavage plates to swell in the center before opening at the margins. By contrast, heat from a blow torch causes rapid exfoliation without this swelling. Rapid heating is also accompanied invariably with a crackling noise, produced by the sudden escape of steam and the forcing open of the plates. The more rapid the conversion of water to steam, the greater (within limits) is the exfoliation. Only those minerals containing water of hydration display the property of exfoliation.

Differential thermal analysis has provided a useful method of examining the loss of water during heat exfoliation. Vermiculites yield characteristic troughs in the differential thermal curves through the temperature range 0° C. to 1000° C. and characteristic plateaus in the equilibrium dehydration curves for the same temperature range. Differential thermal curves have proved more useful than equilibrium dehydration curves in the study of vermiculites, as well as in the study of most common clay minerals.

Characteristic differential thermal curves for natural vermiculite and for hydrobiotite are shown in figure 21. The significant parts of the curves are the endothermic troughs which represent water losses. These losses for each trough may be calculated in per cent total H_2O or in mols per exchangeable cation.

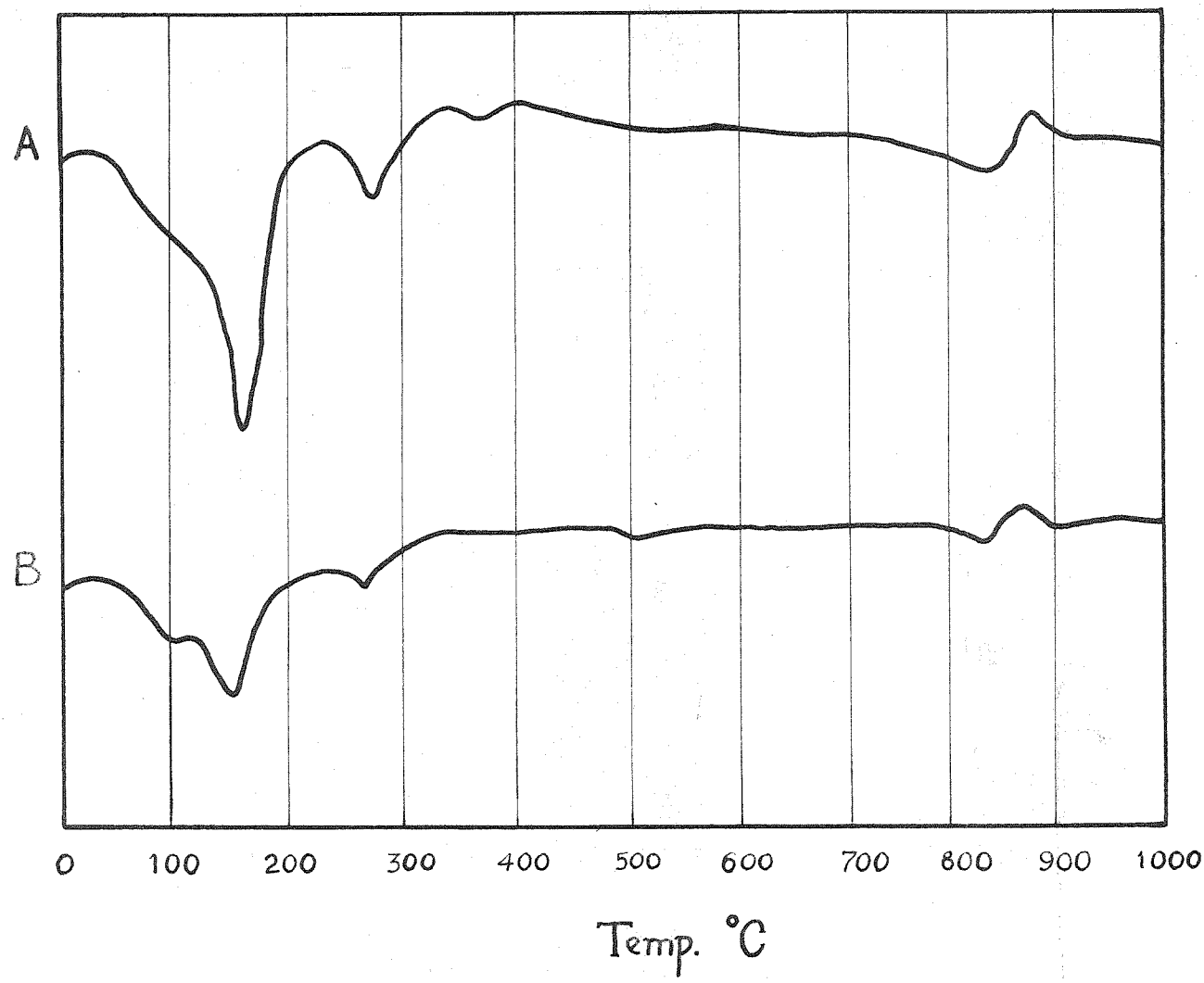

Fig. 21. Differential thermal analysis curves of A: Vermiculite from Brinton's quarry, West Chester, Pa; B: Hydrobiotite, Mpwapwa, Morogoro, Tanganyika; (Walker, 1951, p. 211).

The curve for natural vermiculite shows three troughs, the first at about 150° C., the second at about 240° C., and the third at about 850° C. The first two troughs represent H_2O losses, the third an OH loss.

The hydrobiotite shows reduced peaks corresponding to the reduced ratio of vermiculite in the vermiculite-biotite mixture. Because the area of the trough is proportional to the percentage of vermiculite present in a given weight of the sample, the percentage of vermiculite and percentage of biotite may be determined. Measurement of the trough areas indicates the mixture is 40 per cent vermiculite.

The moisture losses recorded on differential thermal curves assume special significance when correlated with the degrees of exfoliation. The maximum exfoliation corresponds in time with the first water losses shown on the curves. It seems, therefore, that temperatures need not exceed 500° C. to give maximum exfoliation.

Recent investigations shed considerable light on changes in the interlayer structure during heat exfoliation. Barshad (1949, p. 680) indicates that heat exfoliation takes place in steps, each equivalent to a thickness of one molecular layer of water. It is well to keep in mind that the mere loss of water holds no relationship to exfoliation, for the crystal lattice contracts as water is expelled. When vermiculite lattices are contracted, it is probable that the interlayer cations, Mg and Ca, occupy the cavities formed by the hexagonal rings of oxygens on the bases of the linked silica tetrahedra of opposite lattice layers in the typical biotite or talc-like structure.

Walker (1951, p. 206) showed that the height of the water layer in vermiculite is sufficient for each Mg atom to be surrounded by a single hydration shell of six close-packed water molecules arranged octahedrally. Inasmuch as the chemical formula of vermiculite requires 16 water molecules per unit cell, there will be approximately 14 water molecules between the biotite-like layers for each Mg^{+2}. Six of these will be "bound" water and eight will be left over in a loose condition as "unbound" water. According to the chemical formula of vermiculite, 30 per cent of the total water consists of hydroxyl groups so that the "unbound" water will constitute almost half the total water content of the mineral, the half presumably released at 150° C. The loss of the "bound" water molecules would correspond to the water loss at 240° C., causing further exfoliation.

Walker supposes that on the removal of the "unbound" water, the octahedral groups around the Mg ions spread out over the basal plane surfaces in a single layer, but that the strong tendency of the Mg ions to rehydrate causes reversion to the original structure as soon as moisture becomes available.

Chemical exfoliation.- A number of oxidizing agents will produce exfoliation. Drosdoff and Miles (1938, p. 391-393) discovered that cold hydrogen peroxide exfoliates vermiculite. They ascribed the reaction to the presence of traces of catalytic MnO_2 which caused the decomposition of H_2O_2. The liberated oxygen split the vermiculite flakes apart. Groves (1939, p. 554) found that other oxidizing agents

act in a similar manner but not as energetically. He, too, believed liberated oxygen forced the sheets of vermiculite apart. Gruner (1939, p. 423) repeated and verified the experiments of Drosdoff and Miles.

Ruthruff (1941, p. 480-481) showed that when hydrobiotite is saturated with concentrated sulfuric acid and then exposed to air over a considerable period, or steamed for a shorter time, it exfoliates as much as ten fold. This behavior is attributed to the forcing apart of lamellae by sulfate crystals formed between them. Inasmuch as true vermiculite does not exfoliate under these same conditions, an easy means of distinguishing vermiculite and hydrobiotite is thus afforded.

MINERALOGY OF GOLD BUTTE VERMICULITE

X-ray, chemical, differential thermal, and heat exfoliation studies indicate that two distinct types of vermiculite mixtures occur in the deposit investigated. All samples examined were one of these two types or gradations between them. All must be considered as varieties of hydrobiotite, because K_2O is present in every case and represents a contamination by biotite layers.

One type is a vermiculite-biotite mixture with the approximate ratio of 2:1, respectively. Its color in the field is dark green and it has the feel and luster of talc. In general it occurs in mica-like

books which measure half an inch to 3 inches parallel to the basal cleavage.

The second type is essentially a biotite, containing approximately four per cent vermiculite. It is like biotite in general appearance with a dark brown color. No books larger than half an inch were found. Because this mineral displayed marked heat exfoliation in comparison to the pure biotite also present in the deposit, it will be considered as a hydrobiotite.

In order to distinguish the two types in this report the one will be referred to as vermiculite-hydrobiotite, the other as biotite-hydrobiotite. Collectively, vermiculite hybrids will be known by their trade name, vermiculite.

Optical properties of each are discussed in part XI.

X-ray studies

X-ray data are essential to an accurate picture of the structure of a vermiculite. Because basal spacings (d001) are the most significant diffraction lines, these are presented in table 7. Most were kindly furnished by Dr. Isaac Barshad of the University of California. All spacings of the diffraction pattern of the vermiculite-hydrobiotites correspond to those of biotite or vermiculite with the exception of the broad basal spacing, 12.48^{96}Å.

This latter spacing is an average spacing produced by the interleaving of vermiculite and biotite. If these two lattices are interleaved in a regular pattern, as shown to be the case in the hydrobiotite

from Libby, Montana (p. 109), the basal spacing should be an average of the basal spacing for each material (Hendricks and Jefferson, 1939, p. 873-875). In the sample studied the average basal spacing would therefore be (2 x 14.62 + 1 x 10.27) ÷ 3 = 13.17Å, where 14.62Å is the vermiculite basal spacing and 10.27Å is the assumed biotite basal spacing. The spacing actually obtained was 12.48Å, showing that a regular repetitive pattern is absent.

According to Barshad the diffraction pattern of the vermiculite-hydrobiotite sample studied by him shows that all of the biotite is randomly interleaved with the vermiculite, but that some of the vermiculite is present in segregated zones without being interleaved. Calculations by Barshad, based on the 12.48Å spacing, show that 51 per cent of the total vermiculite in the sample is in segregated form, whereas 49 per cent is in interleaved form. Thus the sample can be considered as a 1:1 mixture of vermiculite and hydrobiotite.

Other samples of the same vermiculite-hydrobiotite specimen give diverse results. Barshad (1951, personal communication) reports that one specimen appears to be a mixture of forms, some of which seem identical to the 1:1 vermiculite-hydrobiotite mixture and others that seem far different. Another specimen (Intermediate-1 in table 7), X-rayed by the writer, showed a broad basal spacing of 11.20Å. Bradley (1950, personal communication) studied the X-ray diffraction effects of other samples of the same specimen, reporting that one is a biotite-hydrobiotite mixture and that another contains nearly equal proportions of biotite and vermiculite.

Table 7 Basal spacings of vermiculite from Gold Butte, Nevada

Variety	Basal spacing (d001)
1. Vermiculite-hydrobiotite	12.48Å- strong intensity (average spacing of vermiculite and biotite)
2. Intermediate (1)	11.20Å- strong intensity (average spacing of vermiculite and biotite)
3. Intermediate (2)	10.75Å- strong intensity (average spacing of vermiculite and biotite)
4. Hydrobiotite	10.27Å- strong intensity (essentially biotite spacing)

This total lack of uniformity within one specimen collected from the same small area is indeed astonishing at first, but seems characteristic of the interstratification of sheet structures wherein all kinds of irregularities can and do exist. Probably a more direct explanation in this case involves the high cation-exchange capacity of vermiculite, because cation-exchange is undoubtedly the process of alteration in these sheet structures. With the alteration being completely random, the implication is that initially any layer may be attacked, determined only by chance, but an attacked layer tends to alter completely before other layers are attacked (Bradley, 1950, personal communication).

The biotite-hydrobiotite examined by Barshad has a broad basal spacing of 10.27Å, which is essentially a biotite spacing. In addition all diffraction lines are identical to those of biotite, the vermiculite being present in too small an amount to be detected by X-ray. An X-ray analysis by the writer shows a basal spacing of 10.75Å, indicating a greater number of vermiculite layers than in the specimen analysed by Barshad.

It is interesting to compare these X-ray data for Gold Butte hydrobiotites with X-ray data available for other hydrobiotites. Of 12 mixed biotite-vermiculite structures for which basal spacings have been measured, all fall within the limited range of approximately 11.4-12.1Å. Not a single basal spacing of Gold Butte hydrobiotite

is included in this range, although there is reason to suspect there exist all gradations between the two measured extremes of 10.27Å and 12.48Å.

Chemical analyses

Chemical analyses of the two extreme variations of vermiculite are shown in table 8. Analyses of other vermiculites, hydrobiotites, and a biotite are shown for comparison. The separation of water into uncombined water (H_2O-) and combined water (H_2O+) is ignored, because much of the total water content escapes at temperatures as low as 105° to 110° C. upon prolonged heating. Gold Butte samples were thoroughly dried below 100° C. and only total water reported.

The two most significant oxides in the analyses are K_2O and H_2O. Their relative abundancy establishes the minerals' position within the range biotite to vermiculite. Percentages of K_2O and H_2O for Gold Butte types are compared with average oxide percentages of biotite, hydrobiotite, and true vermiculite in part A of table 9.

Potassium oxide ranges from 0 per cent in true vermiculite to 10.7 per cent in ideal biotite. Water shows a progressive increase of 4.1 to 20.7 per cent from biotite to true vermiculite. The range of averaged analyses for K_2O, MgO, and H_2O is shown in part B of table 9. These do not include the Gold Butte types. As a rule the amount of MgO increases from biotite to vermiculite, but this is not always true, as can be seen by overlap of the range for

Table 8 Chemical analyses[1] of vermiculites, hydrobiotite and biotite
(cont. next page)

	Vermiculite Loolekop, S. Africa	Ideal Vermic-ulite	Vermiculite, Bare Hills, Md.	Impure Vermic-ulite, Wyoming	Vermiculite-hydrobiotite, Gold Butte, Nev.	Hydrobiotite Libby, Mont.	Biotite-hydrobiotite, Gold Butte, Nev.	Hydrobiotite, Loolekop, S. Africa	Ideal Biotite
SiO_2	36.6	36.7	36.1	39.8	43.5	39.0	34.5	39.1	40.9
Al_2O_3	8.4	14.2	13.9	15.4	10.6	17.1	1.6	10.2	11.6
FeO	0.1	-	0.7	1.5	3.1	0.0	1.8	15.6	16.4
Fe_2O_3	4.5	4.4	4.2	4.8	3.8	6.7	12.4		
MgO	26.9	24.6	24.8	19.9	19.4	21.7	36.5	17.1	16.4
CaO	0.0	-	0.2	1.7	0.8	1.4	0.8	0.3	
K_2O	0.1	-	-	0.7	2.4	4.2	7.4	8.3	10.7
Na_2O	0.0	-	-	0.4	0.5	0.0	2.1	0.1	
H_2O	22.10	20.09	18.9	14.7	12.9	9.9	2.1	5.7	4.1
Accessory elements									
TiO_2	0.89		0.24	0.11	0.40		0.5*	2.60	
Cr_2O_3	0.49		-	0.00	0.49		0.5*approx.	-	
MnO	0.02		-	0.12	0.02		0.08	1.40	
NiO	-		0.28	-	0.02		0.001*approx.	-	
P_2O_5	0.00		-	-	Nil		-	-	
F	0.55		-	0.53	Nil		-	0.53	

Table 8 Chemical analyses[1] of vermiculites, hydrobiotite and biotite
(cont. from page 128)

1. Golden yellow vermiculite, most abundant type, main deposit, Transvaal Ore Co. Workings, Loolekop, Palabora, North East Transvaal, Analyst: J. C. Dunne. Listed by Gevers (1948, p. 154).

2. "Ideal" vermiculite, Gruner (1934, p. 560), arrived at by averaging seven available vermiculite analyses.

3. Vermiculite from Bare Hills, Baltimore, Md., Shannon (1928, p. 21).

4. Impure vermiculite, pale yellow to brown, Encampment, Wyoming. Analyst: W. L. Piers. Listed by Hagner (1944, p. 9).

5. Vermiculite-hydrobiotite from Gold Butte, Nevada. Analyst: G. L. Cheney (1951).

6. Hydrobiotite from Libby, Montana, Ruthruff (1941, p. 478).

7. Biotite-hydrobiotite from Gold Butte, Nevada. Analyst: G. L. Cheney (1951).

8. Black hydrobiotite from Transvaal Ore Co. workings, southwest of Loolekop. Analyst: J. C. Dunne.

9. Ideal biotite calculated from theoretical formula.

[1]Per cents are rounded off to nearest tenth.

-R. B. Ellestad found 5.86% K_2O, .011% Na_2O in Libby, hydrobiotite examined by Gruner (1934, p.559).

*Spectrographic approximations.

Table 9 Comparison of significant oxides in biotite, hydrobiotite, and vermiculite

A. Percentages of significant oxides.

Mineral	%K_2O	%MgO	%H_2O	No. analyses averaged
Biotite	10.7	16.4	4.1	Ideal
Biotite-hydrobiotite (Gold Butte, Nevada)	7.4	36.5	2.1	1
Hydrobiotites	6.4	20.2	9.4	5
Vermiculite-hydrobiotite (Gold Butte, Nevada)	2.4	19.4	12.9	1
Vermiculites	0	22.7	20.7	9

B. Ranges of averaged analyses above (excepting Gold Butte types).

Mineral	%K_2O	%MgO	%H_2O	
Hydrobiotites	3.70-8.32	17-21.8	7.5-14.7	
Vermiculites	0-0.14	19.8-26.9	18.9-22.1	

hydrobiotite and vermiculite. A notable exception to the rule is the Gold Butte hydrobiotite which contains up to 36.5 per cent MgO.

The Gold Butte types contain essentially identical percentages of accessory elements with the exception of chromium oxide which totals 0.49 per cent in vermiculite-hydrobiotite, but is almost nil in biotite-hydrobiotite. The greater chromium and/or ferrous iron content in vermiculite-hydrobiotite probably accounts for its greener color.

Chemical formulas

Chemical formulas were calculated from the two chemical analyses of Gold Butte vermiculite in table 8. Calculations are shown in table 10. The ratios of the analyses give, with reasonable accuracy, the following formulas:

Vermiculite-hydrobiotite-

$$22\tfrac{1}{2}MgO.4\tfrac{1}{2}Al_2O_3.Fe_2O_3.1\tfrac{1}{2}K_2O.30\tfrac{1}{2}SiO_2.30H_2O$$

Biotite-hydrobiotite-

$$60MgO.Al_2O_3.5Fe_2O_3.7K_2O.36SiO_2.7H_2O$$

The first formula bears similarities to that calculated for vermiculite by Gruner:

$$22MgO.5Al_2O_3.Fe_2O_3.22SiO_2.40H_2O$$

Significant differences are the increased water content and the absence of K_2O in the ideal vermiculite.

Table 10 Calculations for chemical formulas of vermiculite

A. Vermiculite-hydrobiotite

Constituent	Per cent	Atomic wts.	Proportions		Ratios	Theoretical comp.
SiO_2	43.5	60	.725	.730	.024x30	$30\frac{1}{2}SiO_2$ = 45.5
TiO_2	0.4	80	.005			
Cr_2O_3	0.5	152	.003	.109	.024x4½	$4\frac{1}{2}Al_2O_3$ = 11.2
Al_2O_3	10.6	100	.106			
Fe_2O_3	3.8	159	.024	.024	.024x1	Fe_2O_3 = 3.9
FeO	3.1	72	.043			
MgO	19.4	40	.485	.542	.024x22½	$22\frac{1}{2}MgO$ = 22.5
CaO	0.8	56	.014			
K_2O	2.4	94	.026	.034	.024x1	$1\frac{1}{2}K_2O$ = 3.5
Na_2O	0.5	62	.008			
H_2O-	8.5	18	.472	.716	.024x30	$30H_2O$ = 13.4
H_2O-	4.4	18	.244			
	97.9					100.0

B. Biotite-hydrobiotite

Constituent	Per cent	Atomic wts.	Proportions		Ratios	Theoretical comp.
SiO_2	34.5	60	.575	.581	.016x36	$36SiO_2$= 34.7
TiO_2	0.5	80	.006			
Al_2O_3	1.6	100	.016	.016	.016x1	Al_2O_3 = 1.6
Fe_2O_3	12.4	159	.078	.078	.016x5	$5Fe_2O_3$ = 12.6
FeO	1.8	72	.025			
MgO	36.5	40	.914	.953	.016x60	60MgO = 38.6
CaO	0.8	56	.014			
K_2O	7.4	94	.079	.113	.016x7	$7K_2O$ = 10.5
Na_2O	2.1	62	.034			
H_2O	2.1	18	.117	.117	.016x7	$7H_2O$ = 2.0
	99.7					100.0

Cation-exchange studies

In vermiculites the exchangeable cations are present in the interlayer structures. The interlayer cations in the Gold Butte vermiculites as determined by Barshad include the readily exchangeable ions, Ca and Mg, and the difficultly exchangeable ion, K.

Cation-exchange studies by Barshad show that the exchangeable cations of the vermiculite-hydrobiotite are 59 per cent Mg, 31 per cent K, and 10 per cent Ca. In the biotite-hydrobiotite they are 96.1 per cent K and 3.9 per cent Ca. On the basis of cation-exchange the composition of the vermiculite-hydrobiotite is 69 per cent vermiculite and 31 per cent biotite; the biotite-hydrobiotite is 96.1 per cent biotite and 3.9 per cent vermiculite.

In a specimen similar in composition to the vermiculite-hydrobiotite the ratio of the exchangeable Mg^{+2} to Ca^{+2} was found by Barshad to be 1:1 instead of 6:1 as in the first specimen. It thus appears that there is the same degree of variation between the Ca/Mg cation ratios that exists between the vermiculite-biotite ratio. Relative solubility and active mass are factors which may have influenced the Ca/Mg ratio.

Differential thermal analyses

Differential thermal analyses by Barshad serve to identify the two types of vermiculite at Gold Butte and confirm the X-ray and cation-exchange results.

Differential thermal curves of vermiculite-hydrobiotite and biotite-hydrobiotite are shown in figure 22 where they may be compared with curves of typical vermiculite and hydrobiotite that were discussed on page 120. The curve for vermiculite-hydrobiotite (curve A, fig. 22)

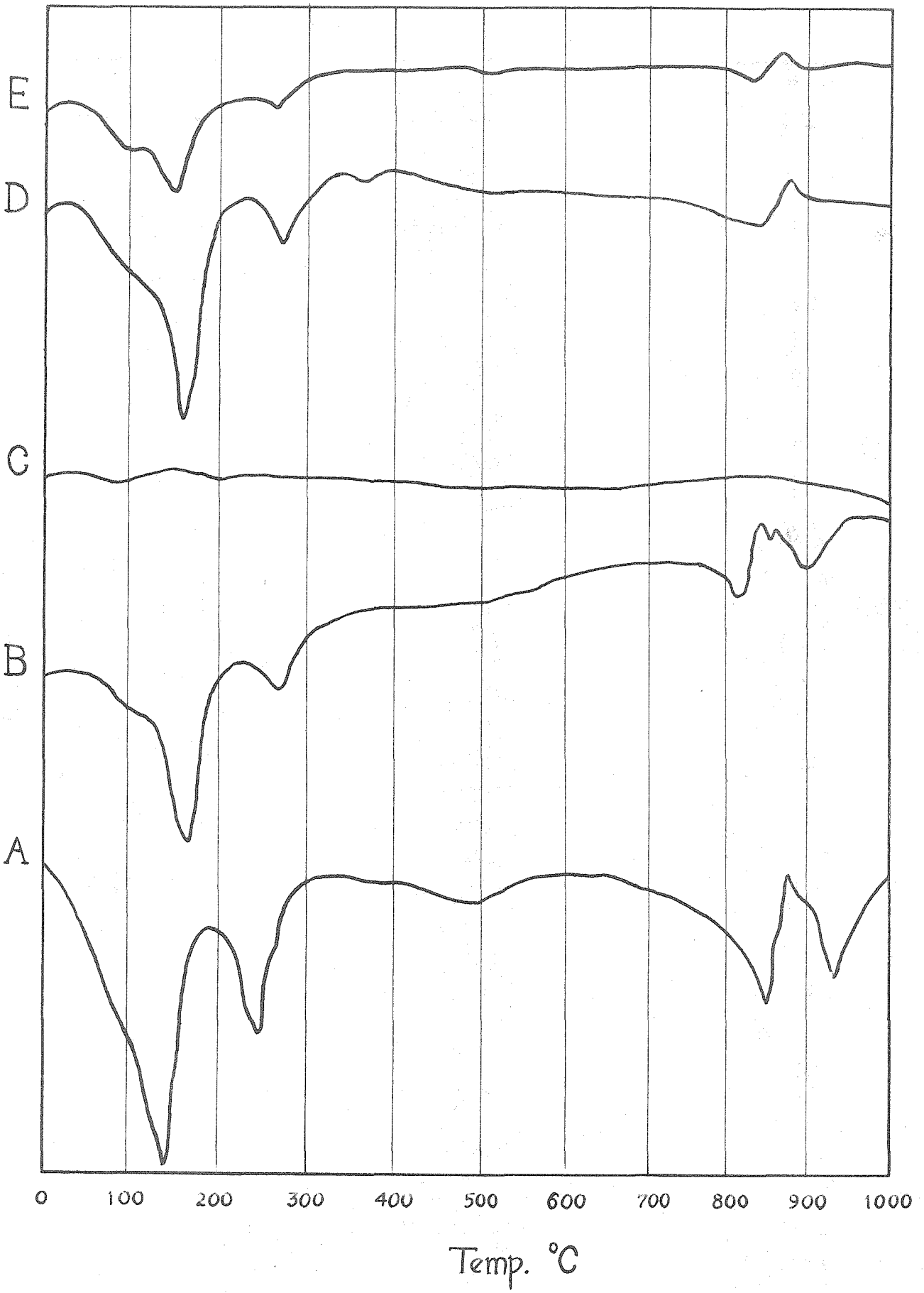

Fig. 22. Differential thermal analysis curves.
A - Vermiculite-hydrobiotite, B - Vermiculite-hydrobiotite, C - Biotite-hydrobiotite, D - Vermiculite from West Chester, Pa., E - Hydrobiotite from Morogoro, Tanganyika. A, B, and C from Gold Butte by Barshad. D and E after Walker (1951, p. 211).

shows water losses of 7.87 per cent at about 150° C. and 2.13 per cent at about 260° C., totalling 10 per cent interlayer water. The specimen is thus very similar in composition to the first vermiculite specimen.

If the three significant water losses on each vermiculite-hydrobiotite curve are expressed as percentages of the total water content, we obtain 57, 17, and 26 per cent, respectively. These percentages are not in good agreement with the theoretical percentages derived by Walker for "unbound" water (40 per cent), "bound" water (30 per cent) (see p. 121). However, if it is assumed that two of the originally "bound" water molecules in each octahedral group become "unbound" by being pressed out into a single layer and are released with the remainder of "unbound" water, some measure of agreement with the experimental data is obtained.

The curve for biotite-hydrobiotite (curve C, fig. 22) is similar to any biotite curve in which no important thermal reactions are registered. Only 0.80 per cent of interlayer water was measured.

Percentages of vermiculite in the two types, vermiculite-hydrobiotite and biotite-hydrobiotite, were calculated from the interlayer water contents by Barshad. On the basis that pure vermiculite contains 20.8 per cent interlayer water, vermiculite-hydrobiotite contains 66 per cent vermiculite and biotite-hydrobiotite contains 3.8 per cent vermiculite. These percentages are in excellent agreement with those calculated from the composition of the interlayer cations.

Heat exfoliation

Degree of heat exfoliation is the most important commercial property of vermiculite. Because few, if any, commercial laboratories have specially designed thermostatic furnaces necessary to determine the exfoliation characteristics of vermiculite under controlled conditions, R. J. Kujawa generously undertook exfoliation tests in the research laboratories of Zonolite Co., Libby, Montana, largest producer of commercial vermiculite in the United States. From such tests a reasonably accurate commercial comparison could be drawn between Gold Butte samples and Libby, Montana hydrobiotite.

A screen analysis was made and each size fraction exfoliated to assure more uniform results. Crushing of a great amount of oversized material was necessary before screening. Thus this screen analysis itself is of no particular significance. Pneumatic means were used to separate the exfoliated fractions. Each fraction was then weighed and its volume measured. Its density was calculated in grams per cubic centimeter. Densities of exfoliated Gold Butte vermiculite for three screen fractions are shown in table 11, wherein they may be compared to average densities of Libby hydrobiotite and to the limits imposed by Zonolite Co. on their expanded products.

Results indicate that Libby material has a superior expansion factor. Only the 3 and 8 mesh fractions of vermiculite-hydrobiotite appear to be within the commercial limits set by Zonolite Co. These fractions are the sizes used for loose-fill home insulation. Based

Table 11 Densities (g/cc) of exfoliated vermiculite

Sample	Tyler screen fractions		
	3(0.263in.)	8(0.093in.)	14(0.046in.)
Vermiculite-hydrobiotite	0.05	0.09	0.10
Biotite-hydrobiotite	0.09	0.15	0.17
Libby hydrobiotite (avg.)	0.06	0.08	0.08
Limits set by Zonolite Co.	0.11	0.09	0.09

Densities by R. J. Kujawa (1951)

on the density of the 8 mesh fraction, the yield of exfoliated vermiculite-hydrobiotite would be 356 cubic feet per ton.

A high degree of correlation between water content and degree of exfoliation in Gold Butte vermiculite is demonstrated in table 12. Thus water content appears to be a fairly reliable index of the degree of exfoliation to be expected within Gold Butte samples. The high density of sample no. 5 is due at least in part to foreign mineral particles adhering to exfoliated vermiculite flakes.

A relationship is inferred between the amount of water expelled during exfoliation and the degree of exfoliation. This relationship supports the view that exfoliation depends upon the rapid formation of water vapor between crystal plates.

Whenever the tightly held crystal lattice water was lost upon exfoliation, the Gold Butte vermiculite became extremely friable. Inasmuch as exfoliation is solely dependent upon the loss of interlayer water and not crystal lattice water, it seems unnecessary to raise the temperature in an expansion chamber above 500° or 600° C., if adequate heat transfer can be accomplished.

Structural formulas

Structural formulas based on the atomic positions of the elements give an accurate, useful, and general picture of related vermiculite-type minerals by indicating the structural distribution of cations and the degree of isomorphous substitution. Accordingly, formulas

Table 12 Correlation of water content and degree of exfoliation in Gold Butte vermiculite

No.	Sample	H_2O^+	Density (g/cc)
1	Vermiculite-hydrobiotite	12.9	0.09
2		9.9	0.09
3		7.3	0.09
4	Intermediate hydrobiotites	6.8	0.10
5		2.7	0.30
6		2.2	0.16
7		2.1	0.16
8	Biotite-hydrobiotite	2.1	0.15

Samples were dried below 100° C. before being analysed. Ignition losses by G. L. Cheney (1951); densities by R. J. Kujawa(1951).

were calculated from analyses in table 8, following the method advanced by Harvey (1943, p. 541-543). Cations were assigned to tetrahedral, octahedral, and interlayer positions by the following procedure:

1. All Si ions were placed in tetrahedral coordination and enough Al^{+3} and Fe^{+3} to make a total of four.

2. The remaining Al^{+3} and Fe^{+3}, together with Fe^{+2}, Ti, Cr, Na, and enough Mg ions to fill the three positions, were assigned to octahedral positions.

3. The remaining Mg and all the Ca and K ions were assigned to interlayer positions.

The calculated distribution of cations in a lattice layer of the Gold Butte types and in Gruner's ideal vermiculite are shown in tables 13 and 14.

If these same calculations are placed into the general structural formula given by Barshad (p.116) we have:

1. Vermiculite-hydrobiotite-

$$(H_2O)_x(K,Mg,Ca)_y(Al,Fe^{+3},Fe^{+2},Ti,Cr,Mg,Na)_z(Si,Al)_4O_{10}(OH)_2$$

2. Biotite-hydrobiotite-

$$(H_2O)_x(K,Mg,Ca)_y(Fe^{+2},Ti,Mg,Na)_z(Si,Al,Fe,Mg)_4O_{10}(OH)_2$$

3. Ideal vermiculite (Gruner)-

$$(H_2O)Mg_{4.44}(Al,Fe^{+3},Mg)_{3}(Si,Al)_4O_{10}(OH)_{2\ 0.337}$$

Several defects in the calculated distribution of cations for no. 1 and 2 are at once apparent. First of all, in no. 2 it is obvious that some divalent cation, presumably Mg^{+2}, must occupy sufficient

Table 13 Calculation of structural formulas of vermiculites

1. Vermiculite-hydrobiotite

Oxide	Wt.%	Metal-Si atoms	Valencies	Metal-Si atoms per 22 valencies
SiO_2	43.5	0.725	2.900	3.290
Al_2O_3	10.6	0.208	0.624	0.944
Fe_2O_3	3.8	0.047	0.141	0.214
FeO	3.1	0.043	0.086	0.199
MgO	19.4	0.481	0.962	2.170
TiO_2	0.4	0.005	0.020	0.023
Cr_2O_3	0.5	0.007	0.021	0.032
CaO	0.8	0.014	0.029	0.064
Na_2O	0.5	0.016	0.016	0.073
K_2O	2.4	0.051	0.051	0.231
H_2O	12.9	0.717		
			4.850	

2. Biotite-hydrobiotite

SiO_2	34.5	0.575	2.300	2.530
Al_2O_3	1.6	0.031	0.093	0.136
Fe_2O_3	12.4	0.156	0.468	0.687
FeO	1.8	0.030	0.060	0.132
MgO	36.5	0.905	1.810	3.980
TiO_2	0.5	0.006	0.024	0.026
CaO	0.8	0.014	0.029	0.062
Na_2O	2.1	0.068	0.068	0.299
K_2O	7.4	0.157	0.157	0.692
H_2O	2.1	0.183		
			5.009	

3. "Ideal" vermiculite (Gruner)

SiO_2	36.7	0.605	2.420	2.866
Al_2O_3	14.2	0.279	0.837	1.320
FeO				
Fe_2O_3	4.4	0.055	0.165	0.261
MgO	24.6	0.610	1.220	2.890
CaO				
Na_2O				
K_2O				
H_2O	20.09	1.110		
			4.658	

Table 14 Calculated distribution of cations in a lattice layer of vermiculite

Sample	Tetrahedral coordination				Octahedral coordination							
	Si	Al	Fe^{+3}	Σ	Al	Fe^{+3}	Fe^{+2}	Ti	Cr	Mg	Na	Σ
1	3.290	.710		4.000	.234	.214	.199	.023	.032	2.170	0.073	2.945
2	2.530	.136	.687	3.353	-	-	.132	.026	-	2.543	0.299	3.000
3	2.866	1.134		4.000	.186	.281	-	-	-	2.553	-	3.000

Sample	Interlayer ions				H_2O (mols)
	Mg	Ca	K	Σ	
1	-	.064	0.231	0.368	2.87
2	1.437	.068	0.692	2.191	.73
3	.337	-	-	0.337	4.44

Sample 1 - Vermiculite-hydrobiotite from Gold Butte, Nevada.

Sample 2 - Biotite-hydrobiotite from Gold Butte, Nevada.

Sample 3 - "Ideal" vermiculite (Gruner, 1934, p. 560).

tetrahedral positions to give a total of 4 ions. Secondly, experimental determinations of interlayer ions by Barshad do not support the calculated findings. In vermiculite-hydrobiotite some of the Mg^{+2} in octahedral coordination should be shifted to interlayer positions and some of the K^{+} should be shifted to octahedral coordination. In biotite-hydrobiotite all of the Mg^{+2} in interlayer positions should be transferred to tetrahedral and octahedral coordination.

By rectifying the above defects and bringing the calculated results into harmony with the experimental results in light of the general structural formula, the approximate structural formulas for vermiculite-hydrobiotite and biotite-hydrobiotite may be written as follows:

Vermiculite-hydrobiotite-

$$\underset{2.87}{(H_2O)}\ \underset{0.368}{(K,Mg,Ca)}\ \underset{2.945}{(Al,Fe^{+3},Fe^{+2},Ti,Cr,Mg,K,Na)(Si,Al)_4}\ O_{10}(OH)_2$$

Biotite-hydrobiotite-

$$\underset{0.73}{(H_2O)}\ \underset{0.754}{(K,Ca)}\ (Fe^{+2},Ti,Mg,K,Na)_3(Si,Al,Fe^{+3},Mg)_4\ O_{10}(OH)_2$$

ORIGIN OF VERMICULITE

Origin of other occurrences

An examination of the literature dating from 1900 reveals few inconsistencies regarding the occurrence of vermiculite and few diverse views regarding its origin. Table 15 presents this information in

Table 15 Occurrences and hypotheses of origin for vermiculite

Location	Host Rock	Author and date	Author's views on origin of vermiculite
Libby, Montana	pyroxenite stock	Pardee & Larson (1929)	Hydrothermal alteration of biotite
" "	" "	Tyler (1936)	Solutions from syenite dikes " " "
Central and northern Vermont	serpentinite belt	Phillips & Hess (1936)	Hydrothermal alteration of serpentine Source of solutions-pegmatitic
Wyoming	serpentinites, hornblendites, mafic & ultramafic schists	Hagner (1944)	Hydrothermal alteration of hornblende biotite, serpentine and possibly others Source of solutions-pegmatites
Chester, Vermont	serpentinite body	Hess (1933)	Hydrothermal alteration of serpentine Source of solutions-acid intrusives
North Carolina & North Georgia	peridotites	Hunter & Mattocks (1936)	Hydrothermal alteration from chlorites and micas, subsequently by weathering
Georgia	peridotites	Prindle & Smith (1936)	Hydrothermal alteration of muscovite, biotite and chlorite. Source of solutions-pegmatites
West Chester, Pennsylvania	serpentinite body	Larsen (1928)	Hydrothermal alteration of biotite and phlogopite Source of solutions-pegmatite
Jackson County, Colorado	hornblende metadiorite	Goldstein (1946)	Hydrothermal alteration of hornblende biotite and phlogopite. Source of solutions-pegmatites
Bare Hills, Maryland	serpentinite body	Shannon (1928)	No conclusions reached
Webster, North Carolina	dunite body	Ross & Shannon (1926)	No conclusions reached
" "	" "	Pratt & Lewis (1905)	" " "
" "	" "	Ross, Shannon & Gonyer (1928)	Hydrothermal alteration of biotite
Llano County, Texas	hornblende schists	McMillan & Gerhardt (1949)	No conclusions reached
Madagascar		Lacroix (1940)	Meteoric alteration of phlogopite
Palabora, S. Africa	pyroxenite body	Gevers (1948)	Mainly meteoric, minor hydrothermal alteration of biotite and phlogopite
Buldium, U.S.S.R.	ultramafic body	Kazantsev (1934)	Alteration from biotite

summary form. The location of the vermiculite occurrence, the host rock body, the author and date of reference, and a brief summary of the author's views concerning the origin of the vermiculite are shown. In some cases authors have merely described the occurrences and presented no theories of origin.

All references testify to the association of vermiculite with ultramafic rocks, particularly pyroxenites, hornblendites, peridotites, dunites, and serpentinites. In all deposits the ultramafic rocks have been intruded by granitic rocks. In most deposits vermiculite is found contiguous or near to pegmatites. All authors favor a secondary rather than a primary origin for vermiculite meaning that they believe it is not deposited as vermiculite, but alters from another mineral. Biotite, phlogopite, serpentine, and hornblende are believed to be the chief parents of vermiculite. Two modes of alteration appear possible, hydrothermal and meteoric.

The most important commercial deposits of vermiculite are discussed below.

The largest commercial deposits in the United States occur near Libby, Montana in a stock of alkaline rocks, two-thirds of which is pyroxenite. The pyroxenite varies in composition from unmixed pyroxene (diopside) to unmixed biotite or vermiculite. According to Pardee and Larsøn (1929, p. 8) the pyroxene has been hydrothermally altered to amphibole asbestos and the biotite to vermiculite. Tyler (1936, p. 1072) believes that a series of syenite dikes were the source of the solutions that altered the pyroxenite in whole or in part into vermiculite in one end of the deposit.

Vermiculite deposits of North Carolina and Georgia rank second to Libby in production. They occur in peridotite intrusives. Hunter and Mattocks (1936, p. 1-10) describe the vermiculite deposits of both states and consider that, "During the last stages in the cooling of the peridotites.....a continued flow of solutions.....attacked the partly cooled basic rocks altering them along the contacts and planes of weakness into chlorite, actinolite, and some biotite. Later, when the hydrothermal solutions became more watery and cooler, the solutions attacked the chlorites and micas, converting them into the various vermiculites depending on the original mineral and the degree of alteration. ....In many cases after hydrothermal activity ceased, ascending and descending meteoric water continued to vermiculize the materials."

Regarding the Georgia deposits Prindle and Smith (1936, p. 41-46) explain that the final stages of an intrusion of peridotite brought in heated mineralized waters that altered the surrounding rocks and perhaps portions of the peridotite. The alteration to vermiculite may or may not have been completed at this stage. They believe it possible that the hydrothermal alteration accomplished by the waters accompanying the intrusion of peridotite simply formed an envelope of such products as muscovite, biotite, and chlorite schists, which were later altered to vermiculite by heated waters that accompanied the intrusion of pegmatites.

Wyoming vermiculite deposits have been investigated by Wagner (1944, p. 1-47). They occur in hornblende schists, hornblendites,

and serpentinites. Hagner regards vermiculite as an alteration product of hornblende, serpentine, biotite, and possibly other minerals. The fact that the ultramafic rocks have altered to vermiculite only where intruded by pegmatites suggests to Hagner that hydrothermal solutions from the pegmatites were responsible for the formation of vermiculite and not solutions from the ultramafic bodies themselves.

Colorado vermiculite deposits of Jackson County are found in pre-Cambrian hornblende metadiorites. Goldstein (1946, p. 13-17) feels there is a direct relation between the intrusion of younger granite pegmatites and the formation of vermiculite. The pegmatites are believed to have supplied the hydrothermal solutions which attacked the hornblende and converted it to vermiculite. Goldstein writes as follows: "Biotite may or may not be an intermediate product in the alteration of hornblende to vermiculite. In the majority of samples studied the vermiculite is a tertiary product replacing biotite or phlogopite."

Outside of the United States, commercial deposits of vermiculite occur in the Ural Mountains, U.S.S.R. and in South Africa. Little information is available on the geology of the Russian deposits which are believed to be of considerable extent. Kazantsev (1934, p. 464-479) describes the alteration of vermiculite from biotite in the Buldym deposit of the Ural Mountains.

The best known deposit in South Africa exists at Loolekop, Palabora in Northeastern Transvaal and has been described by Schwellnus (1938, p. 1-27), and Gevers (1948, p. 133-173). According to Gevers

the deposit represents the largest occurrence of vermiculite in the world. It occurs in a pyroxenite mass intruded by granites and syenites. The process of vermiculitization is believed to result from supergene alteration and only minor hydrothermal alteration of biotite and phlogopite.

Significant observations concerning the origin of minor occurrences of vermiculite are as follows:

Phillips and Hess (1936, p. 333-362) show that the intrusion of pegmatites into serpentinite belts extending from Vermont to Southern Quebec was accompanied by abundant hydrothermal solutions, which attacked the serpentinites and produced around them a complex zonal arrangement of minerals including vermiculite.

Pabst (1942, p. 580-585) in a study of metamorphosed serpentine in Fresno County, California, found that vermiculite composed most of the micaceous crust of several nodules of serpentine. The vermiculite overlay a zone of tremolite.

Larsen (1928, p. 396-432) describes a number of localities where rocks made up chiefly of sodic plagioclase (albitite) or of sodic plagioclase with varying amounts of corundum (plumasite) cut ultrabasic rocks. In every case the ultramafic rock is altered to vermiculite, amphibole, and talc layers outward from the pegmatite. The vermiculite layer is made up of a vermiculite derived from biotite or phlogopite. It contains some apatite and locally talc or anthophyllite. The amphibole zone is sharply separated from the vermiculite but is gradational into the talc zone. Larsen believes that alteration by hydrothermal solutions is the correct explanation of these vermiculite occurrences.

Nickeliferous vermiculite in a dunite mass near Webster, North Carolina has been studied by Ross, Shannon, and Gonyer (1928, p. 528-545). They ascribe its origin to the alteration of biotite and suggest that nickel set free from weathering dunite has been fixed in the vermiculite by cation-exchange.

In South Madagascar phlogopite deposits Lacroix (1940, p. 353-357) showed that alteration of phlogopite to vermiculite is taking place at the present time by the action of circulating meteoric waters at normal temperature.

The distribution of vermiculite is clearly related to the land surface or the water table in other areas, also. In many South African kimberlite pipes, vermiculitic hydrated phlogopite at the surface gives way in depth to ordinary phlogopite (Gevers, 1948, p. 165). At Palabora, South Africa, between 80 and 90 feet from the surface, vermiculite passes into less highly hydrated types and finally into non-expanding biotite (Gevers, 1948, p. 165). Analyses show less water and a higher K_2O content for the latter material. Core-drilling of five vermiculite deposits in Llano County, Texas showed that vermiculite is restricted to within 65 feet of the surface. Unlike the fact that serpentinites have been found to a depth of several thousand feet below the water table, no such evidence for vermiculites has been offered.

Optical and chemical data of minerals in the ultramafic rocks

Crystallographic and chemical studies were made primarily to understand better the geochemistry of vermiculitization. If vermiculite alters from one or a number of other mafic minerals besides biotite, this process must represent a change in crystal structure, chemical composition, or both. Chemical changes in the altered zones bordering solution channelways should reflect additions and subtractions of material to and from solutions, be they hydrothermal or meteoric.

In addition, these data were collected with an intent to furnish quantitative information which has been lacking in past studies of vermiculite deposits. Views concerning the paragenesis of vermiculite have thus far been supported by no quantitative data. No attempt has been made to correlate optical properties of vermiculite with chemical composition or physical properties. Admittedly, data on the biotite-vermiculite series or other vermiculite hybrids are as yet too scarce to permit accurate correlations of optical properties with chemical composition in graphical form. Some of the following data are a step in that direction and at least permit comparison of other vermiculites, commercial and otherwise.

Winchell, among others, has continually emphasized the fact that many minerals vary considerably in composition and has published diagrams showing the relations between variations in composition and corresponding variations in physical properties of those minerals.

As expected from X-ray studies, optical properties of minerals in ultramafic rocks show considerable variation within the Gold Butte area because of isomorphism. Unfortunately, chemical analyses could not be made of all these variations revealed by optical disparities. Another liability was the fact that olivine and enstatite could not be isolated in pure form for chemical analysis. Minerals selected and prepared for chemical analysis were vermiculite-hydrobiotite, biotite-hydrobiotite, hyperesthene, diopside, hornblende, and serpentine. Powders of these important rock-forming minerals that were chemically analyzed were systematically studied and the available optical constants and the nature of the foreign material were recorded.

Procedures

Indices of refraction were measured by means of immersion media differing from each other by 0.002. Indices are considered accurate to within $\pm$0.003, thus making allowance for the accuracy of the oils. Because vermiculite is very difficult to orient with respect to X and Z vibration directions, a new "needle orientor" method suggested by Rosenfeld (1950, p. 908) was used with much success. Several innovations which served to facilitate measurement of indices by this method are recorded as follows:

1. By beveling the 0.06 inch glass needle guides, no additional plate is needed to hold the needle in position.

2. A hatpin three inches long serves as a better needle than a shorter corsage pin and facilitates turning of the spherical knob. A three inch slide base is best suited to the larger needle.

3. Rotation of the needle may be impeded if the needle point is not centered. By forming a waterglass ball on the point this difficulty is eliminated.

Optic angles were measured by three methods (1) estimating the angle from the amount of curvature of the hyperbola in sections cut normal to an optic axis (2) computing the angle from the three indices of refraction according to the equation devised by Wright (1951, p. 543-556) (3) measuring on the universal stage. The method or methods used are indicated under each mineral.

Errors in the optical work may be due to incorrect measurements, presence of impurities, zoning, strain, and heterogeneity of specimens selected. Anomalous values are discussed under each mineral species.

Crystals easily separable from their containing rocks were crushed, lightly ground, and examined under the binocular microscope. A crude separation of undesirable material was made with a needle. The purest material was then studied under the petrographic microscope where further impurities, if apparent, were rejected in a similar manner or by using heavy liquids. Fines and adhering dust were removed by washing and decanting. Vermiculite plates were cleaned with a damp brush. Suitable samples were chemically analyzed by G. L. Cheney.

Errors in the chemical analyses may be of three types:

1. Lack of homogeneity in the minerals, especially in the cases of vermiculite, enstatite-hypersthene, and hornblende. This is one of the chief sources of error.

2. Analytical errors.

3. Contamination of the minerals by foreign substances.

Chemical analyses are believed accurate to the following values: constituents over 5 per cent - $\pm$0.02%; constituents between 1 and 5 per cent-$\pm$0.10; constituents below 1 per cent - $\pm$0.05.

An admixture which could not be entirely removed from all mineral samples was a negligible quantity of amorphous-looking material which was determined chemically to be caliche. This would be recorded in chemical analysis principally as CaO and CO_2. Only in one vermiculite is CO_2 of significant amount, 2.2 per cent. Because CaO in the same analysis is 0.78 per cent, only 0.6 per cent of the CO_2 may be allotted to CaO, leaving 1.6 per cent. This excess could possibly be present in combination with MgO, in which case 1.4 per cent MgO is tied up as carbonate. However, this is not considered likely, because the caliche effervesces freely in dilute hydrochloric acid and contains only 10 per cent $MgCO_3$ in chemical analysis.

Small calcite inclusions in hornblende crystals were removed with acid before the hornblende was powdered.

Specific gravity was measured by means of the pycnometer. Values are believed accurate to at least the first decimal place.

If not otherwise indicated, the specific gravity values were determined by the writer.

Mineral data

Vermiculite

(1) Biotite-hydrobiotite

Class	- Biaxial
Sign	- (-)
2V	- 9° (Univeral Stage)
Dispersion	- (weak)
Refractive indices	- α = 1.568
	β, γ = 1.607
Birefringence	- 0.039
Absorption	- $Z = Y > X$
Pleochroism	- X - nearly colorless
	- Z = yellowish brown to tan to orange

Composition-

	wt.%
SiO_2	34.46
Al_2O_3	1.60
FeO	1.80
Fe_2O_3	12.40
CaO	0.80
MgO	36.50
Na_2O	2.06
K_2O	7.44
MnO	0.05
Cr_2O_3	0.08
CO_2	0.18
H_2O	2.14
total	99.51

Sp. Gr. 2.37
Analyst: G. L. Cheney

(2) Vermiculite-hydrobiotite

Class	-Biaxial
Sign	-(-)
2V	-very small
Dispersion	-(weak)
Refractive indices	- α = 1.528
	-β, γ = 1.550
Birefringence	-0.022
Absorption	-Z= Y>X
Pleochroism	-X - nearly colorless
	-Z = Y- yellowish brown

Composition-

	wt.%
SiO_2	43.50
Al_2O_3	10.56
FeO	3.10
Fe_2O_3	3.76
CaO	0.78
MgO	19.44
Na_2O	0.50
K_2O	2.40
MnO	0.02
Cr_2O_3	0.49
NiO	0.02
TiO_2	0.40
P_2O_5	Nil
CO_2	2.20
F	Nil
H_2O	8.52
H_2O	4.38
total	100.07

Sp. Gr. 2.26
Analyst: G. L. Cheney

The variety of vermiculite in the perknites is considerably more biotitic than that in the peridotites. This difference reflects the higher percentage of iron and potassium and the lower percentage of magnesium and water, as compared with those within peridotites,

as well as the less intense alteration of the perknites. Chemically, the alteration of biotite to vermiculite is accompanied by a loss of iron, preceded by oxidation of ferrous to ferric, loss of potassium, and a gain in water. This is shown by the analyses on page 123.

Refractive indices and birefringence of all vermiculites whose optical constants are recorded in the literature are shown in table 16. The relation of specific gravity, refractive index, and per cent iron is treated in table 17. All minerals in table 16 that are listed below the vermiculite from Fresno, California are actually hydrobiotites, with the exception of the nickeliferous vermiculite from Webster, North Carolina. From the data available the range of refractive indices for expandable vermiculites is α = 1.525-1.568 and β,γ = 1.545-1.607; the range of birefringence is 0.020-0.039; the range of specific gravity is 2.15-2.78. These ranges may be compared to the ranges found at Gold Butte. Refractive indices are α = 1.528-1.568, β,γ = 1.550-1.607; birefringense is 0.022-0.039; specific gravity is 2.37-2.40. Varieties of vermiculite with refractive indices between the extremes given were confirmed. Thus it appears that Gold Butte vermiculites nearly run the gamut of possible optical properties. It also appears that a change from biotite to vermiculite involves a decrease in specific gravity, refractive indices, and birefringence and a marked color change from a dark to a lighter color (usually dark brown to golden yellow).

Optical characteristics of vermiculite may be summarized as follows: All are optically negative with a small 2V. The acute

Table 16 Refractive indices and birefringence of vermiculites

Refractive indices α	Refractive indices β, γ	$\gamma - \alpha$	Mineral, locality and examiner
1.525	1.545	0.020	Vermiculite, Bare Hills, Md.,Shannon
1.528	1.550	0.022	Vermiculite-hydrobiotite, Gold Butte, Nev., Leighton
	1.552		Vermiculite, Fresno, Calif., Pabst
1.537	1.557	0.020	Jefferisite, Delaware County, Pa.,Larsen
	1.558		Hydrobiotite, Loolekop, S. Africa, Gevers
1.540	1.560	0.020	Vermiculite,Corundum-Hill, N.C., Larsen
1.542	1.573	0.031	Nickeliferous vermiculite, Webster,N.C.,Ro
1.545	1.582	0.037	Hydrobiotite, Haddam Neck, Berman
	1.606		Hydrobiotite, Loolekop,S. Africa, Gevers
1.560	1.607	0.047	Vermiculite, Glenrock,Wyoming, Hagner
1.561	1.581	0.020	Jefferisite, West Chester,Pa.,Larsen
1.568	1.607	0.039	Biotite-hydrobiotite,GoldButte, Nev.,Leigh

Table 17 Correlation of specific gravity, refractive index, and total iron of vermiculites

Specific gravity	β, γ	%Total iron	Mineral, locality, and examiner
2.15	1.558	4.4	Hydrobiotite, Loolekop,S. Africa, Gevers
2.29	1.552	-	Vermiculite,Fresno, Calif., Pabst
2.37	1.550	6.9	Vermiculite-hydrobiotite,Gold Butte,Nev., Leighton
2.40	1.607	14.2	Biotite-hydrobiotite,Gold Butte,Nev., Leighton
2.67	1.606	15.6	Hydrobiotite,Loolekop,S.Africa, Gevers
2.78	1.582	-	Hydrobiotite, Haddam Neck, Berman
-	1.607	16.9	Hydrobiotite, Wyoming, Hagner

bisectrix (X) is nearly normal to the perfect basal cleavage. Pleochroism is strong, usually increasing with the iron content. Refractive indices and birefringence are extremely variable.

Optically, vermiculites may be confused with chlorites and biotites. The optical differences between chlorites and vermiculites are that (1) vermiculites are all optically negative, (2) the birefringence of chlorite is considerably less, (3) the chlorites are usually green, whereas vermiculite, unless nickeliferous, is generally not green under transmitted light. Vermiculites differ optically from biotites by generally having a lower birefringence and lower indices of refraction. However, as can be seen by table 16 the two minerals merge into each other.

The biotite-vermiculite series should not be considered as mixtures of end member "molecules". This would be inconsistent with present ideas of isomorphous cation-exchange in crystal structures. Correlation between chemical composition and optical constants should be viewed in this light.

From scanty data it seems that iron content is the chief control of refractive index. A vermiculite high in refractive index is also high in iron. Because iron increases in passing from true vermiculite to hydrobiotite to biotite, the refractive index also increases in that direction. The comparative influence on the refractive index of iron in a higher state of oxidation to iron in a lower state is not known, because in all chemical analyses of vermiculite iron in a higher state predominates.

Effects of admixtures are difficult to assess because few vermiculites contain appreciable amounts of these elements and in many analyses these elements have not been sought. However, Shannon believes (1928, p. 4) that nickel increases the refractive indices and birefringence. This is confirmed from inspection of the chemical analysis of nickeliferous vermiculite from Webster, North Carolina and inspection of table 16. Though there is no direct evidence of TiO_2 and Cr_2O_3 increasing the refractive index and specific gravity of the Gold Butte vermiculite-hydrobiotite, this is suspected because of the extremely low iron content and the somewhat high specific gravity.

Hypersthene

Optical properties

Class - Biaxial
Sign - (-)
2V - 55° (calculated)
Dispersion - (weak)
Refractive indices - In altered cortlandtite
α = 1.690
β = 1.701
γ = 1.704
Birefringence - .014 (moderate)
Absorption -
Pleochroism - X= red to brownish pink
Y= pink to yellowish to colorless
Z= pale green

Composition-	wt.%
SiO_2	54.14
Al_2O_3	1.88
FeO	4.60
Fe_2O_3	17.04
CaO	0.56
MgO	21.58
K_2O	Trace
total	98.80
MnO	approx. 0.1%

Sp. Gr. 3.35 - Analyst: G. L. Cheney

Correlations of optical and chemical data for orthopyroxene by six different authors do not differ materially (Poldervaart, 1950, p. 1075), hence the determination of the composition of orthopyroxenes by optical means appears to be reasonably accurate.

According to Larsen and Berman (1934, p. 241) the most reliable optical means of determining composition is by refractive index. Compositions indicated by plotting indices of refraction on a diagram prepared by Poldervaart (1950, p. 1066) are compared below with compositions determined by chemical analysis.

Composition from Poldervaart chart			Chemical analysis		
oxide		wt.%			wt.%
SiO_2	-	55	SiO_2	-	53.1
FeO	-	20	$FeO-Fe_2O_3$	-	21.6
MgO	-	25	MgO	-	21.6

Alumina, amounting to 1.88 per cent, appears to be the only important admixture which might cause the slight disparity between the true and theoretical chemical compositions.

Hess believes that all natural orthopyroxenes contain about 1.5 per cent CaO (Poldervaart, 1950, p. 1076). The present analysis reveals only 0.56 per cent CaO.

Diopside (from altered cortlandtite)

Optical properties

Class	- Biaxial
Sign	- (+)
2V	- 58° (Universal Stage) and 59° (calculation)
Optic angle	- 39° (distinct)
Refractive indices	- α = 1.667
	β = 1.674
	γ = 1.696
Birefringence	- 0.028-0.029 (strong)
Color	- faint green tint
Pleochroism	- none

Composition-

	wt.%
SiO_2	51.46
Al_2O_3	0.54
FeO	1.58
Fe_2O_3	9.44
CaO	21.68
MgO	13.98
K_2O	Trace
total	99.68

Sp. Gr. - 3.34
Analyst: G. L. Cheney

Most optical property curves for the diopside-hedenbergite series draw largely from data on synthetic specimens. A recent diagram published by Hess (1949, p. 641) includes 13 new chemical analyses of natural clinopyroxenes belonging to this series, four lying within the diopside zone.

If plotted on this diagram the extinction angle, optic angle, specific gravity, and α and γ indices of refraction establish compositional values that are in close agreement with those in chemical analysis. The average graphical composition is that of a true diopside containing 5 per cent Fe atoms of the total Ca-Mg-Fe,

the three major variables under consideration. On the other hand the chemical analysis contains approximately 16 per cent Fe atoms. This is a sufficient number of Fe atoms for salite, yet the optical properties which were determined agree with those plotted for diopside.

Either much of the iron is an impurity, or Fe^{+3}, unlike Fe^{+2}, has little effect on the optical properties. No impurities such as exsolution lamellae or limonite stains were noted. According to Hess (1949, p. 626) if the chemical analysis is accurate and the material analyzed is pure, the total number of Si and Al ions will come within about 2 per cent of equaling the total of other ions, excluding O ions. The ratio of these two groups is 870:872, evidence of a completely satisfactory analysis.

This is the first analysis of a pyroxene known to contain a greater number of Fe^{+3} than Fe^{+2}. Although Fe^{+3} is included in the total Fe of the diagram by Hess, the effect of Fe^{+3} on optical properties is not the same as Fe^{+2} as pointed out by him. From analyses 1 and 2 by Hess it seems that Fe^{+3} does not increase the indices in diopside nearly as much as Fe^{+2}. Nevertheless, an almost negative effect on refractive indices measured by this writer is difficult to explain. It may be that analyses are not numerous enough to draw reliable curves. At least there seems no reason to suspect that all optical properties are incorrect.

The ratio of Ca:Mg:Fe recalculated to 100 per cent is $Ca_{44.3}$ $Mg_{39.7}$ $Fe_{16.0}$. Hess states that the per cent of Ca (of total Ca-Mg-Fe)

is close to 50 throughout the diopside-hedenbergite series. The number of Ca ions, 44.3 per cent, is well within the range published by Hess. The average diopside analyzed by Hess is $Ca_{47.5}\ Mg_{48}Fe_{4.5}$; the average salite analyzed is $Ca_{48.5}\ Mg_{26.5}\ Fe_{25}$.

Hornblende (from perknite)

Optical Properties

Class - Biaxial
Sign - (-)
2V - 82°30' (calculated)
Dispersion -
Refractive indices- $\alpha = 1.650$
$\beta = 1.659$
$\gamma = 1.666$
Birefringence - 0.016 (moderate)
Adsorption - $X<Y<Z$
Pleochroism - variable shades of green

Composition-

	wt.%
SiO_2	43.86
Al_2O_3	13.54
FeO	8.06
Fe_2O_3	7.20
CaO	12.70
MgO	6.77
Na_2O	5.46
total	97.59

K_2O	-- approx.	0.5
TiO_2	"	0.5
Mn	"	0.1
Cr	"	0.1

Sp. Gr. 3.11
Analyst: G. L. Cheney

The hornblende series is well-known for showing considerable variation in composition. The principal chemical feature which characterizes the series is the presence of both Ca and Na, the former predominating (Larsen and Berman, 1934, p. 220). So many departures are noted in the tables of physical and chemical properties

of calciferous amphibole by Winchell (1945, p. 38-43) that it does not seem worthwhile attempting any correlation. No property or set of properties appears anomalous in the light of these tables.

Serpentine

Optical Properties

Class	- Biaxial
Sign	- (-)
Refractive Indices	- 1.56-1.57
Birefringence	- low
Color	- tan

Composition-	wt.%
SiO_2	40.10
Al_2O_3	0.44
FeO	0.72
Fe_2O_3	0.32
CaO	1.08
MgO	40.63
K_2O	0.10
CO_2	0.10
H_2O	15.47
H_2O	0.63
total	99.59

Sp. Gr. 2.32
Analyst: G. L. Cheney

Serpentine is considered by most mineralogists as the end member of the chlorite series. It is the Mg-rich, Fe- and Al-free end of the series. It includes antigorite and its dimorph chrysolite, although the latter is orthorhombic and is not usually included within the chlorite series. Both may be distinguished from the rest of the chlorite series by lower indices of refraction and the absence of

pleochroism. Most, if not all the serpentine present is antigorite which can be distinguished from chrysolite by its optic sign and lamellar habit.

The chemical analysis is in close agreement with the theoretical formula for serpentine, $Mg_3Si_2O_5(OH)_4$, which contains 43 per cent MgO, 44.1 per cent SiO_2, and 12.9 per cent H_2O. The 16 per cent of H_2O is unusually high.

Olivine (Forsterite)

Optical Properties

Class	- Biaxial
Sign	- (-)
2V	- 85° (graphical plot-Poldervaart and estimate from optic axis figure)
Refractive indices	- β = 1.650
Birefringence	- strong
Colorless	

The solid solution series of fayalite-forsterite has been studied thoroughly (Deer and Wager, 1939, p. 18-25; Poldervaart, 1950, p. 1066-1079), and variations of optical properties with composition are known with accuracy. The composition of the olivine was found by determining the optic axial angle and refractive index and observing their position on a composition-optical diagram prepared by Poldervaart (1950, p. 1073). Chemical results for both optical determinations were about the same. The olivine appears to be pure forsterite with no more than 5 per cent of the fayalite molecule. In view of the quantity of secondary iron associated with olivine and serpentine in thin section, an olivine member richer in iron is expected. If calcium were an important

admixture, it would tend to lower the index of refraction somewhat (Larsen and Berman, 1934, p. 829), thus lowering the apparent iron content on the diagram. Allowing for 5 per cent CaO, which is probably much too high, extrapolation shows more than 5 per cent iron is probably not present and certainly no more than 10 per cent.

Plagioclase (chief variety in ultramafic rocks)

Optical Properties

Class	- Biaxial
Sign	- (-)
2V	- 80-90° (estimated)
Refractive indices	- α = 1.563
	γ = 1.574
Birefringence	- 0.011
Maximum extinction angle	- 39° (Michels-Levy method)
Composition	- An_{65-70}

This mineral series has been studied in more detail than any other. Correlations of optical properties with chemical composition in simple plagioclase members should be very accurate. Optical data assembled above agree closely with one another and with values given by curves plotted by Kennedy (1941, p. 568) and Poldervaart (1950, p. 1069). All fall within the compositional range An_{65-70} with the exception of the birefringence, which is within the limits of possible errors derived from measurement of refractive indices.

The chemical composition, based upon optical properties, is as follows in wt. per cent:

SiO_2----50-52
Al_2O_3---31-32
CaO-----14-15
Na_2O---- 3-4

Because plagioclase was an accessory constituent of the ultramafic rocks and because the chemical composition of simple plagioclase members is readily ascertained from optical properties, chemical analysis seemed unnecessary. In addition, zoning and intergrowths are absent and provide no problem.

These factors may produce anomalous optical properties, the presence of K_2O, excessive Al_2O_3, and admixtures of Fe, Ba and Sr. A K_2O content up to 2 per cent apparently does not affect the optical constants of plagioclase (Chudoba and Engeld, 1937 by Poldervaart, 1950, p. 1070) and, therefore, is probably not an important factor. Excessive Al_2O_3 is apparently not common in normal plagioclase (Ferrier, 1930 by Poldervaart, 1950, p. 1070) and, therefore, is probably not present here. Significant admixtures of Fe, Ba, and Sr are absent in other basic minerals and so are probably also absent in plagioclase. Inversion to low temperature modifications of plagioclase was shown by Tuttle and Bowen (1950, p. 572-583) to extend only as high as An_{35}; therefore, this phenomenon would have no effect here.

Origin of Gold Butte vermiculite

The minerals of the primary unaltered ultramafic rock are thought to have been olivine, diopside, enstatite-hypersthene, hornblende, biotite, and magnetite-chromite. This conclusion is based on the mineralogy of the least altered rocks in the area, and on comparison

with the normal composition of ultramafic rocks of similar composition and modes of origin.

Inasmuch as vermiculites are associated with only mafic minerals, they must have formed at theexpense of one or more of them. From table 18 it is apparent that chemical additions and subtractions are necessary to produce vermiculite-hydrobiotite, biotite-hydrobiotite, or a vermiculite intermediate between the two from each of the mafic minerals chemically analyzed. However, if the bulk composition of all mafic minerals in certain proportions is considered, only a small amount of silica must be subtracted and considerable potassium and water added to give either type of vermiculite. This suggests that vermiculite has altered from biotite by the process of cation-exchange or has formed from a combination of hornblende, hypersthene, diopside, serpentine, biotite, and possibly other mafic minerals with water being added and silica subtracted.

Trace elements shown in table 19 supply no clues as to which minerals did or did not take part in the alteration. All minerals contain at least traces of the following minor constituents: chromium, titanium, manganese, barium, nickel, vanadium, strontium, boron, copper, and cobalt. Zirconum and gallium are found in all except diopside and hypersthene. Biotite-hydrobiotite is the only mineral containing lead.

Because the majority of the peridotites are sufficiently weathered to crumble readily in the hand, thin sections could not readily be made. Hence samples were ground and examined in immersion media under the

Table 18 Comparison by weight and volume of compositions of mafic minerals

	Weight per cent					
Oxide	1	2	3	4	5	6
SiO_2	40.3	34.5	43.9	53.1	51.5	40.1
Al_2O_3	11.8	1.6	13.5	1.9	0.5	0.4
FeO	0.7	1.8	7.2	4.6	1.6	0.7
Fe_2O_3	10.3	12.4	6.1	17.0	9.4	0.3
MgO	17.4	36.5	6.8	21.6	14.0	40.6
CaO	2.6	0.8	12.7	0.6	21.7	1.0
K_2O	3.2	7.4	0.5*	-	-	0.1
Na_2O	1.0	2.1	5.5	-	-	-

	Mg/cu cm x wt. per cent x 10					
Oxide	1	2	3	4	5	6
SiO_2	912	817	1370	1760	1720	928
Al_2O_3	266	38	420	64	16	9
FeO	16	43	224	154	53	16
Fe_2O_3	232	294	252	570	310	7
MgO	390	865	212	725	467	942
CaO	59	19	395	20	725	23
K_2O	72	175	16*	-	-	2
Na_2O	23	50	171	-	-	-

*approximate from qualitative spectrograph

(1) Vermiculite-hydrobiotite. Sp. Gr. 2.26
(2) Biotite-hydrobiotite. Sp. Gr. 2.37
(3) Hornblende. Sp. Gr. 3.11
(4) Hypersthene. Sp. Gr. 3.35
(5) Diopside. Sp. Gr. 3.34
(6) Serpentine. Sp. Gr. 2.32

Table 19. Minor constituents of mafic minerals*

	A	B	C	D	E
Ba	0.05	0.1	0.001	0.001	0.001
Mn	0.01	0.05	0.1	0.05	0.1
V	0.005	0.01	0.001	0.001	0.005
Zr	0.01	0.01	-	-	0.01
Sr	0.005	0.01	0.001	0.005	0.05
B	0.001	0.001	0.001	0.001	0.001
Pb	-	0.001	-	-	-
Ga	0.001	0.001	-	-	0.001
Cu	0.001	0.001	0.001	0.001	0.001
Ni	0.01	0.001	0.005	0.005	0.005
Co	0.001	0.001	0.001	0.001	0.001

*Qualitative spectrographic analyses by T. C. McBurney.

Quantities reported are approximately accurate to the nearest factor of ten.

A - Vermiculite-hydrobiotite

B - Biotite-hydrobiotite

C - Hypersthene

D - Diopside

E - Hornblende

petrographic microscope. Microscopic study of these specimens from a number of locations was made to determine the average compositions of altered specimens. Comparison of the mineralogy of unaltered and altered rocks yields the following results in volume per cent:

Constituent	Unaltered	Altered
Serpentine	5 - 10	20
Olivine	30	-
Hornblende-pargasite	10-15	15
Actinolite	0	10
Diopside	20	5
Vermiculite	0	40
Biotite	10	0
Hypersthene	0	5
Enstatite	15	-
Magnetite-Chromite	3-4	2
Calcite-Magnesite	-	3
Other accessories	1%	2%

The most prominent mineralogic changes in the altered specimens are the addition of vermiculite, calcite-magnesite, actinolite, and an iron-rich enstatite (hypersthene), the deletion of biotite, olivine, and enstatite, the decrease in amount of diopside and magnetite-chromite, the increase of serpentine. Three of these changes are especially significant in the formation of vermiculite.

1. Minerals in addition to primary biotite must have altered to vermiculite.

2. Higher percentages of serpentine in less altered specimens indicate that serpentine has undergone alteration to vermiculite or has been extracted and concentrated in other places.

3. As indicated by thin section study and supported by quantitative and qualitative microscopic study of crumbled specimens, pyroxene has altered to amphibole and serpentine.

The chemical changes shown in table 20 shed light on the nature of the mineralogic changes. The most notable changes involve both subtraction and addition of elements. From the unaltered material iron and the alkalies have been leached, and water and carbon dioxide have been added. The constancy of MgO is noteworthy. These changes suggest supergene rather than hypogene alteration. There is no surface indication of the fate of the material leached from the rock.

If the chemical data are significant the following mineralogic inferences can be made:

1. No new MgO was introduced during vermiculitization.
2. Most of the K_2O has been subtracted from biotite.
3. Formation of vermiculite and serpentine account for the increased water content in the altered rock.
4. The source of the iron that has been extracted is not restricted to any one mineral. It has come from some combination of magnetite-chromite, biotite, diopside-hedenbergite, and olivine.

Table 20 Chemical changes in alteration of peridotite

Oxide	(1) Wt.%	(1) mg/cu cm[1]	(2) Wt.%	(2) mg/cu cm[1]
SiO_2	44.6	1390	43.6	1370
Al_2O_3	2.5	79	4.2	123
FeO	0.8	25	1.2	34
Fe_2O_3	19.8	617	10.5	297
MgO	20.3	640	21.8	617
CaO	4.9	154	4.7	133
K_2O	4.3	135	0.1	3
Na_2O	2.0	63	0.7	20
Cr_2O_3	0.25	8	0.5	14
CO_2	0.08	3	2.7	76
H_2O-	0.19	6	4.4	124
H_2O-	0.20	6	5.5	156
Total	99.72		99.9	

1. Unaltered material, 250 feet NNE of cabin. Bulk density-3.15.

2. Altered material, average composition of samples studied under microscope. Bulk density - 2.83.

[1]Milligrams per cubic centimeter is equal to the weight per cent multiplied by the bulk density times 10.

5. If serpentinization occurs without substantial change in volume, it appears that the formation of serpentine involves the removal in solution of MgO and SiO_2. Because the amount of MgO has decreased only slightly in altered peridotites, some MgO must have entered another alteration product, the most likely one being vermiculite.

As stated earlier, vermiculite ~~present~~ in the perknites is a biotite-hydrobiotite. It appears that biotite-hydrobiotite has formed directly from biotite. Sufficient K_2O to form biotite-hydrobiotite is not present in any other primary mineral, and biotite-hydrobiotite is a stage of alteration not far advanced beyond biotite.

Could not biotite-hydrobiotite have been deposited as such? A serious objection is that no interlayer water can be retained above 300° C., and that much of the total water content escapes at temperatures as low as 105° to 110° C. upon prolonged heating. Temperature of formation is thus an important factor. Under magmatic conditions only crystal lattice water can be retained; hence hydrobiotite cannot form. But if the environment is epithermal, hydrobiotite could theoretically be deposited, allowing that K_2O is somewhat scarce and that all essential constituents are present in sufficient amounts. Strong testimony against such an origin is furnished by the random interstratification of biotite and vermiculite layers, the implication being that the mineral has developed vermiculite layers through the alteration of an initial pure biotite structure. Furthermore, inasmuch as some of the biotite-hydrobiotite in the perknites is

early and probably magmatic, at least a portion of the mineral must have altered from biotite. Considering the pronounced cation-exchange property of vermiculite and the likelihood of reversals in the exchange process under changing environmental conditions, the concept of direct alteration to the present composition of hydrobiotite would be an over-simplification of the case.

Because the relatively pure specimens of vermiculite occur in or contiguous to serpentinized rocks, vermiculitization is likely related to serpentinization. Field relations reveal that serpentinization manifests itself wholly within the ultramafic rocks. Serpentinized rock is not restricted to the core of the ultramafic bodies as has been reported (Gevers, 1948, p. 160). It shows a haphazard distribution unrelated to rock contacts. However, it is nowhere, as far as can be determined, in direct contact with large pegmatites injected into the ultramafic rocks.

In the light of laboratory investigations by Bowen and Tuttle (1949, p. 439-460) serpentinization is not a late magmatic or deuteric process, but rather a process involving hydrothermal solutions derived from nearby sediments or from intrusive bodies of granitic magma. Facts brought out by Bowen and Tuttle which seem applicable here are as follows:

1. Above 500° C. olivine-enstatite mixtures cannot be converted to serpentine by any means.

2. Serpentine can form from olivine-enstatite mixtures under the action of pure water.

3. Replacement of both olivine and enstatite precludes the possibility of autometasomatism.

Therefore, it seems reasonable to assume that serpentinization of the peridotites in question has not been produced by autometasomatism but by low temperature highly aqueous solutions. Because nearby granitic and pegmatitic intrusions are available as a source of water, serpentinization is believed due to the introduction of magmatic water into the ultramafic mass. Hydrothermal activity is so intimately associated in time and space with pegmatitic activity that it can be differentiated only on the basis of its mineral products such as serpentine.

Serpentine not only occurs as a constituent of the periodtite proper, but also as megascopic veins which cut weathered peridotite. A typical vein exposed in a trench 150 feet east of the cabin contains a central zone, 1½ to 3 inches wide, of almost pure serpentine. The serpentine is pale green, fine- to medium-grained, and flaky. Sharply in contact on both sides are dark green zones half an inch to one inch wide. Dark brown vermiculite is the most abundant mineral in this zone, comprising over 60 per cent by weight. Serpentine averages 30 per cent and actinolite 10 per cent. The texture of this zone is similar to that of the central zone. Progressing outward the vermiculite-serpentine-actinolite zone grades into typical altered peridotite within a distance of one inch. Discontinuous hypersthene-rich seams of relic country rock are in places present between the two inside zones, showing that wall-rock has been replaced and that we are not dealing with a simple fissure-filling. From the essentially matching "walls" of the vein, the symmetry of the two sides, and the changing mineralogy

and chemical composition outward from the center, it seems that a portion of the central serpentine zone was once an open conduit.

Obviously, there has been a rearrangement of material, taking place within the peridotite bodies. Some of the serpentine whose absence in the altered peridotite was unaccounted for, has apparently moved in solution and been redeposited in veins which transect the former altered mass. Under solution attack, the walls of the solution channelway have altered to a different mineral assemblage. Thus successive zones of alteration have formed outward from the solution channel.

Assuming that the altered zones were formerly of the same chemical composition, chemical analyses in table 21 reveal the chemical changes which have taken place. Some transfer of material has occurred between zones. The most conspicuous changes are the addition of MgO and H_2O into the wall-rock, and the subtraction of iron and silica from the wall-rock.

The space relations of mineralogic changes induced by solutions are determined by a number of variables, to wit: the nature of the solution and the wall-rock, the temperature-pressure relations, and the character of the fissure. Examining these variables one by one, the following points are inferred:

1. Inasmuch as MgO increases outward and serpentine is the only mineral stable in the particular chemical environment of the central zone, solutions must have been Mg-rich. They may be regarded

Table 21 Chemical changes in alteration by serpentine vein.

Oxide	(1) wt.%	(1) mg/cu cm[1]	(2) wt.%	(2) mg/cu cm[1]	(3) wt.%	(3) mg/cu cm[1]
SiO_2	40.1	930	36.3	820	43.6	1230
Al_2O_3	0.4	9	3.6	81	4.2	119
FeO	0.7	16	1.5	34	1.2	34
Fe_2O_3	0.3	7	0.2	5	10.5	297
MgO	40.6	940	37.7	851	21.8	617
CaO	1.1	26	5.8	131	4.7	133
K_2O	0.1	2	1.0	23	0.1	3
CO_2	0.1	2	0.9	20	2.7	76
H_2O-	15.5	360	11.0	25	5.5	156
H_2O-	0.63	15	1.0	23	4.4	124

1. Serpentine in central vein zone. Bulk density 2.32.

2. Vermiculite-serpentine-actinolite zone. Bulk density 2.26.

3. Rock unaffected by vein solutions. Bulk density 2.63.

[1]Milligrams per cubic centimeter is equal to the weight per cent multiplied by the bulk density times 10.

as the product of deliquescence of the ultramafic rocks under the influence of aqueous liquids migrating out from intrusive magmas. They were probably dilute in their early stages, but later became relatively immobile.

2. The wall-rock was ultramafic with a chemical composition indicated presumably by the least altered rock outward from the channel. Only a small width on both sides of the channel has been affected.

3. Temperature was always less than 500° C. Stress was not active during mineral formation as shown by the random orientation of serpentine and vermiculite flakes.

4. Seams of relict country rock limit the width of the former channel to three inches, which is the average maximum width of the central zone. As a result, most of the serpentine in the central zone may not be a replacing mineral, but rather a fissure-filling. Furthermore, the minerals just outside the central zone have replaced minerals of the wall-rock.

The amount of material that has migrated to and from the zones cannot be estimated, because the width of the former channelway is unknown. Nevertheless, a few qualitative conclusions are in order.

Symmetrical zones of alteration such as these seem explainable only by diffusion of material through pore solutions. This movement by diffusion depends upon a concentration gradient induced principally

by differences of either chemical composition or temperature. A nearly isothermal condition probably prevailed because of the relatively rapid heating of the wall by hydrothermal solutions and nearby magmas. Composition gradient is believed to have been the chief control of diffusion.

If silica is to be removed from the wall-rock, it is only necessary that the pore solution in the wall-rock be more nearly saturated with silica than the solutions moving through the fissure. Because the solutions we are dealing with are Mg-rich, upon passing through an iron-rich rock cation-exchange would be promoted, the Mg^{+2} of the solution moving outward and perhaps proxying for Fe^{+2} which moves inward. Inasmuch as the replaced rocks originally contained CaO, actinolite and serpentine would form. As the solution becomes supersaturated with MgO and relatively immobile, serpentine would be precipitated within the fissure. Diffusion of MgO outward would take place until all the MgO in the fissure had precipitated or until the MgO concentration in the wall-rock was equalized.

The formation of actinolite is usually assumed to be a rather high temperature hydrothermal phenomenon. This suggests that vermiculite was formed at a later date than actinolite, because vermiculite is not stable above 150° C. If this be the case, one possibility is that vermiculite is a weathering product of actinolite and serpentine. However, the chemical composition of actinolite and serpentine, and the zonal relationships in space and time militate against such a view.

The chemical zonal relationships, especially the increase of MgO and H_2O in the inner zones, suggest that vermiculite and some serpentine formed while hydrothermal solutions were still active and the temperature had dropped below 150° C. Thus, the zonal vermiculite must have a complex paragenetic history, for it formed from the reconstitution of some combination of biotite, serpentine, diopside, hypersthene, and possibly actinolite. Serpentine, hornblende, and biotite are believed to be the essential contributors, although many questions regarding the paragenesis are left unanswered.

Although vermiculite in thin sections of perknites appears to be replacing several of the above minerals, the reactions are much more complex than simple substitution, involving substances not contained in either vermiculite or the host mineral. In the same way, a crystal of vermiculite growing within the outer zone of the vein owes part of its substance (water and some magnesia) to the impregnating solution and part of its substance to minerals initially present in the host rock.

Evidence is accumulating that serpentine formed over a longer time interval than other hydrothermal constituents. High and low temperature formation of actinolite and vermiculite, respectively, during serpentinization, probable transection of previously serpentinized material by veins of serpentine, and the occurrence of serpentine in outer and inner zones of veins - all support this view. Two or more epochs of serpentinization are possible but not probable.

The evidence presented thus far definitely favors a hydrothermal rather than a meteoric origin for vermiculite. In summary form, the evidence favoring hydrothermal origin is listed below.

1. Zoning relations of vermiculite and other minerals in serpentine veins suggest cooling hydrothermal solutions.

2. The relatively pure forms of vermiculite occur in or next to serpentinized rocks.

3. Vermiculite is more abundant and coarser adjacent to pegmatitic diopside and plagioclase veinlets which crosscut the badly altered peridotite.

4. Vermiculite is most abundant and pure where large pegmatites occur, as in the southeastern part of the area.

5. Vermiculite flanking one large pegmatite decreases in quantity and quality away from the pegmatite and grades into original ultramafic minerals.

Such evidence would seem to rule out a meteoric origin. However, the facts that caliche veins occupy fractures and former serpentine veins, and contain the largest and purest books of vermiculite in the area, strongly suggest that vermiculitization has progressed along the veins by meteoric means.

Gevers (1948, p. 166) cites as evidence against a meteoric origin the various degrees of alteration of phlogopite to vermiculite laterally at the surface. To this writer such chemical variability, if heterogeneous

and not zonal, reflects differential cation-exchange. All gradations from almost pure vermiculite to biotite-hydrobiotite within the same vein sample is more in keeping with a hypothesis of meteoric alteration by cation-exchange. In the interlayer structure of the vermiculite analyzed from the veins, Ca^{+2} and Mg^{+2} are the replacing cations. Both are available in the caliche which surrounds the crystals.

Other facts which suggest a meteoric origin are as follows:

1. In all caliche veins vermiculite is oriented with its maximum dimension parallel to the vein.

2. Serpentine was never found transecting vermiculite flakes.

3. In some vermiculite flakes penetration of water along cleavage lines could be followed under the microscope by means of the traces of oxidation left behind.

In summary, it is believed that meteoric solutions continued the process of vermiculitization after hydrothermal activity ceased and perhaps, in some cases initiated it. In order to prove that any of the vermiculite is wholly supergene, it appears that vermiculite would have to be found crosscutting the caliche. Certainly, this relationship would be very difficult to identify, if present.

Although there is evidence that some of the caliche veins were once occupied by serpentine, obviously serpentine is not the direct parent of vermiculite. The extreme poverty of serpentine in iron, aluminum, and potassium is a bar to such an origin. Biotite is the only ultramafic mineral rich in all these constituents and is, therefore, the most likely direct ancestor of vermiculite.

The fact that all samples examined in the whole area show either biotite interlayered with vermiculite, or non-expandable biotite along with vermiculite is perhaps the most convincing evidence that all vermiculite has altered from biotite, which in most cases, is an intermediate product in the alteration of other ultramafic minerals.

Vermiculitization of biotite involves the following chemical changes:

1. Progressive subtraction of the alkalies, mainly K_2O.
2. Hydration and formation of loosely-bound interlayer water.
3. Progressive oxidation of ferrous to ferric iron.

All varieties of vermiculite at Gold Butte reflect the degree to which these changes have been carried, cation-exchange being the essence of the process.

In view of the fact that vermiculite may have a hydrothermal or meteoric origin, it may be much more common than heretofore supposed in altered biotitic rocks.

REFERENCES

Barshad, I. (1948) Vermiculite and its relation to biotite as revealed by base exchange reactions, X-ray analyses, differential thermal curves, and water content, Am. Mineral., vol. 33, p. 655-678.

_____ (1949) The nature of lattice expansion and its relation to hydration in montmorillonite and vermiculite, Am. Mineral., vol. 34, p. 675-684.

_____ (1950) The effect of the interlayer cations on the expansion of the mica type of crystal lattice, Am. Mineral., vol. 35, p. 225-238.

Barth, T. F. W. (1931) Proposed change in calculation of norms of rocks, Min. Pet. Mitt., Band 42, p. 1-7.

Bowen, N. L. and Tuttle, O. F. (1949) The system of MgO-SiO_2-H_2O, Geol. Soc. Am. Bull., vol. 60, p. 439-460.

Bradley, W. F. (1945) Diagnostic criteria for clay minerals, Am. Mineral., vol. 30, p. 704-713.

_____(1950) personal communication, March 16.

Bragg, W. L. (1937) Atomic structure of minerals, Cornell University Press, 292 pages.

Bugge, J. A. W. (1945) The geological importance of diffusion in the solid state, Skrifter Norske Videnskaps- Akad. i. Oslo, I, Mat.-Naturv. Klasse, no. 13.

Cameron, E. N. et al. (1949) Internal structure of granitic pegmatites, Econ. Geol. Monograph 2, 115 pages.

Chayes, F. (1948) A petrographic criterion for the possible replacement origin of rocks, Am. J. Sci., vol. 246, p. 413-425.

Daly, R. A. (1933) Igneous rocks and the depths of the earth, New York, McGraw-Hill Company, 598 pages.

Dana, E. S. (1945) A textbook of mineralogy, 4th ed., revised by W. E. Ford, New York, John Wiley and Sons, p. 476.

Davis, F. A. W. and Johnson, M. (1936) Research work on North Carolina vermiculite, 1936, Geol. Bull. 5, T. V. A., Knoxville, Tenn., p. 11-21.

Deer, W. A. and Wager, L. R. (1939) Olivines from the Skaergaard intrusion, Kangerdluqssuak, East Greenland, Am. Mineral., vol. 24, p. 18-25.

Drosdoff, M., and Miles, E. F. (1938) Action of hydrogen peroxide on weathered mica, Soil Sci., vol. 46, p. 391-393.

Eskola, P. (1933) On the differential anatexis of rocks, Comm. geol. Finlande, Bull., no. 103, p. 12-25.

Fenneman, N. M. (1930) Map of the physical divisions of the United States.

Fenner, C. N. (1914) The mode of formation of certain gneisses in the highlands of New Jersey, Jour. Geol., vol. 22, p. 594-612, 694-702.

Gevers, T. W. (1948) Vermiculite at Loolekop, Palabora, North East Transvaal, Trans. Geol. Soc. of S. Africa, 173 pages.

Gilluly, J. (1933) Replacement origin of an albite granite near Sparta, Oregon, U. S. Geol. Survey Paper 175-C, p. 65-81.

Goldstein, A. (1946) The vermiculites and their utilization, Colorado School of Mines Quart., vol. 41, 63 pages.

Grim, R. E. (1950) personal communication, March 21.

_____(1950) personal communication via M. M. Leighton.

Groves, R. C. (1939) Exfoliation of vermiculite by chemical means, Nature, vol. 144, p. 554.

Gruner, J. W. (1932) The crystal structure of kaolinite, Zeit. f. Kriet., vol. 83, p. 75-88.

_____(1934) The structures of vermiculites and their collapse by dehydration, Am. Mineral., vol. 19, p. 557-575.

_____(1939) Ammonium mica synthesized from vermiculite, Am. Mineral., vol. 24, p. 428-433.

_____(1948) Progress in silicate structures, Am. Mineral., vol. 33, p. 679-691.

Hagner, A. F. (1944) Wyoming vermiculite deposits, Wyoming Geol. Survey Bull. 34, 47 pages.

Harker, A. (1939) Metamorphism, Methuen, London, 362 pages.

Harvey, C. O. (1943) Some notes on the calculation of molecular formulas for glauconite, Am. Mineral., vol. 28, p. 541-543.

Hendricks, S. B. and Jefferson, M. E. (1938) Structures of kaolin and talc-pyrophyllite hydrates and their bearing on water sorption of the clays, Am. Mineral., vol. 23, p. 863-875.

_____(1938) Vermiculite structure, Am. Mineral., vol. 23, p.851-862.

_____(1939) Polymorphism of the micas, Am. Mineral., vol. 24, p. 729-771.

Hess, H. H. (1933) The problem of serpentinization, etc., Econ. Geol. vol. 28, p. 634-657.

_____(1949) Chemical composition and optical properties of common clinopyroxenes, Am. Mineral., vol. 34, p. 621-666.

Hunter, C. E. and Mattocks, P. W. (1936) Vermiculites of Western North Carolina and North Georgia, Geol. Bull. 5, T. V. A., Knoxville, Tenn., 51 pages.

Hutton, C. O. and Fannkuchen, I. (1938) The stilpnomelane group of minerals, Mineral., Mag., vol. 25, p. 172-206.

Jackson, W. W. and West, J. (1930a) Muscovite, Zeit. f Krist., vol. 76, p. 211-227.

_____(1933b) Muscovite, Zeit. f. Krist., vol. 85, p. 160-164.

Johannsen, A. (1939) A descriptive petrography of the igneous rocks, vol. 1, Univ. of Chi. Press, Chicago, 318 pages.

Kazantsev, V. P. (1934) The structure and properties of vermiculite, Soc. russe mineralogie Mem., Ser. 2, vol. 63, p. 464-479.

Kennedy, G. C. (1941) Charts for correlation of optical properties with chemical composition of some common rock-forming minerals, Am. Mineral., vol. 32, p. 561-573.

Lacroix, A. (1940) Secondary transformation in the Phlogopite Deposits of South Madagascar, Soc. geol. France Compte rend., vol. 210, p. 353-357.

Larsen, E. S. (1928) A hydrothermal origin of corundum and albitite bodies, Econ. Geol., vol. 23, p. 398-433.

Larsen, E. S. and Berman, H. (1934) The microscopic determination of the nonopaque minerals, U. S. Geol. Survey Bull. 848, 266 pages.

Laschinger, J. E. (1946) Vermiculite and the working of the Palabora Deposit, Union of South Africa, Dept. Mines, G.M.L. Memoir No. 3, 23 pages.

Longwell, C. R. (1928) Geology of the Muddy Mountains, Nevada, U. S. Geol. Survey Bull. 798, 152 pages.

_____(1937) Sedimentation in relation to faulting, Geol. Soc. of Am. Bulletin, vol. 48, p. 433-441.

MacEwan, D.M.C. (1951) X-ray identification and crystal structures of clay minerals edited by G. W. Brindley, contributions by numerous authors, London Mineralogical Society, 345 pages.

McMillan, W. D. and Gerhardt, A. W. (1949) Investigation and laboratory testing of vermiculite deposits, Llano County, Tex., U. S. Bu. Mines, R. I. 4486, 42 pages.

McMurchy, R. C. (1934) Structure of chlorites, Zeit. f. Krist., vol. 88, p. 420-432.

Noble, J. A. (1952) Evaluation of criteria for the forcible intrusion of magma, Jour. Geol. vol. 60, p. 34-57.

Nockolds, S. R. (1932) The contaminated granite of Bibette Head, Alderney, Geol. Mag., vol. 69, p. 433-452.

_____ (1937) On the association of granite and dolerite in igneous bodies, Upsala Univ., Geol. Inst., Bull. 26, p. 265-278.

Pabst, A. (1942) The mineralogy of metamorphosed serpentine at Humphrey's, Fresno County, California, Am. Mineral., vol. 27, p. 580-585.

Pardee, J. T. and Larsøn, E. S. (1929) Deposits of vermiculite and other minerals in the Rainy Creek District near Libby, Montana, U. S. Geol. Survey Bull., 805-B, 12 pages.

Pauling, L. (1930) The structure of the chlorites, Proc. Nat. Acad. Sci., vol. 16, p. 578-582.

_____(1930) The structure of the micas and related minerals, Proc. Nat. Acad. Sci., vol. 16, p. 123-129.

Phillips, A. H. and Hess, H. H. (1936) Metamorphic differentiation at contacts between serpentinite and siliceous country rocks, Am. Mineral., vol. 21, p. 333-362.

Poldervaart, A. (1950) Correlation of physical properties and chemical composition in the plagioclase, olivine, and orthopyroxene series, Am. Mineral., vol. 35, p. 1067-1079.

Pratt, J. H. and Lewis, J.V. (1905) Corundum and the peridotites of Western North Carolina, North Carolina Geol. and Econ. Survey Bull., vol. 1.

Prindle, L. M. and Smith, R. W. (1936) Kyanite and vermiculite deposits of Georgia, Georgia Geol. Survey Bull. 46, p. 41-46.

Ramberg, H. (1945) The thermodynamics of the earth's crust, Norsk Geol. Tidsskr, Bind 24, p. 98-111.

Reiche, P. (1950) A survey of weathering processes and products, Univ. of N. Mex., no. 3, 95 pages.

Reynolds, D. L. (1946) The sequence of geochemical changes leading to granitization, Quart. J. Geol. Soc. London, vol. 102, p. 389-446.

Rosenfeld, J. L. (1950) Determination of all principal indices of refraction on difficulty oriented minerals by direct measurement, Am. Mineral., vol. 35, p. 902-905.

Ross, C. S. and Kerr, P. F. (1931) Clay minerals and their identity, J. Sed. Pet., vol. 1, p. 55-64.

Ross, C. S. and Shannon, E. V. (1926) Nickeliferous vermiculite and serpentine from Webster, North Carolina, Am. Mineral., vol. 11, no. 4, p. 90-93.

Ross, C. S., Shannon, E. V., and Gonyer, A. (1928) The origin of nickel silicates at Webster, North Carolina, Econ. Geol., vol. 23, p. 528-552.

Ruthruff, R. F. (1941) Vermiculite and hydrobiotite, Am. Mineral., vol. 26, p. 478-481.

Schwellnus, C. M. (1938) Vermiculite deposits in the Palabora area, Northeast Transvaal, Union of S. Africa, Dept. Mines, Geol. Ser. Bull. 11, 27 pages.

Shannon, E. V. (1928) Vermiculite from the Bare Hills near Baltimore, Maryland, Am. Jour. Sci., vol. 115, p. 20-24.

Thomas, B. E. (1949) Geology and ore deposits of the Wallapai District, Arizona, doctorate thesis, Calif. Inst. of Tech., 187 pages.

Turner, F. J. (1949) Mineralogical and structural evolution of the metamorphic rocks, Geol. Soc. of Am. Mem. 30, 343 pages.

Turner, F. J. and Verhoogen, J. (1951) Igneous and metamorphic petrology, McGraw-Hill, New York, 602 pages.

Tuttle, O. F. and Bowen, N. L., (1950) High-temperature albite and contiguous feldspars, Jour. Geol. vol. 58, p. 572-583.

Tyler, P. M. (1936) Minor nonmetals, U. S. Bur. Mines Minerals Yearbook, p. 1072.

Wahlstrom, E. E. (1960) Theoretical igneous petrology, J. Wiley, New York, 365 pages.

Walker, G. F. (1949) Water layers in vermiculite, Nature, vol. 163, p. 726.

_____(1951) X-ray identification and crystal structures of clay minerals, Min. Soc., London, p. 199-223.

Webb, T. H. (1824) Vermiculite, Am. Jour. Sci.,vol. 7, p. 55.

Winchell, A. N. (1945) Elements of optical mineralogy, Part II, John Wiley and Sons, 459 pages.

_____(1945) Variations in composition and properties of the calciferous amphiboles, Am. Mineral., vol. 30, p. 27-50.

Wright, F. E. (1951) Computation of the optic axial angle from the three principal refractive indices, Am. Mineral., vol. 36, p. 543-556.

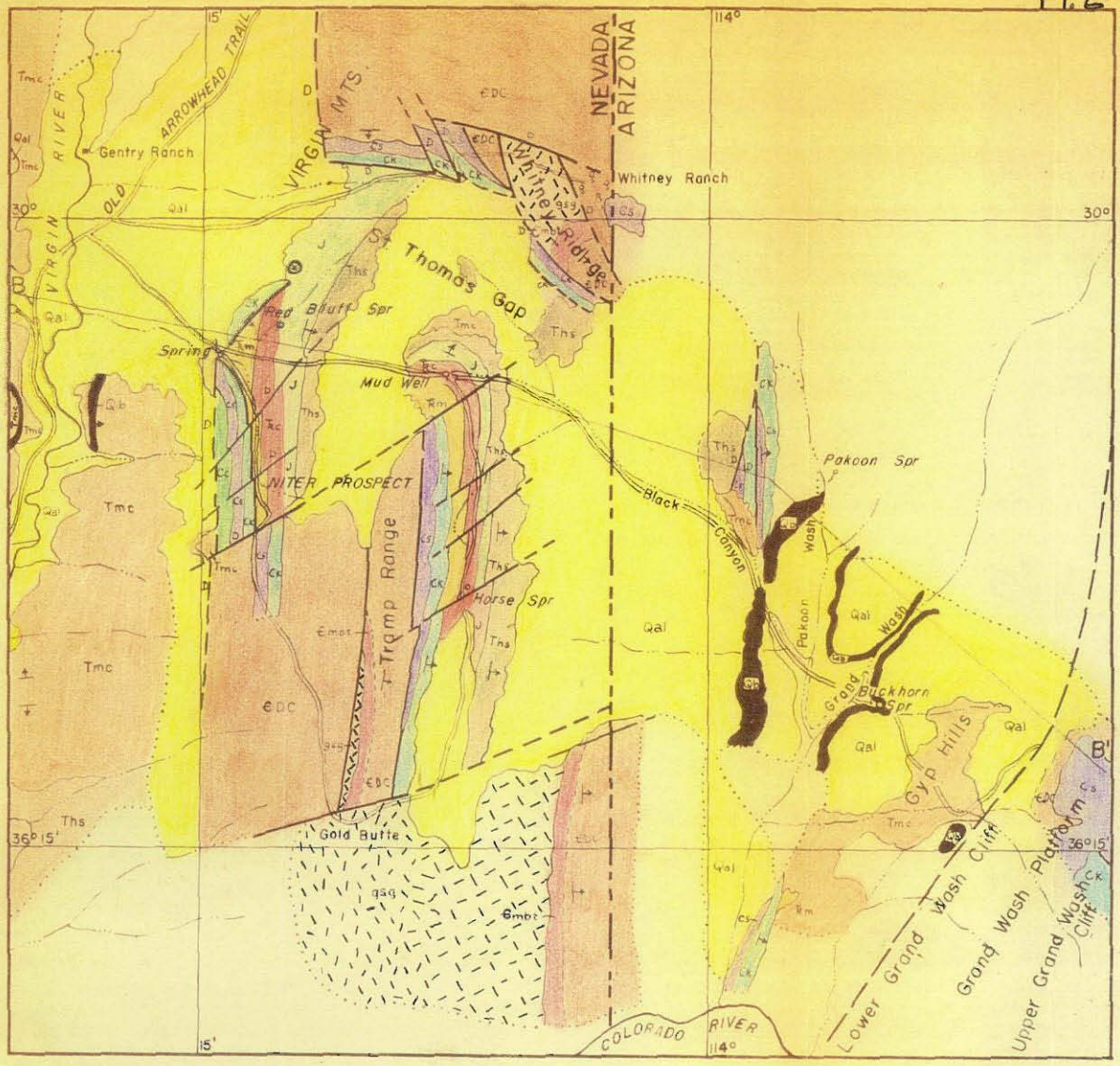

Geologic map and section across northern portion of Southern Virgin Mountains, from Virgin River to Upper Grand Wash Cliff. (From C. R. Longwell, 1928, plate I.)

Scale 1:250,000

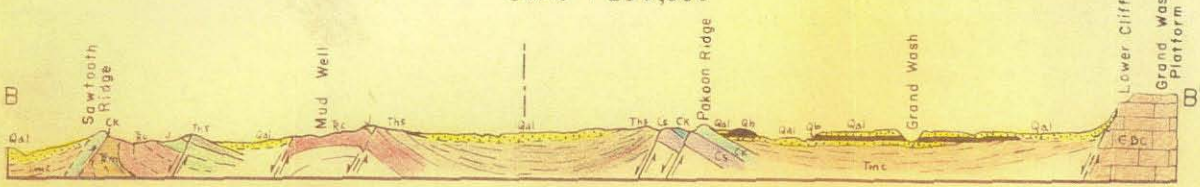

EXPLANATION

SEDIMENTARY ROCKS

Recent and Pleistocene	Qal — Alluvial deposits	Quaternary	
Unconformity			
Miocene(?) Pliocene(?)	Tmc — Muddy Creek formation	Tertiary	
Unconformity			
Miocene(?)	Ths — Horse Spring formation (including Overton conglomerate in places)	Tertiary	
Great Unconformity			
	J — Cross-bedded sandstone	Jurassic(?)	
Upper Triassic	Rc — Chinle formation (Underlain by Shinarump conglomerate probably Upper Triassic)	Triassic	
Unconformity			
Lower Triassic	Rm — Moenkopi formation	Triassic	
Unconformity			
Permian	Ck — Kaibab limestone (With some Cocomino sandstone at base in Grand Wash and Grand Wash cliffs)	Carboniferous	
Pennsylvanian(?)	Cs — Supai formation	Carboniferous	
Pennsylvanian	Cc — Callville limestone	Carboniferous	
	Embt — Muav (?) limestone, Bright Angel(?) shale, and Tapeats(?) sandstone	Cambrian	
	EDC — Paleozoic undifferentiated	Cambrian(?) and younger	

METAMORPHIC ROCKS

qsg	Gneiss, schist, and granite

IGNEOUS ROCKS

Qb	Basaltic flows

Quaternary and Pliocene

D — D Downthrown side of normal fault
→ Direction of horizontal displacement of thrust fault

Faults

Strike and dip of rocks.

OGIVES OF THE EAST TWIN GLACIER, ALASKA--
THEIR NATURE AND ORIGIN

INVESTIGATIONS IN THE TAKU GLACIER FIRN

Minor theses by

Freeman Beach Leighton

In Partial Fulfillment of the Requirements

For the Degree of

Doctor of Philosophy

California Institute of Technology

Pasadena, California

1952

OGIVES OF THE EAST TWIN GLACIER, ALASKA—THEIR NATURE AND ORIGIN

FREEMAN BEACH LEIGHTON

Reprinted for private circulation from
THE JOURNAL OF GEOLOGY
Vol. 59, No. 6, November 1951
PRINTED IN U.S.A.

OGIVES OF THE EAST TWIN GLACIER, ALASKA THEIR NATURE AND ORIGIN[1]

FREEMAN BEACH LEIGHTON
California Institute of Technology

ABSTRACT

The perfection, fine exposure, and unusual accessibility of ogives on East Twin Glacier, Alaska, make this an exceptional place in which to study the nature and origin of this phenomenon. The origin of ogives is discussed, and previous hypotheses are critically analyzed. With the exception of a hypothesis first suggested by R. T. Chamberlin, that ogives are the surficial expressions of shearing planes, no other hypothesis satisfactorily accounts for the fact that these ogives are exposed edges of layers of denser and dirtier ice than the intervening layers. Concepts of glacier flow evolved by Demorest provide a reasonable mechanism for understanding their formation, namely, periodic obstructed extrusion flow down-glacier from an icefall. Debris which was originally basal is believed to become, by upthrusting and ablation, the surface manifestation of an ogive.

INTRODUCTION

TERMINOLOGY

Agassiz (1847, p. 216)[2] first applied the term "ogives" to the series of curved layers of debris-rich ice whose surface manifestation in the ablation area of a glacier resembles large-scale pointed arches. This usage is believed to have special merit and will be followed in this paper.

Ribboned structure, alternating thin blue and white ice layers, was considered to be a type of ogive by H. and A. Schlagintweit (1850, pp. 78–86, 101), but this broad usage has not been followed and is undesirable. Ribboned structure is a distinct phenomenon in occurrence, if not in origin. Most glaciers form ribboned structure; few form ogives.

The terms "dirt bands" (Forbes, 1842, p. 89), "Forbes' dirt bands" (Quincke, 1905, p. 543; Fisher, 1942, pp. 1–17), and "periodic annual banding" (Washburn, 1935, p. 1885) have been applied to the features herein called "ogives." "Dirt bands" is an unsatisfactory term, because it has also been widely applied to annual dirt layers in stratified firn and ice. These are the German *Schmutzbänder* of present usage. "Ogives" has priority over all the other terms mentioned and has the further advantage of identical form in English, French, and German.

In addition, "periodic annual banding" and "Forbes' dirt bands" are not entirely apropos as terms. The annual formation of an ogive has not been clearly demonstrated, and it is controversial whether J. D. Forbes, for whom "Forbes' dirt bands" were named, was their first discoverer. With the exception of Tyndall (1876, p. 130), nineteenth-century glaciologists attributed the first

[1] Manuscript received February 28, 1951.

[2] Actually, the term appeared earlier in an article by M. E. Desor (1843, p. 308).

PLATE 1

Aerial view of Taku glacier system, looking southwest. Lettered locations: *A*, East Twin Glacier; *B*, West Twin Glacier; *C*, Taku Glacier; *D*, Twin Lake; *E*, Taku Inlet; *F*, approximate location of Juneau, 24 air miles from Twin Lake. U.S. Air Force photograph.

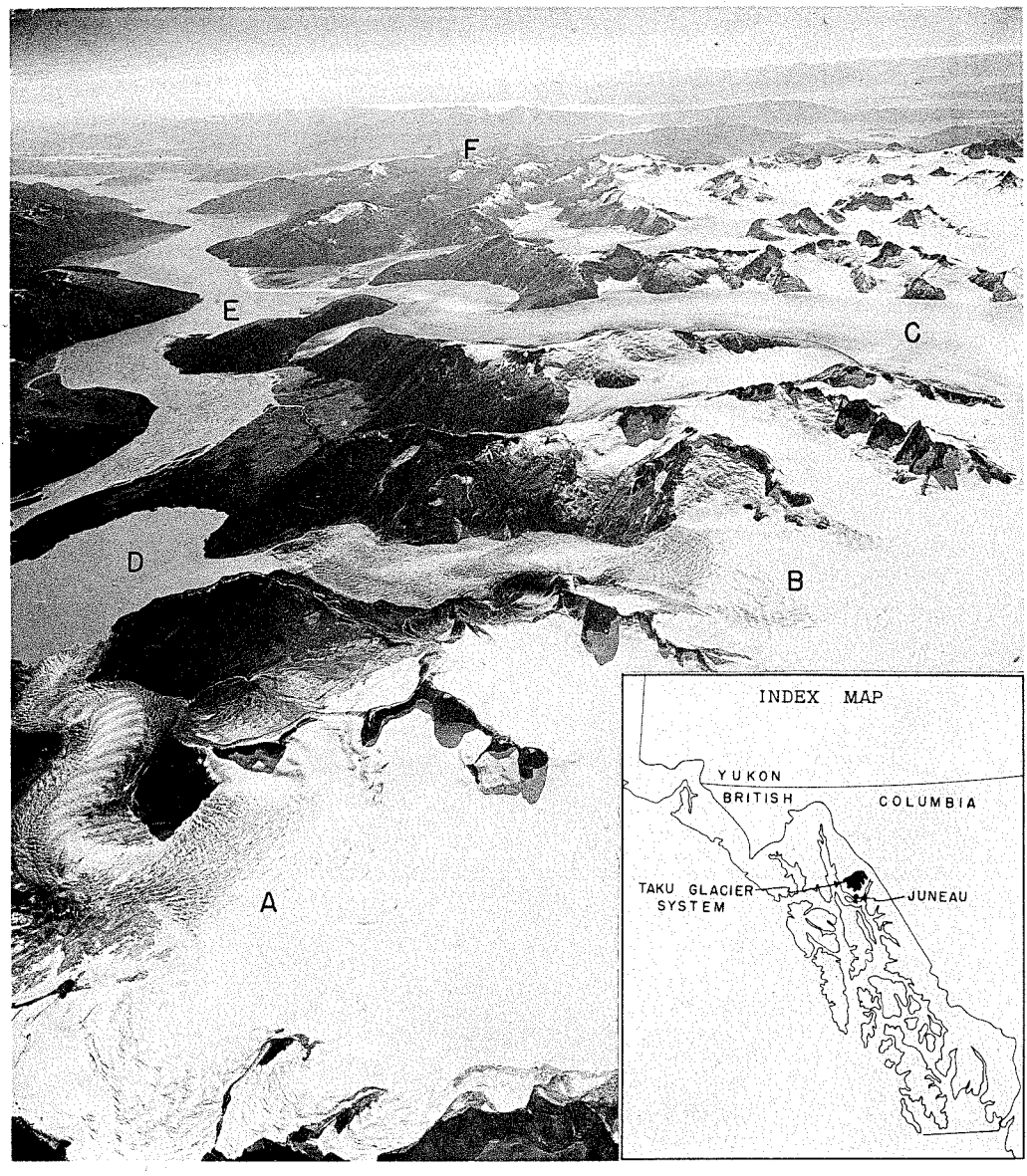

Aerial view of Taku glacier system

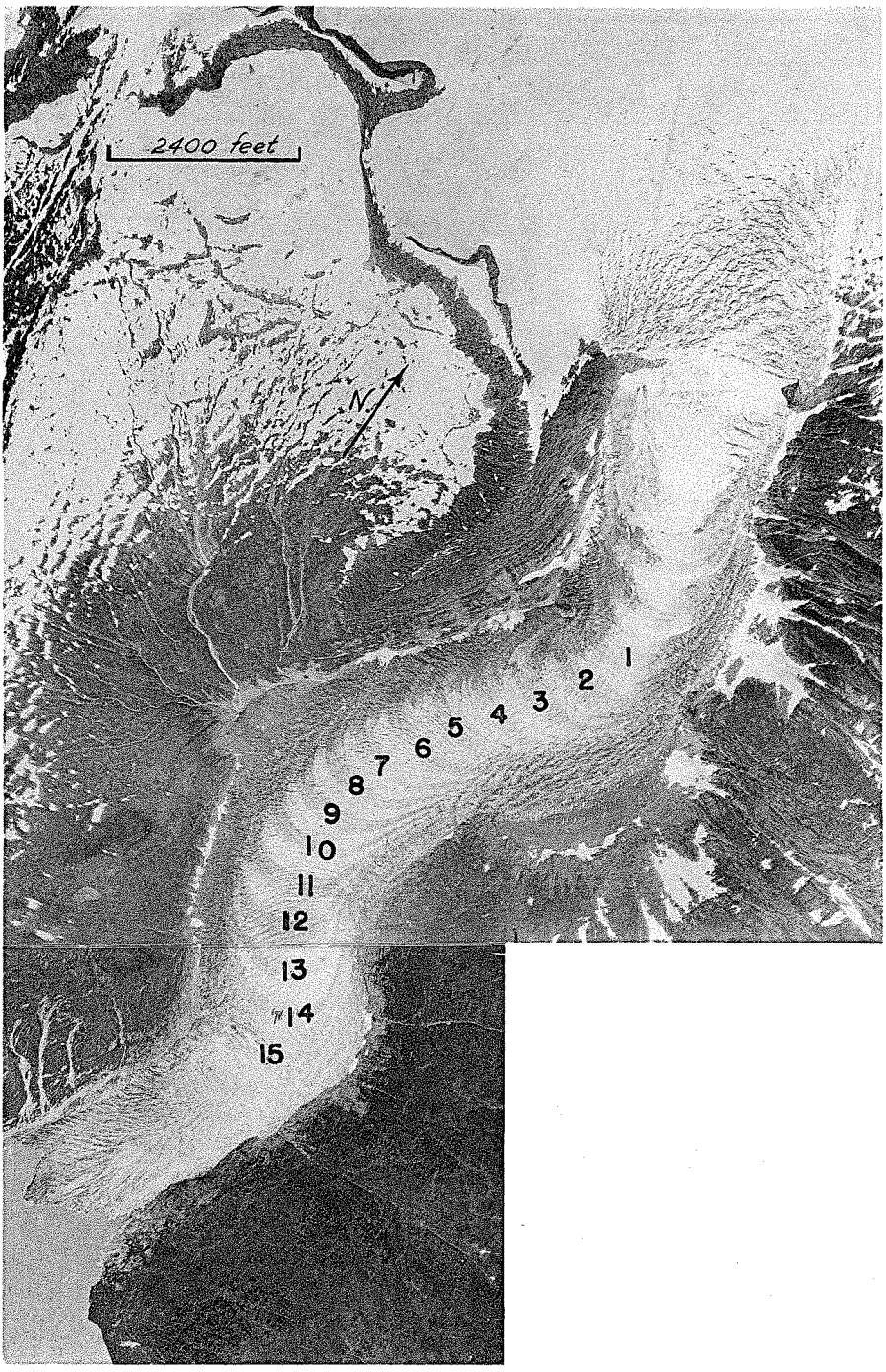

Ogives of the East Twin Glacier

recorded mention of this feature to Guyot (unpublished paper, 1838) and Agassiz (1840, pp. 120–121). The fact that Agassiz and Guyot failed to discriminate between ribboned structure, primary stratification, moraines, and ogives may have been largely responsible for the resulting variance in nomenclature.

Subsequent authors have also confounded ogives with dissimilar phenomena. Russell (1897, pp. 43–44) apparently confused ogives with the outcrops of primary stratification on Sierran glaciers. Fisher (1942, pp. 1–17; 1947, pp. 137–145) confused what he termed "Alaskan bands" with what in reality are ogives.

"Margins" as used in this paper refers to the lateral margins of a glacier. "Lateral moraine" refers to the accumulation of debris on and within a glacier along its margins.

SCOPE OF WORK

This study of ogives is based upon brief observations made during the Juneau Ice Field Research Project of 1949, sponsored by the American Geographical Society and carried out under contract with the Office of Naval Research, with the active co-operation of the Department of the Army and the Air Force, the Forest Service, and other civilian agencies.

Ten days, September 4–13, 1949, were spent on the Twin Glaciers, six of which were devoted to studying ogives. Since then an extensive study has been made of the literature. Although the paucity of field data is recognized, it is felt that the field data and information compiled from published observations as interpreted here in the light of modern concepts of glacial mechanics constitute a contribution to the understanding of ogives.

PHYSICAL SETTING

The East Twin is a small valley glacier, roughly 3 miles long and an average of 1 mile wide. Its source is the same accumulation area as the West Twin Glacier, which is roughly parallel in position and symmetry (pl. 1). Both descend icefalls and calve icebergs into Twin Glacier Lake. These are the only two glaciers in the Taku system that form ogives. Because ogives on the East Twin are regularly spaced and conspicuous and those on the West Twin are irregular and indistinct, the former were accorded particular attention and will be described here.

Roughly 2 miles above its terminus, East Twin Glacier descends 1,100 feet in a horizontal distance of 1,000 feet as an icefall over a steep, narrow cliff. The ogives occur below this icefall. Inasmuch as the zone of the icefall is believed to be a critical factor in their formation, attention will be given it first.

DESCRIPTION

THE ICEFALL AND ITS RELATIONSHIPS

Above the icefall, the East Twin Glacier is broken by tension forces into a great number of curved crevasses pointing up-glacier (pl. 2). No glacier-wide crevasses are present above the icefall; in fact, none extends even half the width of the glacier. In the course of its descent the ice becomes so badly shattered and disrupted that no crevasse retains its identity (pl. 3, *A*). Even seracs in the upper icefall are pulverized by the cascading.

PLATE 2

Ogives of the East Twin Glacier. The definite ones are numbered. U.S. Navy photograph.

Although the firn limit lay at least 1,000 feet above the icefall, the disintegration within the icefall was so complete that all evidence of the dirty summer surface on the glacier was destroyed. Moreover, there was no visible contamination of ice within the icefall by morainic debris to the depth of observation of roughly 75 feet.

In an icefall the ice is necessarily thinner than at places either upstream or downstream therefrom, because increased velocity is accompanied by decreased thickness. Owing to extensive exposures of the bedrock riser which restricts the icefall to a narrow gap, it is not likely that the icefall is very thick. This would imply that the ice is also broken up in depth and that plastic flow, if present at the base, is not considerable.

For 3,000 feet below the foot of the icefall, crevasses are lacking except along the glacier margins. Ogive banding is also absent. The glacier surface is firm, unbroken, and relatively clean, only the margins being strewn with detritus. Roughly 1,500 feet below the icefall the glacier surface becomes mildly undulating. A series of indistinct pressure ridges are faintly outlined by narrow discontinuous white bands, which represent residual accumulations of snow on the south sides of the ridges. Small ponds occupy the depressions between several ridges.

The ridges are 200–500 feet in width and four in number. They are crudely concentric, pointing downstream, and gradually become cuspate toward the glacier sides. Short crevasses cross the crest of the downstream ridge at right angles to its trend.

The ridges die out 3,500 feet below the foot of the icefall, and they are succeeded by the first faint appearance of an ogive. This transition from pressure ridge to ogive is gradual, and the general relations suggest that the down-glacier sides of the ridges become ogives and that the upstream sides, including the narrow intervening troughs, become the cleaner bands. The termination of pressure ridges also marks the beginning of intense transverse crevassing. This is believed to be in response to topographic control, inasmuch as a resistant bedrock ridge projects transversely from both sides of the glacier 3,500 feet below the icefall and narrows the glacier perceptibly. Beyond this ridge the glacier floor again appears to increase in gradient.

OGIVES

East Twin ogives are most striking when viewed from an elevated position (pls. 1 and 2). Traced downstream, they at first become increasingly distinct, but farther down they gradually become less distinct. Fifteen successive ogives were definitely identified and are numbered in plate 2. Pressure ridges just below the icefall are believed to be incipient ogives. These and the remains of several other ogives in the terminal portion, if included, would bring the count to twenty ogives in roughly 2 miles of glacier.

PLATE 3

A, Middle portion of East Twin icefall.

B, Lower East Twin Glacier viewed from west bank. Discordance between bands at far right is an optical illusion caused by foreshortening and unevenness in the glacier surface.

C, Longitudinal section of East Twin terminus. Remnant ogive stratigraphically below most prominent debris layer.

D, Ogive ice on left; bubbly, white ice on right. Twin Glacier.

A

B

C

D

Icefall and ogives of the East Twin Glacier

Plate 2 reveals the remarkable regularity of size, shape, and spacing of the ogives. They are mostly 250–350 feet wide in the center of the glacier. This approaches the average width of the intervening areas. Ogives near the icefall are lunate, becoming gradually more parabolic toward the terminus. Unlike the ogives viewed from air photos of other Alaskan glaciers, these did not become more closely spaced or more hyperbolic toward the terminus. The ogives die out before the terminus is reached, as a result of intense crevassing preparatory to iceberg calving.

All narrow toward the glacier margins, and most of them lose their identity upon merging with the morainic debris of the margins. On the east side of the glacier, where the margin is relatively clean, ogives *8*–*11* could be traced up-glacier as narrow subparallel bands, which finally coalesced. It was possible to follow ogive *11* to a point opposite the apex of ogive *5*, a distance of almost 3,000 feet.

Lateral morainic detritus is much more prominent on the west than on the east margin of the glacier (pl. 3, *B*). Aprons of avalanche debris on the west margin at the base of the icefall have been dragged into arcuate stringers by the more rapid movement of the center of the glacier. Farther down-glacier, concentrations of morainic detritus emphasize and coincide with the west sides of the ogives. It is also present in intervening areas, but in most cases it does not extend so far toward the center of the glacier in these areas (pl. 3, *B*). Hence the ogives appear to incorporate more morainic detritus than do the intervening areas.

A traverse was made of ogives from the terminus of East Twin Glacier to ogive *8* (pl. 2). Measurements and particular observations were made of ogives *8*, *9*, and *10* and of the intervening areas. The distinction between ogives and intervening areas is relative only, but the following general differences are noted:

1. Ogives are composed of denser and dirtier ice than the intervening areas (pl. 3, *D*). The difference in color is imparted by the concentration of debris in ogives and by the contrast between the predominantly bubble-free blue ice of ogives and the predominantly bubbly white ice of the intervening areas.

2. Debris within the ogives is more abundant, coarser, and more evenly distributed than in the intermediate areas.

3. Owing to differential ablation caused by a difference in albedo, the cleaner and whiter intervening areas project a few inches to a foot above them (pl. 3, *D*).

Ogives *8*, *9*, and *10* are nearly spoon-shaped structurally, dipping 70°–80° toward the center of the glacier at the margins and 35°–50° up-glacier at the vertices of the ogives. They are conformable with the intervening layers and with the ribboned structure, which is less conspicuous in ogives than between them. The average true thickness of ogives *8*, *9*, and *10* measured 240 feet and that of the intervening areas 255 feet.

On a small scale, ribboned structures resemble ogives, inasmuch as dense, bubble-free, blue-ice layers alternate with bubbly white-ice layers. The blue layers of ribboned structure have long been attributed to differential movement accompanied by recrystallization through refreezing of meltwater produced by friction along shear planes (Philipp, 1920, p. 439). For this reason the blue ice of ogives is also considered ice that has recrystallized in this manner, with elimination of air bubbles.

Excavations showed that the surficial debris of ogives is derived from the ice by ablation and not from an extra-glacial

source. The surficial debris is predominantly angular and poorly sorted. Sizes range from clay and silt to boulders several feet in diameter. The clay and silt are rather uniformly distributed, and the coarser debris is localized along certain layers. Concentrated superglacial deposits of coarse sand and pebbles form debris cones. Striated cobbles and boulders suggest that some of the detritus was once subglacial. Ogives also contain bubbly-ice layers up to 25 feet thick which are mostly debris-free, but a few

TABLE 1

SECTION OF PART OF AN INTEROGIVE ICE LAYER

Type of Ice	True Thickness (Feet)
Clean, bubbly white ice	12
Bubbly white ice with many parallel thin dirt layers	4
Dirty blue-ice lens	1
Clean, bubbly white ice	14
Bubbly white ice with many parallel thin dirt layers	4
Dirty blue ice	2
Clean, bubbly white ice	18
Total	55

contain dust and silt. By contrast, all the blue ice contains layers of debris parallel to the ogive structure.

Dirty ice in the relatively clean ice areas between ogives is of two types: first, parallel dust and silt layers 0.25–0.50 inch thick within white, bubbly-ice layers and, second, debris-laden blue-ice layers and lenses. The debris in nonogive areas is similar to that in ogives, but less abundant. The clean layer between ogives *9* and *10* measured 306 feet in width and 252 feet in true thickness. The section in table 1 of a part of this layer adjacent to ogive *9* is believed to be representative.

The dirt in all the glacier ice is so small in amount that it has often been mistakenly assumed that the surficial debris must have been introduced onto the glacier surface from an outside source instead of being concentrated by ablation (Forbes, 1842, pp. 348–352; Tyndall, 1876, pp. 127–132; Scherzer, 1907, pp. 50–60). The difficulty in tracing the ogive and nonogive dust and silt layers in depth is analogous to the difficulty in detecting annual dirt layers in pits dug in firn. In such pits it may be several days before ablation concentrates the debris sufficiently so it is visible on the pit walls.

Where East Twin Glacier enters Twin Glacier Lake, a striking longitudinal section of the glacier is exposed (pl. 3, *C*). Debris planes are clearly shown, dipping upstream. The most prominent debris plane pictured is believed to be the upper surface of an ogive, because, stratigraphically, below this debris plane is the dense, dirty, schistose ice characteristic of ogives and above the debris plane are the bubbly, relatively debris-free characteristics of ice between ogives.

HYPOTHESES OF ORIGIN

Ogives have been reported from valley glaciers in the Alps, the Himalayas, Canada, the United States, Alaska, and Patagonia and are therefore a feature of wide geographical distribution. Six contrasting hypotheses have been advanced to explain the origin of ogives, as follows:

1. Ogives are original dirty layers in the firn carried through an icefall or restricted channelway and eventually exposed by ablation in the lower part of the glacier.

2. Ogives are surficial bands related to alternating zones of porous and compact ice formed at the base of an icefall, with dirt of surficial origin lodging in the porous ice more readily than in compact ice.

3. Ogives are formed by surficial concentration of debris in depressions at and below an icefall.

4. Ogives are glacier-wide blocks of dirty ice which are separated by the clean, snow-filled crevasses of an icefall.

5. Ogives are formed in an icefall by alternate winter snowfalls and summer dust accumulations.

6. Ogives are the surface expressions of shearing planes and associated phenomena of glacial flow.

All hypotheses were first developed from study of ogives in the Alps, with the exception of no. 5, which has been applied only to the ogives of East Twin Glacier, Alaska. Hypotheses 3 and 4 have subsequently been applied to Alaskan ogives. All except hypotheses 2 and 6 have had proponents within the last two decades.[3]

ORIGIN OF OGIVES OF EAST TWIN GLACIER

Any plausible explanation of the East Twin ogives must account for the following characteristics: (1) location down-valley from an icefall in the ablation area; (2) continuity across the width of the glacier; (3) three-dimensional character; (4) regularity in size, shape, and spacing; (5) thickness in excess of 200 feet; (6) dip up-glacier and inward from the margins; (7) complete disruption of pre-existing stratification in the icefall; (8) gradation from pressure ridge to ogive; (9) layers of dense, bubble-free, seemingly recrystallized ice; (10) coarseness of detritus; (11) abraded clastics; (12) increasing prominence and increasing abundance of detritus down-glacier to the terminus.

1. *Stratification hypothesis.*—This is the only hypothesis which does not demand the presence of an icefall up-glacier from the ogives. This hypothesis, originally proposed by Agassiz (1847, pp. 205–218), was subsequently supported by Hess (1904, pp. 169–178) and Vareschi (Godwin, 1949, pp. 325–332).

Hess formed miniature ogives experimentally with layers of red and white wax. From these experiments he concluded that parallel horizontal firn strata, moving from a wide firn area into a constricted valley, would become thickened and spoon-shaped and that the dirty layers would be accented through the removal by intensified ablation of the surficial seracs produced in an icefall.

Vareschi's pollen studies on the Aletsch Glacier, Switzerland, lend support to the stratification hypothesis. Samples of pollen collected from successive dark and light bands are interpreted as showing a seasonal sequence, the dirty ice representing summer, spring, and autumn accumulations and the cleaner ice corresponding to winter accumulations.

The complete disruption of pre-existing stratification by East Twin icefall definitely eliminates this hypothesis from consideration here. Other facts just as fatal to the hypothesis are (1) the 200-foot-plus thickness of some ogives; (2) the coarseness of detritus; and (3) the failure of the theory to recognize the dynamics of glacial flow.

2. *Porosity hypothesis.*—J. D. Forbes (1842, pp. 348–352; 1859, pp. 17–26, 210–220, 268; 1900, pp. 154–162, 379–380) was the lone proponent of this hypothesis. He was the first to recognize an icefall as a general requisite to the formation of ogives.

The presence of alternating zones of porous and compact ice on the East Twin was verified, but in the reverse relationship from that proposed by Forbes. The ogives are the compact, not the porous, zones. In addition, the porous

[3] W. V. Lewis (in Orowan, 1949, p. 239) by inference seems to favor a shear origin.

zones are not perforated enough to collect particles of rock, and the compact zones are not smooth enough to be washed clean by rain, as Forbes visualizes.

Other facts which oppose Forbes's hypothesis are (1) the East Twin ogives have a three-dimensional character; (2) the surficial debris increases in abundance down-glacier; (3) the amount of debris bearing the characteristics of subglacial action is greater than would be expected to be introduced in the icefall zone.

3. *Depression hypothesis.*—Tyndall (1876, pp. 127–132; 1896, pp. 372–375) believed that Forbes had confused cause and effect and that the greater porosity observed in the ogives was merely the result of the ice surface's being pitted by dirt. His explanation involves three considerations: "(1) the transverse breaking of the glacier on the cascade, and the gradual accumulation of the dirt in the hollows between the ridges; (2) the subsequent toning down of the ridges to gentle protuberances which sweep across the glacier; (3) and the collection of the dirt upon the slopes and at the bases of these protuberances."

Washburn (1935, pp. 1885–1889) followed this thesis in its entirety, apparently failing to recognize that Tyndall had introduced the idea years before. Though Tyndall merely speculated on the annularity of ogives, Washburn was convinced of it.

Scherzer (1907, pp. 50–60, 118–119), Tutton (1927, pp. 113, 121–22), and Streiff-Becker (1943, pp. 111–132) favored the accumulation of debris in troughs at the base of an icefall. Scherzer held that the troughs were due to the incomplete healing of transverse crevasses in an icefall. On the other hand, Streiff-Becker considered that the undulations at the base of the icefall were formed from strong differential pressure from above (Fisher, 1947, p. 140) and by the damming-up of the glacier below an icefall through a narrowing of the glacier bed (Seligman, 1949, p. 330). Tutton (1927, p. 121) regarded the swells as "due to the forces at work in effecting the stream-like movement of the glacier, faster in the middle and at the surface than at the sides and bottom (bed), rather than to mere change of declivity of bed."

Application of this hypothesis to the East Twin ogives is weakened by the lack of glacier-wide crevasses and block ridges in the East Twin icefall and the lack of surface debris available at the icefall. Troughs exist below the icefall, but there was no sign of dirt collecting in them. On the contrary, the pressure ridges appear darker than the depressions.

The increasing abundance of debris down-glacier is also a cogent argument against the accumulation of debris in troughs. Had the debris collected in icefall crevasses, progressive ablation down-glacier might well remove a sufficient thickness of ice to bring most or all of the debris to the surface by the time it reached the glacier terminus; yet all ogives develop and retain a well-defined three-dimensional form despite unlimited ablation.

4. *Block-ridge hypothesis.*—Fisher (1947, pp. 137–145), in contrast to Washburn, believed that the block ridges become ogives and that the glacier-wide crevasses become white bands. In his opinion (1947, p. 140), "the dark bands are the lineal descendants of the old (dirty) névé surface above the icefall, and the clean bands are inlays of clean ice that filled up the crevasses."

The facts which prevent acceptance of

this theory include: (1) lack of glacier-wide crevasses and dirty block ridges in the icefall; (2) coarseness of the debris in the ogives; and (3) increasing clarity of ogives down-glacier. In addition, the "inlays of clean ice" in 75-foot crevasses would be depleted by ablation before the bands reached the glacier terminus, assuming an arbitrary velocity of flow of 300 feet per year and an ablation rate of 2 feet per year.

5. *Snowfall-dust accumulation hypothesis.*—After observations of ogives on the East Twin Glacier, Miller (1949, p. 25) reports:

> It seems fairly clear that the alternation of bands represents, in turn, the white clean ice of winter snow carried over the seracs from late autumn to spring, and darker bands of ice made dirty by accumulations of summer dust carried through the seracs in that segment of the glacier which moved over this point during the warmer months. This summer dirt is concentrated by virtue of ablation and a narrower channel of flow below the icefall.

This concept ignores the fact that much of the debris is not dust, that it is much greater in quantity than any seasonal accumulation, and that much of the debris shows subglacial abrasion. Furthermore, this hypothesis assumes that the area of dust accumulation would be limited to that portion of the glacier's surface which had not moved "over the seracs from late autumn to spring." It also implies that the glacier descends the icefall in roughly half a year. If this premise were true, each ogive should be over 500 feet wide. In all fairness to Miller, he also suggested:

> It is considered very desirable for next season's field party to investigate closely the possibility that here, shearing at depth, may be a factor in bringing out the pattern of dirty summer ice, intercalated with cleaner winter ice, resulting from possible thrusting of many thin layers of ice one against another.

6. *Shearing hypothesis.*—Although T. C. Chamberlin (1895, pp. 206–208) did not discuss ogives as such, his explanation of the means of introducing debris into the small-scale foliation within the ice of ablation areas is especially significant:

> The original stratification could not have been pronounced. Perhaps it was intensified somewhat during subsequent consolidation, but some new agency was necessary to produce the more definite partings and to introduce the layers of debris. This agency appears to have been a shearing movement between the layers.

According to R. T. Chamberlin (1928, pp. 24–26), "where an icefall behind develops strong thrusting, relief is obtained by upward movement of the ice mass as well as by forward movement. This is both by granular adjustment and by shearing." R. T. Chamberlin did not distinguish between the large-scale ogives and smaller-scale foliation, nor did he attempt to account for the periodicity of ogives. He regarded each ogive as a special surface expression of many closely spaced shearing planes.

This mechanism accounts for features not readily explained by other hypotheses. The three-dimensional character of the ogives, their form, the general coarseness of debris, the similarity to thrust layers exposed in longitudinal section in the terminus of the glacier (pl. 3, *C*), and the similarity of the ice in ogives and in the blue bands of ribboned structure, all attest to a shearing origin. Furthermore, the occurrence of pressure ridges at the base of the icefall is an intimately related phenomenon produced by the dynamics of the glacier.

Concepts of glacier flow proposed by Demorest (1942, pp. 29–66; 1943, pp. 363–400) lend support to the shearing hypothesis. His analysis of glacier flow establishes four types of ice movement,

each characteristic of different conditions of underlying topography and surface configuration. These are extrusion flow, obstructed extrusion flow, obstructed gravity flow, and gravity flow. Extrusion flow is "pressure-controlled" because it depends upon differential pressures arising from the slope of the glacier surface. Gravity flow is "drainage-controlled" because it results from the force of gravity, bear the thrust of the steeper portions behind. This obstruction causes the flowing ice to pile up below the icefall and increase its thickness. Compressive stresses accumulate faster than they can be accommodated by plastic flow during the thickening process. Under these conditions the slower-moving thinner ice ahead is overridden by the obstructed ice. Movement of the thrusted layers is

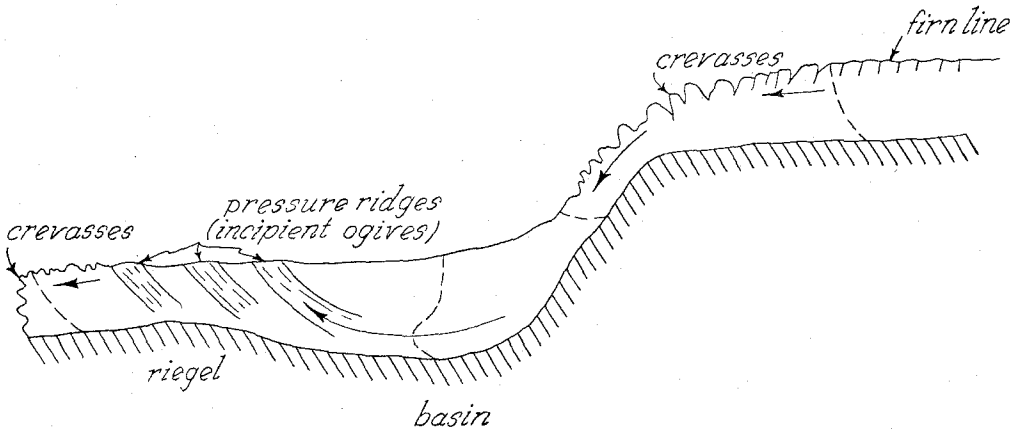

FIG. 1.—Diagrammatic longitudinal section of East Twin Glacier icefall. Dashed lines show profile of rate of flow; arrows show the locus of maximum velocity in different parts of the glacier (after Matthes and Demorest). Ogives form below icefall where flow is obstructed by slower-moving masses.

whose effect is dependent upon the slope of the glacier floor.

East Twin ogives seem best explained by the periodic occurrence of obstructed extrusion flow at the base of an icefall. A condition of obstruction to flow, such as is present here, was suggested in principle by R. T. Chamberlin, namely, the sudden flattening of bed slope beneath an icefall.

In making its steep descent, the ice in a fall is accelerated by gravity and attains a high velocity. This velocity increases with the height and gradient of the icefall and the constriction of the cross section of flow. At the base of the icefall this motion is in part arrested, and the relatively level portion of the glacier has to forward and upward, deforming the upper zone of relatively nonplastic ice and forming transverse pressure ridges.

The absence of tension crevasses from the base of the East Twin icefall to the constriction 3,500 feet down-glacier indicates the absence of gravity flow. Thus the type of flow, we infer, changes from "drainage-controlled" in the icefall to "pressure-controlled" below the icefall, and the level of maximum velocity shifts from the surface to the bottom of the glacier (fig. 1).

It is a matter of common observation that lakes are often located below bedrock steps in valleys of homogeneous rock. Pressure-controlled flow down-glacier from the East Twin icefall implies

that the glacier floor is either basin-shaped or has a gradient too low to enable the force of gravity to overcome the frictional resistance of the rock bed. It seems likely that the former is the case. The bedrock restriction which projects laterally into both sides of the glacier and marks the boundary between the continuous compact ice and the crevassed ice may be a surface indication of a basin sill. If this restriction exists as a riegel (buried ridge) at the lower end of the basin, it may be a factor influencing the resistance to thrusting and hence may have a part in controlling the spacing and regularity of ogives.

In all probability, the shearing and thrusting occur near the lower end of the smooth reach below the icefall, where pressure ridges are most prominent and where the transition from bottom to top current takes place (fig. 1). It is here that what was originally subglacial detritus is believed to become, by upthrusting and ablation, the surface manifestation of an ogive.

PERIODICITY OF FORMATION

Because the ogives on the East Twin Glacier are rather uniformly spaced, a roughly periodic relation must exist between velocity of flow and episodes of thrusting. Presumably, the obstruction below the icefall is a fairly constant force, and the stresses which produce the obstructed flow are accumulative until that type of flow occurs. The stresses are not relieved solely by thrusting of the bottom current, because small-scale shear foliation (ribboned structure) of conformable orientation is also found in the ice layers between ogives. These represent minor yieldings along planes parallel to the ogives and are a product of the same applied stresses. Hence the over-all thrusting is a general periodic movement involving thick masses of ice which carry along thinner slices in the direction of easiest relief, which in this case, owing to the obstruction, is surfaceward. This relieves the obstructing effect temporarily, and plastic flow then dominates. When stresses again accumulate to a point where plastic flow is overcome, thrusting again takes place.

Obviously, it would be wholly fortuitous under the shearing theory if East Twin ogives were formed only by annual thrusting, although annual changes in ice volume or velocity of flow might be an important factor. Glacier flow is sometimes accelerated above firn line during the winter, owing to heavy snowfalls (Streiff-Becker, according to Seligman, 1947, p. 16; Orowan, 1949, pp. 232–233), and it may be retarded at the same time of year below firn line, where accumulative snowfalls are less and where a proportionately thicker surface layer yields less readily in subfreezing weather (R. T. Chamberlin, 1936, p. 104). Such a difference in rate of flow during the winter on East Twin Glacier would increase the obstruction below the icefall and possibly influence the regularity of large-scale thrusting at this point. Seasonal observations, if and when possible, should contribute to this problem.

SCARCITY OF GLACIERS WITH WELL-DEVELOPED OGIVES

Glaciers with well-developed ogives are relatively uncommon as compared to glaciers with indistinct and deranged ogives. From a comparison of the two Twin Glaciers and a study of available photographs of ogives, the following possible explanations for the absence, indistinctness, or derangement of ogives below icefalls are suggested:

1. The glacier is of too great thickness or is too short to permit obstructed ex-

trusion flow in depth to be revealed by ablation.

2. The icefall is composite or complicated by other icefalls, which disrupt the regularity of thrusting at the base.

3. No abrupt flattening of bedrock slope occurs below the icefall.

4. The icefall lacks the size or vigor to develop large periodic thrust movements at its base.

5. At the base of an icefall the glacier makes a sharp turn.

6. A tributary glacier may disrupt or conceal ogives in a trunk glacier.

7. If the distance from an icefall to the glacier terminus is not great, thrust layers formed near the glacier terminus as a result of thinning of the ice may derange thrust layers formed at the base of the icefall.

8. No portion of the glacier below the icefall is in the ablation area.

SUGGESTIONS FOR FURTHER STUDIES

It is natural to refer a phenomenon to a single cause, even though it is rare that any phenomenon is wholly the result of a single cause. If it is demonstrable that this cause is effective in one area, the tendency is to extend its application elsewhere. Therefore, the writer suggests careful study by others of the following points.

For those ogives occurring down-glacier from an icefall the writer is inclined to believe that the factor of thrusting may be universally applicable. That all ogives are related to an icefall has not been established, although this is suspected from studies of the aerial photographs of nine Alaskan glaciers which display ogives below an icefall. Further observations in other glacier regions are needed to prove this.

Studies made at the bottoms of steep declivities in recently deglaciated valleys may aid in reconstructing the flow characteristics and indicate whether topographic and geologic relations would have favored obstructed extrusion flow.

ACKNOWLEDGMENTS.—I am greatly indebted to the American Geographical Society, which sponsored the Juneau Ice Field Research Project of 1949, of which the study described here was a part. Special thanks are due Maynard M. Miller, field director of the project, for making this investigation possible, and to William O. Field, of the American Geographical Society, for permission to publish here. I am extremely grateful to Professor Robert P. Sharp, of the California Institute of Technology, for his valuable advice in the writing of the manuscript. To Charles Harrington, Zach Stewart, and Dick Ward, my sincere thanks for their co-operation and assistance in the field. Miss Ellen Powelson kindly drafted the illustrations.

REFERENCES CITED

AGASSIZ, L. (1840) Études sur les glaciers, Neuchâtel, privately printed.

——— (1847) Système glaciaire ou recherches sur les glaciers, pt. 1: Nouvelles études et expériences sur les glaciers actuels, Paris, V. Masson.

CHAMBERLIN, R. T. (1928) Instrumental work on the nature of glacier motion: Jour. Geology, vol. 36, pp. 1–30.

——— (1936) Glacier movement as typical rock deformation: *ibid.*, vol. 44, pp. 93–104.

CHAMBERLIN, T. C. (1895) Recent glacial studies in Greenland: Geol. Soc. America Bull. 6, pp. 199–220.

DEMOREST, M. (1942) Glacier thinning during deglaciation, pt. 1: Glacier regimens and ice movement within glaciers: Am. Jour. Sci., vol. 240, pp. 29–66.

——— (1943) Ice sheets: Geol. Soc. America Bull. 54, pp. 363–400.

DESOR, M. E. (1843) Report of the researches of M. Agassiz: Edinburgh New Philos. Jour., vol. 35, p. 308.

FISHER, J. E. (1942) Forbes' dirt bands on glaciers, New York, privately printed.

——— (1947) Forbes' and Alaskan dirt bands on glaciers and their origins: Am. Jour. Sci., vol. 245, pp. 137–145.

FORBES, J. D. (1842) Third letter on glaciers, addressed to Professor Jameson: Edinburgh New Philos. Jour., vol. 32, pp. 84–91.
——— (1859) The theory of glaciers, Edinburgh, A & C. Black.
——— (1900) Travels through the Alps, Edinburgh, A. & C. Black.
GODWIN, H. (1949) Pollen analysis of glaciers in special relation to the formation of various types of glacier bands: Jour. Glaciology, vol. 1, pp. 325–332.
GUYOT, A. (1838) Paper read before Acad. Sci. Paris.
HESS, H. (1904) Die Gletscher, Braunschweig, F. Vieweg & Sohn.
MILLER, M. M. (1949) Progress report of the Juneau Ice Field Research Project, New York, Am. Geog. Soc.
OROWAN, E. (1949) Joint meeting of the British Glaciological Society, the British Rheologists Club, and the Institute of Metals: Jour. Glaciology, vol. 1, pp. 231–240.
PHILIPP, H. (1920) Geologische Untersuchungen über den Mechanismus der Gletschertextur: Neues Jahrb. Mineralogie, Geologie, Paläontologie, vol. 43, pp. 439–556.
QUINCKE, G. (1905) The formation of ice and the grained structure of glaciers: Nature, vol. 72, pp. 543–545.
RUSSELL, I. C. (1897) Glaciers of North America, Boston, Ginn & Co.
SCHERZER, W. H. (1907) Glaciers of the Canadian Rockies and Selkirks: Smithsonian Contr. to Knowledge, vol. 34, pp. 1–131.
SCHLAGINTWEIT, A., and SCHLAGINTWEIT, H. (1850) Untersuchungen über die physikalische Geographie der Alpen, Leipzig, T. O. Weigel.
SELIGMAN, G. (1947) Extrusion flow in glaciers: Jour. Glaciology, vol. 1, pp. 12–18.
——— (1949) Discussion: *ibid.*, pp. 330–332.
STREIFF-BECKER, R. (1943) Beitrag zur Gletscherkunde Forschungen am Claridenfirn im Kt. Glarus: Schweizer. naturf. Gesell. Denkschr., vol. 75, pp. 111–132.
TUTTON, A. E. H. (1927) The high Alps; a natura history of ice and snow, London, K. Paul, Trench Trubner & Co.
TYNDALL, J. (1876) The forms of water, New York, D. Appleton & Co.
——— (1896) The glaciers of the Alps, New York J. M. Dent.
WASHBURN, H. B. (1935) Morainic banding o Malaspina and other Alaskan glaciers: Geol. Soc. America Bull. 46, pp. 1879–1890.

INVESTIGATIONS IN THE TAKU GLACIER FIRN

By F. B. Leighton

from

Report of the Juneau Ice Field Research Project, Alaska
1949 Field Season

Department of Exploration and Field Research
American Geographical Society
Broadway and 156 Street
New York 32, N. Y.

Excerpt from:
J.I.R.P. Report No. 6 November. 1951

B. INVESTIGATIONS IN THE TAKU GLACIER FIRN

By F.B. Leighton[1]

(This section describes, analyzes, and interprets the results of firn studies made between August 12 and September 4, 1949, on the broad and relatively flat main branch of the upper Taku Glacier. Both qualitative and quantitative measurements of melt-water, its generation and movement in the firn, and various firn structures influenced directly or indirectly by melt-water behavior are considered.)

The site selected for these studies (Fig.3) was representative of the meteorological and firn conditions for the glacier at 3,600 feet elevation. This site, hereafter known as Camp 10A, lies 35 air miles from the city of Juneau, 16 miles from the sea level terminus of the Taku Glacier, and 8 miles inside the 1949 firn line limit which rested at approximately 3,200 feet elevation. The depth of the glacier beneath Camp 10A (approximately 1,200 feet from the eastern edge of the glacier at the main base, Camp 10) was on the order of 600 feet.

Hourly temperature records, 4-hour psychrometric readings, and daily sunshine and precipitation records were made at Camp 10A with standard U.S.Weather Bureau and Army Signal Corps equipment (see meteorological section of this overall report). Weather conditions for the 24 day period on the upper Taku Glacier were generally mild during the daytime, typifying the maritime summer climate of Southeastern Alaska. At night freezing or near-freezing temperatures were the rule at Camp 10A. The maximum temperature at this site for the period of observations was 58°F., the minimum temperature 28°F. Despite an extremely wet summer there was little rainfall during the period of study and no snowfall. In as much as the Juneau Ice Field is at a melting point in summer months, it is of Ahlmann's Temperate Type[2] and Lagally's Warmen Type[3] in a geophysical classification.

The ablation season extended roughly from May to September. The thickness of the 1948-49 accumulation layer at Camp 10 was 14.8 feet

1 Mr. Leighton is Assistant Professor of Geology at Whittier College, California.

2 Ahlmann, H.W:son, "The Swedish-Norwegian Arctic Expedition", Geogr. Ann. Vol. 15.

3 Lagally, M., "Zur Thermodynamik der Gletscher", Zeit. für Gletsch. Vol. 19, 1932.

on August 14 and had an average density of 0.55. This amounts to 98 inches of water, an exceptionally large amount of accumulation considering the ablation losses before August 14. After deducting measured ablation losses up to September 12, the surplus of accumulation over ablation at this site for 1948-49 was approximately 85 inches.

I am indebted to Dr. Robert P. Sharp of the California Institute of Technology, under whose expert supervision the field work and the writing of this paper were done. Many field procedures should be credited to experience gained as Dr. Sharp's assistant on upper Seward Glacier, Yukon Territory, in 1948[4]. Rudolf von Huene, California Institute of Technology technician, constructed most of the equipment. To R. Lange, M.M. Miller, F. Pooler, Z. Stewart, and N.E. Turner, I am deeply appreciative for their help and cooperation in the field.

1. Measurements of Melt-water Percolation

Glaciologic investigations on Isachsen's Plateau, West Spitsbergen[5] and on the Mönchfirn near the Jungfraujoch, Switzerland,[6] represent two contrasting approaches to melt-water study. Ahlmann measured the amount of melt-water formed at the surface; Hughes and Seligman studied melt-water movement at depth. Following considerable experimentation on upper Seward Glacier, Alaska, in 1948[7], an attempt was made to combine these two equally important phases of melt-water study on the Taku firn in 1949.

(a) Equipment and Methods:

Ablation Measurements. At this particular site surface ablation was measured every 12 hours by averaging the lowering of the firn surface at three stationary vertical stakes. The stakes were reset daily. Considering possible errors caused by surface irregularities and settling, measurements are believed accurate to within two millimeters.

4 Note: M.M. Miller of the American Geographical Society also assisted Dr. Sharp on the same expedition in 1948 and has made firn studies on the Juneau Ice Field.

5 Ahlmann, op. cit., pp. 290-291

6 Hughes, T.P. and G. Seligman, "The Temperature, Melt-water Movement and Density Increase in the Névé of an Alpine Glacier," Roy. Astro. Soc., Mon. Notices Geophy. Supp., Vol.4, 1939, pp. 616-647.

7 Leighton, F.B., "Contributions to the Glaciology of the Seward Ice Field, Canada, and the Malaspina Glacier, Alaska", unpublished master's thesis, Calif. Inst. of Tech., 1949, pp. 1-101.

The quantities of melt-water passing through the firn are best gauged by the amounts of surface ablation and rainfall, but these measurements give no indication as to the nature and rates of melt-water movement through the firn. Therefore, the latter were the principal matters investigated in this work.

Melt-water Collection. Ten metal pans of 730 square centimeters were used to collect vertically moving melt-water. They were of two kinds, an open-box type and a funnel type (Figs. 16 and 17). Two pans of 100 square centimeters collecting area were designed to receive the horizontal component of movement to the exclusion of vertically moving water. Each was built with a top, but without a back side. The term pans, unless referred to as horizontal component pans, will connote either the box or funnel type.

Five pits were excavated to depths of 6, 8, 10, 14, and 23 feet, and the pans were buried in the pit walls. Hughes and Seligman[8] completely buried their box-type pans in the firn so that they would not be influenced by radiation and air temperatures, but before doing this they filled the pans with snow and therefore, ~~in a sense, as far as setting was concerned, they~~ produced unnatural conditions. On the Juneau Ice Field small tunnels were cut laterally in the pit walls at different depths below the firn surface. Pans were pushed upward into the roofs of these tunnels until the firn was in contact with the bottom of the pan, or in the case of the funnel pans, in contact with a screen. In this way the firn above the pans was not disturbed, and conditions of melt-water flow into the pans were not altered. Pans which received the horizontal component of flow were inserted laterally into the back faces of tunnels. Before burial all pans were cooled to the temperature of the firn to prevent melting of the snow upon contact.

Twenty-four to thirty inches of packed firn protected the buried pans from atmospheric influences related to the walls of the large pit. The adequacy of this protection was demonstrated by the agreement in melt-water production of two pans placed at the same level, but on opposed sunny and shady sides of a pit.

Melt-water gathering in pans drained through a rubber tube to a receptacle (Fig. 15). The receptacles were covered with funnel tops to exclude extraneous water or snow. Hourly measurements were made during the daytime and frequently at night.

The position of melt-water pans in pit 1 and their relationship to

[8] Hughes and Seligman, op. cit., p. 636

to ice structures[9] and density[10] are shown in Fig. 24. Funnel-type pans IF, $2F_1$, $3F_1$, $3F_2$, $4F_1$, 5F, 6F, 7F, and 8F were installed at 16, 50, 53, 80, 105, 144, 168, and 192-inch levels, respectively. The symbol $4F_1$, as an example, refers to the first funnel-type pan located at the fourth level (80 inches) beneath the firn surface.

Utility pans $1B_1$, $1B_2$, 3B, and 4B of the box type and $2F_2$ and $4F_2$ of the funnel type were reinserted periodically in other pits at the 16, 50, 53, and 80-inch levels so that melt-water collection at these higher levels could be compared at several places. Box-type and funnel-type pans proved equally satisfactory. Pans at the 16-inch level and pans that collected no melt-water were removed after a week to ten days and placed elsewhere in the firn. The two pans, H_1 and H_2, measuring the horizontal component of flow, were buried at progressively deeper levels for short periods. All pans in the same pit wall were in staggered positions.

Pans were purposely positioned directly above and below ice structures in order to study the effect of the latter upon melt-water circulation (Fig. 24). At the 50-inch level in the main pit, pan $2F_1$ was placed directly above a two-inch ice layer. Pans $3F_1$ and $3F_2$ were placed just below the ice layer; pan $3F_1$ also lay under an ice column three to four inches in diameter which transected the ice layer and extended to the firn surface. Subsequently, at the same level in another pit, pan $2F_2$ was placed above the ice layer and pan 3B below the ice layer. No ice column descended to pan 3B.

At the 80-inch level in the main pit (Fig. 24) a pan was fortuitously placed beneath an ice column that descended from the tapered termination of an ice lens nine inches above the pan. Pans were installed in other pits at the same 80-inch level but where there ~~was~~ were no ice structures directly above or below them.

(b) Concentration of Melt-water with Depth:

Fig. 25 presents graphically the average hourly melt-water collections at four different levels during the daytime and the average total melt-water received at night. In general, the deeper the pan the later its maximum melt-water production was attained. Pans buried at 16-inch levels delivered their average maximum flow between 2 and 3 p.m.; pans at the 50-inch levels delivered their maximum flow between 7 and 8 p.m. However, the deeper pans behaved so irregularly that the impression of a descending melt-water front is nullified.

Some of the deeper pans, such as $3F_1$, $4F_1$, and 7F, redeived large

9 Ice structures include ice layers and ice columns which are discussed in detail elsewhere in this report.

10 Firn densities were determined by weighing a sample of firn taken from a hole of known volume with a toothed pipe.

quantities of melt-water; others, such as 3B, $4F_2$, 4B, 4F, 6F, and 8F, received little or no melt-water. For those pans that received melt-water, the amounts increased with depth. Thus the quantity of water measured in deeper firn layers is not representative of the total melt-water produced at the surface in terms of the same units of area. This increased concentration of melt-water with depth is strikingly brought out by Table 1.

Abundant evidence indicates that the concentration of melt-water can be attributed to the influence of ice structures in the firn.

Above the pan at the 16-inch level, the firn is more homogeneous, because it is in the zone of transmitted radiation.[11] All ice structures in this zone are permeable. Pans at the 16-inch level received similar amounts of melt-water and reached their maximum rate of production at nearly the same time of day (Fig. 26).

Table 1 shows that the melt-water generated each day at the surface (column 2) is less than that measured at the 16-inch level. This difference in most instances is beyond the limits of error of ablation measurements from which the calculations of surface melt-water were made. This discrepancy must be due either to concentrations of melt-water in its descent to the pan level or to generation of melt-water beneath the surface. Because all pans at the 16-inch level collected similar amounts of melt-water, the additional melt-water is probably produced beneath the surface by transmitted radiation.

Table I.

	Column 1				Column 2	Column 3		
				Density	Calculated	Measured Melt-water		
	Ablation	Rain	Ablation	at	Melt-water	cc/730cm^2		
Date	(mm)	(mm)	Rain (mm)	Surface	cc/730cm^2	16 in.	50 in.	80 in.
8/15	12.7	2.3	15.0	0.48	614	620	1093	
8/16	14.2	2.0	16.2	0.48	642	682	832	1487
8/17	7.9		7.9	0.50	288	597	472	1587
8/18	15.7		15.7	0.50	574	653	877	1964
8/19	15.7		15.7	0.55	631	773	1048	1969
8/20	14.2		14.2	0.55	570	895	745	1816
8/21	12.7		12.7	0.55	510	858	1120	1760
8/22	15.7		15.7	0.55	631	987	1458	1352
8/23	17.5		17.5	0.55	703	996	1919	1667
8/24	17.5		17.5	0.55	703	996	1018	1419
8/25	15.7		15.7	0.55	631	925	862	1563
8/26	14.2		14.2	0.55	570	816	458	1424
8/27	12.7		12.7	0.55	510	742	322	1249
8/28	19.1		19.1	0.53	739	878	1627	1456
8/29	22.4		22.4	0.55	900	887	597	1429
8/30	27.0		27.0	0.55	1085	1011	772	1626
8/31	19.1	8.4	27.5	0.48	1277	1066	1979	2738
9/1	25.4	4.8	30.2	0.48	1241		3360	3392

[11] The maximum depth of penetration of transmitted radiation was estimated to be 26-40 inches. The phenomenon is discussed in the section on firn structures.

Note: Data in column 2 were calculated from data in column 1 for a pan area of 730cm^2.
Data in column 3 represent daily melt-water totals averaged for the 16, 50, and 80-inch levels.

Furthermore, on most cloudy days when radiation was at a minimum the calculated melt-water approximated the measured melt-water.

Results of melt-water collection at the 50 and 53-inch levels are given in Fig. 28. Despite the fact that five pans were located roughly at the same level, they varied greatly in melt-water volumes and melt-water cycles. Pans $2F_1$ and $2F_2$ placed above ice layers produced more water than pans $3F_1$, $3F_2$, and 3B beneath ice layers. In fact pans 3B and $3F_2$ received almost no melt-water until August 31, and are therefore not shown in Fig.28. Thus, these ice layers served as barriers to melt-water flow. Melt-water reaching the ice layers was arrested and compelled to flow laterally until it reached openings in the ice layers or terminations of the ice lenses.

Even greater variance in flow was measured at the 80-inch level. Little or no water was collected by pans $4F_2$ and $4B_1$, but pan $4F_1$ collected more melt-water than any higher pan.

Hour to hour results of pan $4F_1$ are compared to those of pans $2F_1$ and $3F_1$ in Fig. 29. The maximum flow to pans $2F_1$ and $3F_1$ shows no correlation whatsoever to the maximum flow of pan $4F_1$. Hour to hour flow was also more erratic and the maxima less well-defined in the case of pan $4F_1$.

The position of pan $4F_1$ with relation to ice structures in the firn (Fig.24) is believed to be the reason why it was the only pan to collect melt-water at the 80-inch level, and also why it collected melt-water so erratically. The ice column that descended to the pan from the tapered end of an ice lens at 71 inches depth, apparently controlled the flow of melt-water which had moved along the lens to its tapered end. Other ice structures above the lens may have also played a part in complicating and concentrating the drainage.

The remaining four pans at deeper levels produced minor amounts or no melt-water with the exception of pan 7F. The increase in size and number of ice structures in depth apparently caused greater irregularity of flow. Pan 7F collected almost no melt-water the first week after it was installed, but on August 30 it suddenly began producing melt-water in large quantities. Water formerly flowing in another direction was apparently diverted to pan 7F. This possibly was the result of a recess dug adjacent to pan 7F the day before.

The aforementioned pan records have shown to the writer's

satisfaction that below the zone of transmitted radiation melt-water is diverted and concentrated along certain channels of flow by impermeable ice structures, both horizontal and vertical. Owing to the increased complexity of these ice structures with depth, loci of flow became more unevenly distributed. Once established, these loci continued to exist as evidenced by the fact that on successive clear days, melt-water maxima for any one pan occurred in sequence, and usually with the same time interval separating them. The record of pan 7F indicates diversion of melt-water, but this may have been man-made as shown above.

(c) Correlation of Melt-water Flow with Meteorological Record:

In all pans the ascent to daily maximum flow was generally much more rapid than the descent from it (Figs. 26,28, and 29). This trend followed that of daytime temperatures which increased rapidly to a maximum and then decreased gradually. Melt-water flow at the 16-inch level was more closely correlated to air temperature changes than at the deeper levels. The shallow pans also show sharper and steeper peaks on the graphs than the deeper pans. Pans at the 16-inch level ceased receiving flow during nocturnal sub-freezing temperatures while pans at the 50, 53, 80, and 168-inch levels continued to deliver substantial quantities of melt-water.

Meteorological data are compared with ablation and melt-water data in Fig. 30. The daily rates of ablation and melt-water flow, and the average daily temperatures all show a similar trend during clear days. Although air temperature appears to be the most important factor influencing ablation, no single meteorological factor can be used to predict daily ablation. Ablation would be a reliable indicator of the volume of melt-water flow, if it were not for the varying density of the firn surface and the amount of melt-water received as rainfall.

Although ablation and melt-water production were high on rainy days (Table I and Fig. 30), rainfall itself does not appear to be the principal cause. The well-established computation for ablation from rainfall is:

$$A = \frac{P(Tw-32)}{144 \times D}$$

where P is the rainfall in mm, Tw is the wet-bulb temperature (assumed to be the temperature of the rain), and D is the density of the firn. Substituting the data of September 2 in this equation, 42°F for Tw, 4.5 mm for P, and 0.48 for D, the maximum ablation accounted for by rainfall would be only 0.65 mm of water as compared with the measured ablation of 20 mm of water. Even a wet-bulb temperature of 60°F under the same circumstances would produce no more than 2 mm of water.

Consequently, high ablation and copious melt-water on rainy days

must result from the average temperatures, extremely high humidity accompanied by condensation, and moderate winds which accompanied the rain.

(d) Rates of Flow:

Volumetric Flow Rates. The greatest rate of flow recorded was from pan 4F1, 80 inches below the surface. For the pan area of 730 cm^2 this rate was 0.46 $cc/cm^2/hr$. Seligman[12] recorded an identical maximum rate on the Mönchfirn for a pan at 40 inches depth. The average maximum rates in $cc/cm^2/hr$. for the different pan levels were as follows: 16-inch level, 0.14; 50-53-inch level, 0.17; 80-inch level, 0.20; 168-inch level, 0.15,

Velocity of Flow. Water soluble fluorescein dye was used successfully as a tracer to enable visual observation of the velocity of melt-water flow. Its characteristic yellow-green color can be distinguished at a dilution of one part in 10,000,000. The diffusive power of the dye in extremely dilute solution and at near-freezing temperatures was determined to be ~~nil.~~ limited.

During nine sunshine-days dye was spread on the firn surface hourly from 9 a.m. to 6 p.m. Trenches were dug after each ensuing hour to determine the depth of penetration of the dye in the firn. The average of these hour by hour records is shown below.

Hour of Day	Rate (inches per hour)
9-10	8
10-11	16
11-12	20
12-1	23
1-2	25
2-3	19
3-4	15
4-5	16
5-6	12

The rates of dye percolation in ice columns ranged from one to eleven inches per hour more than the tabulated figures.

The maximum hourly rate of dyed melt-water flow shows a close correlation with the hour of maximum melt-water flow at the 16-inch level which varied between 1 and 3 p.m. When it rained the percolation rate increased, the amount depending upon the intensity of the rain. The rate of flow is obviously a function of the rate of water supply.

Long-period measurements were made by noting the rate of descent of

12 Seligman, op. cit., p.637

dyed melt-water from the surface to groups of small cylindrical holes bored 2 feet horizontally into the walls of a pit along specified levels. An extremely dilute solution of fluorescein dye was spread evenly on the firn surface above the pit walls. The dye reached the core-holes of each horizontal plane at different times, the advancing dyed-water front becoming more irregular with depth. For example, at the time that the first traces of dye reached a depth of 14 feet at one place in the main pit, the maximum penetration below the surface in neighboring areas was only 9 feet. At 23 feet depth the differences in penetration along different parts of this same pit wall had increased from 5 to at least 12 feet. In addition to this vertical range the lateral configuration of the dye front became more irregular with depth.

The dye reaching the 14-foot level had moved at an average rate of 10 - 11 inches per hour. This is much less than the average rate of percolation, 19 inches per hour, in the upper three feet of firn. The decrease in rate of flow and the increasing irregularity of the dye front can be attributed to the increase of density and heterogeneity within the firn at depth.

If the maximum flows recorded by the various pans shown in Fig.25 all belong to the same daily melt-water wave, the average velocities of flow between pan levels in the main pit would be as follows:

Firn Layer (inches)	Inches per hour
16-50	6-9
16-80	32 plus
16-168	38-76

These figures show that no uniform melt-water wave is in evidence here; nor is one in evidence if the peaks on the curves of Fig. 25 are considered to be one wave out of phase. Velocities of the lower firn layers computed for a two-day instead of one-day wave cycle are 2-6 inches per hour. These velocities are probably nearer the true order of magnitude of melt-water flow at depth, but they also indicate the irregularity of melt-water front.

Horton[13] and Oechslin[14] have recorded constant velocities for water moving through snow and firn of certain densities. Such relations do not attain on the Juneau Ice Field where there are so many complicating factors. These factors in order of estimated importance are the size and number of ice structures, the rate of water supply, and the

13 Horton, R.E., "The Melting of Snow", Mon. Wea. Rev., Vol.43, p. 603.
14 Church, J.E., "Snow and Snow Surveying; Ice," Chapt. 4 in Hydrology, McGraw-Hill, New York, 1942, p. 132.

texture and density (permeability) of the firn itself. Below the zone of transmitted radiation, velocities of flow are only local and are not constant for similar sections of the same firn layer.

2. Nature of the Melt-water Movement

Firn by definition is a porous medium, the voids between ice crystals being filled with water and air. The water in firn may be of two types: first, capillary water which is held by surface tension in the crystal interspaces and as a film about the crystals, and secondly, gravity water which drains through the influence of gravity. Although the vapor pressure over ice is less than over water, transport of melt-water as a vapor is believed to have been negligible, since the temperature of the Taku firn was isothermal, and since the relative humidity in the firn is assumed to be nearly 100 per cent.

When cakes of firn were lowered into contact with a water surface, the firn acted as a sponge to soak up the water gradually. The height of the rising water was nearly horizontal at all times as though the water were moving upward in thin parallel tubes of nearly equal diameter. According to the laws of capillarity the height to which the water would eventually rise is chiefly dependent upon the radius of the capillaries. Therefore, the openings in the firn were assumed to be relatively uniform.

Disregarding the influence of ice structures and the rate of water supply, the most important factor in the percolation of melt-water is the size of the firn grains and their interspaces. As in soil of uniform texture, the finer the grains, the larger is the amount of water that may be retained by capillary force. In early summer the near-surface firn is generally less coarse and less dense than in mid-summer. Despite the coarseness of the near-surface firn in late August in the Taku accumulation area, the influence of capillarity was still significant. This was concluded in the light of the following observations.

Dyed melt-water percolating downward through the firn moved around rather than into tunnels excavated horizontally into the walls of a pit. This indicated that the capillary attraction of the firn was greater than the force of gravity.

A lag of at least several hours occurred between the time of burial of melt-water collecting pans and the time that they first delivered water. This was not related to the short distance of transport of melt-water from pan to receptacle. Instead it was probably a direct consequence of capillarity, because the firn in contact with the pan had to become saturated before water flowed into the pan. This is suggested by a one to two-inch saturated layer of firn found above the bottoms of all pans producing melt-water. Where pans failed to produce melt-water no saturated layers were found. In

one instance, pan $1B_1$ was removed, its saturated layer sliced away, and the pan placed in its original position. As a result it was almost 24 hours before the pan again collected melt-water.

The behavior can be explained as follows. As the liquid water content[15] of the firn within the pan gradually increases, the cohesion between water molecules becomes greater than adhesion of water for the firn grains. When the firn becomes saturated, capillarity is overcome. The rate at which saturation takes place depends, of course, upon the rate of water supply and the porosity of the firn.

The horizontal component of flow was measurable only in the near-surface firn. Fig.27 graphically compares the horizontal component of flow with the vertical component at the 16-inch level. Maximum horizontal flow was always less than 10 cc per hour, while maximum vertical flow was close to 100 cc per hour. The horizontal pans show a marked, if somewhat erratic, trend of rapidly reaching their maximum output in early morning and then gradually declining to zero in late afternoon. In all but one case, daily maxima were reached five hours before maxima of pan $1F_1$. Significant, also, is the fact that pans H_1 and H_2 began and terminated their melt-water collection at the same time as pan $1F_1$.

These results seem best explained by the effect of capillarity in the firn. In the unsaturated firn of early morning, capillary forces dominate, and movement is confined to the smaller pores. Melt-water may move in any direction, because capillary forces act in all directions. Thus, melt-water moves laterally as well as upward and downward. This was demonstrated by the irregular anastomosing veinlet paths of dyed melt-water in unsaturated firn. Where capillary channels carrying dyed melt-water became obstructed by large firn grains or by impermeable small grain clusters, the flow changed direction along lines of lesser resistance. There was also a tendency for the water to keep to the crystal aggregations and avoid the large inter-crystal spaces. As surface melting increases in late morning, the water in the firn will exceed capillary saturation. Gravity necessarily becomes the controlling force, and the rate of downward movement materially increases.

[15] Liquid water content was measured by one of Bader's non-calorimetric methods (Bader, H., "Theory of Non-calorimetric Methods for the Determination of the Liquid Water Content of Wet Snow", Schweiz. Min. Petr. Mitt., Vol.28, 1948, pp. 355-361). This involved measuring the dilution of a known amount of normal solution with a precision thermometer. Owing to the lack of satisfactory equipment results are considered of limited value.

Seligman[16] contends that capillary action is more effective than gravity in controlling water movement through firn, except when melt-water has melted the snow grains and formed free-fall channels or has saturated a layer of firn from which it can free-fall through space. It is believed that gravity flow predominates at depth, because the firn there, at least in certain areas, is saturated. Ice structures have already been shown to have the effect of damming, diverting, and concentrating melt-water flow. Where melt-water is concentrated, the firn becomes saturated, and gravity flow supplants capillary flow. In these saturated zones the rate of downward movement is restricted by the permeability of the least permeable horizon. Thus, impermeable ice layers act similarly to funnels with constricted stems in controlling the movement of melt-water in the firn above them.

3. Observations on Diurnal Surface Crusts and Sun Cups

(a) Diurnal Surface Crusts

At the 3,600-4,000 foot elevation during the period of observations in late summer, a surface crust began to form each clear day between 5 and 6 p.m. It would grow from the surface downward to a maximum depth of 8 inches and melt by 1 p.m. the following day.

A study of the effects of freeze and thaw upon firn density contributed to the study of melt-water behavior in the surface crustab layer. The chief aim was to determine the day by day change in density of the crust for as long a period as density samples could be cored in the same stratum before that stratum was ablated. Ideal conditions for these measurements were successive clear days when sufficiently thick crusts formed. It was found that cores could be taken at an initial depth of three inches for no longer than four days. Records for the period August 25-28 are shown below. Each sample was cored and weighed between 8 and 10 a.m. before the crust had melted.

Date	Density at Initial Depth 3 Inches		Maximum Crust Thickness(inches)
	No.1 Station	No.2 Station	
8/25	0.63	0.59	3-5
8/26	0.57	0.54	$2\frac{1}{2}$ -$4\frac{1}{2}$
8/27	0.54	0.52	$4\frac{1}{2}$ -6
8/28	0.53	0.52	5 - 8

16 Seligman, G., "Snow Structures and Ski Fields", Macmillan and Co., London, 1936, p.280.

A significant progressive decrease in the density of the crust is evident from these data. A crust containing a small amount of moisture will freeze into a less dense mass than one which is relatively wet. However, this progressive decrease is believed to be directly related to changes in the firn fabric and not to the liquid water content. A very dry surface firn will harden more slowly than a wet firn. Because the crusts were observed to form every evening between 5-6 p.m. and grow at a similar rate until 10 p.m., the liquid water content is believed to have been fairly constant.

During the daily thawing period the smaller ice crystals melted more rapidly than the larger ones; leaving a porous texture with a lower density. When freezing took place at night a coating of ice was added to these larger crystals. It seems likely that there was further minor growth of these crystals by accretion in the morning when the first surface melt-water, in seeping downward, encountered the sub-freezing temperatures of the lower crust. With the increase in coarseness and porosity the surface tension was diminished. As a result, less capillary water was retained by the firn. Thus, the increase in porosity and decrease in capillary water were responsible for reducing the density.

Density samples were taken at depths of three and twelve inches in order to compare densities inside and outside the crustal zone. These measurements were made three times daily. The results are given below.

	INITIAL DEPTH AND STATION			
	3 Inches		12 Inches	
Date	Station 1	Station 2	Station 1	Station 2
8/25				
9-10 a.m.	0.63	0.59	0.53	0.51
1-2 p.m.	0.56	0.56	0.54	0.52
5-6 p.m.	0.55	0.54	0,54	0.50
8/26				
8-10 a.m.	0.57	0.54	0.54	0.49
1-2 p.m.	0.53	0.49	0.56	0.51
5-6 p.m.	0.52	0.49	0.54	0.51
8/27				
8-10 a.m.	0.54	0.52	0.54	0.50
1-2 p.m.	0.50	0.49	0.54	0.53
5-6 p.m.	0.49	0.49	0.53	0.52
8/28				
9-10 a.m.	0.53	0.52	0.52	0.51
5-6 p.m.	0.49	0.49	0.50	0.52

Comparison of the daily trend of densities at the initial three-inch level with those at the initial twelve-inch level is especially

illuminating. It is evident that the changes in density at the twelve-inch level are less significant and are not affected appreciably by atmospheric influences.

Melting by transmitted radiation beneath the firn surface (without concomitant settling) probably played the greatest part in reducing the density at the initial three-inch level after the crust disappeared. The fact that the preceding table shows an increase in density at this level between 5-6 p.m. and 8-10 a.m. the following morning supports this thesis. In general, greater densitites were recorded between 1 and 2 p.m. than between 5 and 6 p.m. This is attributed not only to the time factor of greater melting in a whole than half day, but also to the greater amount of melt-water in circulation near the surface at mid-day.

(6) Suncups

Introduction. F.E. Matthes[17] proposed the term suncups for cuspate hollows, only a few inches in depth, on snow and firn surfaces usually at moderate to high elevations. Under favorable conditions at even higher elevations intensified forms of suncups called sunpits[18] grow to depths of a number of feet.[19]

These terms not only indicate the form of the hollows, but link them with their principal genetic agent, the radiant heat of the sun. Suncups are not to be confused with indirect ablation phenomena, nor with ripples and ridges formed by the wind. The shape of suncups is similar to the "scalloped" surfaces of Workman[20] and Sharp[21] which are the "cuspate" or "negatively mammillate" surfaces of Leighly.[22] However, the latter forms occur in sheltered spots protected from the direct rays of the sun.

Suncups and sunpits are generally interpreted as the result of evaporation. This theory is based on observations that suncups and sunpits develop best on high mountain glaciers and snowfields in latitudes below 50° and in a dry summer climate. It was surprising, therefore, to find suncups on the Juneau firn under conditions of relatively low elevation, high latitude, and humid summer climate. This occurrence requires a description and interpretation.

Description. During sunny periods, firn on the Juneau Ice Field was suncupped (Fig.12). Intervals of cloudy weather and rain

17 Matthes, F.E., "Mount Rainier and its Glaciers", Dept. Interior, Washington, D.C., 1914, pp. 17-18

18 Matthes, F.E., "Ablation of Snow-Fields at High Altitudes by Radiant Solar Heat", Trans. Amer. Geophys. Un., 1934, p.381.

19 The pinnacles or pillars between the sunpits are the well-known nieve penitente.

20 Workman, W.H., "A Study of Nieve Penitente in Himalaya", Zeit. für Gletsch., Vol.3, 1909, p.263.

21 Sharp, R.P., "The Wolf Creek Glaciers, St. Elias Range, Yukon Territory," Geogr. Rev., Vol.37, 1947, pp. 46-47.

22 Leighly, J., "Cuspate Surfaces of Melting Ice and Firn", Geogr. Rev., Vol. 38, 1948, p.300.

destroyed the cups entirely on two occasions, but in both instances they were renewed by two to three days of sunshine.

The suncups were best developed on flats or on gentle slopes facing the sun and were present on all gentle slopes receiving direct sunlight. Typical depressions on a horizontal surface were almost symmetrically cuspate, having a slight east-west elongation. They averaged roughly 10-12 inches from rim to rim and 3-4 inches in depth, with a maximum depth of 6 inches. Aside from some coalescence, their maximum size appeared to be related generally to their initial size. Measured footprints in the firn, for example, would eventually show an enlargement in width three times as much as depth.

Well-developed suncups had a steep south wall and a gently sloping north wall, making the north-south profile across the alternating ridges and depressions saw-toothed. The steeper walls were inclined toward the south at a uniform angle, approximately that of the sun's elevation at mid-day.

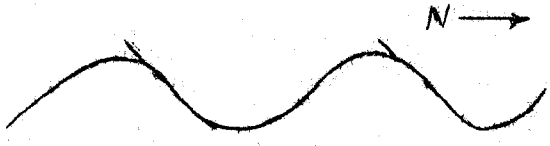

On clear evenings a thin ice layer formed on the steep south wall. As a result of differential melting the following morning, this ice layer projected as a lip, an "ice shingle", above the wall (see above sketch). Where numerous, these gave the firn field the appearance of a minature wind-tossed sea with white caps. This effect was lost when looking south-ward. By mid-day the "ice shingles" had melted.

On slopes where the suncups are elongate, the long axis of the cups was invariably aligned downslope. The steeper the slope, the greater was this elongation and the shallower the cups. Suncups, two feet long and two inches deep, were not uncommon on a 15° slope.

Origin. Heretofore, suncups at high elevations have been regarded as sun-evaporated hollows. However, during August when the writer made his observations meteorological measurements indicated that evaporation on the Juneau Ice Field was relatively ineffective. On only one day during the month was the dew point of the air next to the firn surface below freezing. In addition, there was little movement of air. Thus, it can be concluded that ablation was chiefly by melting.

The cups themselves are the product of differential melting. The question arises, was this selectivity caused by differences in density or by slight initial depressions in the surface of the firn, or both. The absence of dust ruled out indirect ablation. Differences in density

were apparently not a factor. In general, the density was uniform at the surface except where there were ice columns. Even they failed to form the walls of sun cups. Atmospheric eddy currents were not considered a factor. Had they been, they might act to reduce the more vulnerable rims once the depressions were formed.

Original slight depressions, with their north slopes producing a concentration of the sun's rays, appear to have initiated the cups, and subsequently in their evolution other factors played a part.

A horizontal firn surface reflects about 60 per cent of the solar radiation when the incidence of the sun's rays is 45°. Because of a greater angle of incidence more solar heat is absorbed by the initial slope on the north side of the depression, and more firn is melted there. Furthermore, a fraction of the radiation impinging on the north face is reflected and caught by the slopes of the depression. More melt-water is thus produced in the depression than on the ridge top.

An additional factor that promotes greater melting in the depressions than on the ridge tops is the freeze-thaw process. This occurs on all clear days and nights, and it acts in two ways: first, to form "ice shingles" (already described) and secondly to form a crust which reached a thickness of one to eight inches between 4 and 6 a.m.

"Ice shingles" formed in early evening. The only melt-water, usually small in amount, produced this late in the day was on those slopes where the sun's rays were concentrated. This melt-water was trapped and frozen as a thin ice layer, or "ice shingles", which retarded melting of the firn on the south wall the following day.

The thickness of the diurnal crust was measured early each morning. A fluorescein dye pattern observed in vertical section provided a check as to the exact depth of the crust. It was always thicker in the ridges than in the hollow of the suncup. This is attributed to the greater surface area exposed to sub-freezing temperatures in the ridges. As a consequence of the diurnal freeze-thaw process, melting was more effective in depressions than on ridges the greater part of the sunshine day.

The maximum depth of the suncups was controlled by the relative rates of downmelting of ridges and hollows. Deepening of a hollow below the ridge-top level increased the surface area and sharpness of the ridge exposed to melting and, therefore, its susceptibility to melting. The suncups deepened until the ridges and depressions were melted equally.

The reasons that the suncups did not display a more pronounced east-west orientation are not at once evident. The sun warmed the depressions first on their east-facing side, then more so on the south-

facing side, and in the afternoon with less intensity on the west-facing side, while the north-facing side remained comparatively unaffected. The tendency for the suncups to develop a crescent shape is attributed to this relation.

However, atmospheric heat, which was generally at its maximum elevation, acted to overcome the sun's effect of differential melting by melting all sides equally. Moreover, it is believed that drainage of melt-water to the centers of the depressions aided in accentuating the cone-shaped form. Dye patterns showed greater downward percolation of melt-water below the centers than below the sides.

4. Ice Layers and Ice Columns in the Firn[23]

(a) Ice Layers:

Introduction. Horizontal ice layers in glacial firn were first reported by Saussure.[24] The term ice lens will be employed synonomously with ice layer, because all but one of the horizontal ice layers above a depth of 23 feet (the deepest level investigated) were non-uniform in thickness, were discontinuous within 20 feet, and tapered at both ends. The one exception was a 4-10 inch continuous ice layer which is believed to mark the top of the 1947-48 annual firn layer. This will be referred to as the annual ice layer.

Correlation of ice layers from pit to pit was made unusually difficult by their lensing habit. Only the ice lenses at depth 51.5 inches could be correlated with confidence across the 50 yard strip investigated.

Description. Before solar radiation had caused "frosting" of ice layers exposed in vertical section, their color was a deep blue which distinguished them from the firn layers and produced a distinct layering.

The ice layers averaged two inches in maximum thickness. They increased in thickness irregularly with depth, never exceeding three inches with exception of the annual ice layer. The number of ice layers also increased with depth. Where they occurred in clusters they were less than 1.5 inches thick. Sometimes they were grouped so closely that the thickness of individual ice layers exceeded that of the intervening firn layers.

[23] Ed. note: See Miller, M.M., "Preliminary Report of Field Operations, The Juneau Ice Field Research Project - 1949 Season", American Geographical Society, January 20, 1950, pp. 12,13.

[24] Agassiz, L., "Systeme Glaciare", Paris, 1847, pp.201-202.

On the vertical wall of the 23-foot pit, ice layers constituted 8 per cent of the area. Nearly all layers had level bases, but uneven, mildly undulating upper surfaces.

Density samples of ice layers were taken with a brace and bit. The results from this method were not wholly satisfactory. The density of ice layers was above 0.88 as compared with the maximum density, 0.71, of the firn at a depth of 22 feet. This increase is produced principally by the refreezing of melt-water between firn crystals. The firn just under the ice layers was less dense than the firn just above, with differences as great as 0.13. The minimum density measured, 0.48, was under an ice layer at a depth of 11 feet.

Ice layers below three feet in depth were commonly inequigranular. Crystal shapes were irregular, but generally nearly equant. Where elongate, crystals were oriented with their long diameters perpendicular to the firn surface. Diameters ranged from 0.04 - 0.55 inches, with an average of 0.16 - 0.24 inches. Contact surfaces of crystals were irregular and tightly interlocked. All ice layers observed were bubbly. Air bubbles were generally spherical, but a few were ovoid. A semblance of horizontal stratification was preserved in the ice layers.

Crystals in ice layers within the zone of sunlight penetration (above roughly three feet in depth) had average diameters of 0.20 - 0.28 inches. In the diurnal crustal layer within 8 inches of the surface, the average was closer to 0.40 inches.

Two processes were responsible for this increase in crystal size. Above the maximum depth of sunlight penetration, destruction of smaller crystals by melting predominated because of their greater surface area per unit volume. In the surface crustal layer, melt-water refroze on the remaining crystals to increase their size. Both of these processes, therefore, increased the average crystal size of the firn as well as of the ice layers.

Below three feet in depth, the individual crystals[25] composing ice layers were difficult to distinguish. Only occasionally were the crystal boundaries defined by entrapped air bubbles. However, when directly exposed to the sun or to above-freezing temperatures, crystals developed visible sutures at their boundaries. These sutures were integrated and enlarged during continued exposure until the ice layers became masses of loose crystals.

Ice layers near the surface were greatly affected by solar

[25] Crystals were distinguished only megascopically and therefore, may occasionally consist of more than one individual crystal.

radiation. Of a given quantity of radiation reaching the firn surface at least 60 per cent will be reflected.[26] The transmitted radiation reaches a depth dependent upon the inclination and wave length of the rays and on the "groundglass scattering effect" of the ice crystals. The maximum penetration of transmitted radiation was empirically measured by observing to what depth the ice layers were disarticulated. Extremely dilute fluorescein dye solutions penetrated the permeable ice layers to a maximum depth of 26-40 inches. This may be compared to the 51 inch maximum radiation penetration depth measured by Olsson[27] with a photoelectric cell, and to the 20-inch maximum depth (in snow) measured by Gerdel[28] with a pyrheliometer.

The depth of penetration varies with firn density, texture, and melting conditions. As pointed out by Gerdel[29] melt-water may absorb radiation as it percolates downward, and thus carry heat to a lower depth. In view of the slow rate of melt-water percolation through firn, this depth is not only within the magnitude of error in measuring the depth of disarticulation, but stratigraphically above the maximum penetration of short-wave radiation whose heating effects are nil.

Below the lowermost depth of melting, dye solutions flowed laterally along impermeable ice layers to points where the ice layers became discontinuous. As the surface was lowered by ablation, the ice layers not only became disarticulated and permeable, but also became carriers of melt-water. When an ice layer came within 20 inches of the surface, dye solution penetrated the ice layer and flowed laterally through it, instead of along the top of the layer.

Incipient disarticulation preceded visible melting. This fact indicates either that the melting point at crystal contacts was lower than that of the bulk of ice or that there was greater heat absorption at crystal contacts.

Origin. Despite the fact that Agassiz[30] initially recognized two types of ice layers, namely, the primary ice layers in the firn and the secondary "blue bands" of the lower glacier, the origin of ice layers in the firn had long been attributed to differential movement and to

26 Wilson, W.T., "An Outline of the Thermodynamics of Snow-melt", Trans. Amer. Geophys. Un., 1941, pp. 182-195;
Wallen, C.C., "Glacial-Meteorological Investigations on the Kårsa Glacier in Swedish Lapland", Geogr. Ann., Vol.30, 1948, pp. 494-496.

27 Olsson, H., "Radiation Measurements on Isachsen's Plateau," Geogr. Ann., Vol. 18, p.240.

28 Gerdel, R.W., "Penetration of Radiation into the Snow Pack", Trans. Amer. Geophys. Un., Vol.29, 1948, p. 372.

29 Gerdel, op. cit., p. 371

30 Agassiz, L., "Geological Sketches", New York, 1894, pp. 248, 260-261.

the refreezing of melt-water produced by friction along shear planes.[31] Agassiz related the ice layers to former surface crusts and to the freezing of rain which spread along the top of a dense firn layer below the surface.

As far as is known, Sverdrup[32] was the first to suggest that ice layers form from downward percolating melt-water. This conclusion was drawn from observations of ice layers on Isachsen's Plateau, West-Spitsbergen. At a campsite on the North East Land Icecap, Moss[33] found a four-inch layer of saturated firn at a depth of five feet which lent support to this theory.

As a result of their crystallographic investigations of the Jungfraujoch firn, Perutz and Seligman[34] concluded that ice layers "originated in a stratum of water in firn... where melt-water is either held up by a crust or by a particularly fine-grained layer of firn of high capillarity."

Many lines of evidence attest to this origin of ice layers in the areas investigated. The gently undulating upper surfaces and the even base surfaces of ice layers, the continuity of horizontal stratification in the ice layers with the stratified structure of the firn and ice columns, the lower density of firn below an ice layer support the view that their growth takes place by the refreezing of downward percolating melt-water.

Further confirmation of this origin was provided by actual observation of the formation and growth of ice layers at the firn surface inside the camp tent. Wooden boxes and other non-conductors became perched on firn pedestals owing to differential ablation. Melting of the pedestals furnished water which seeped downward to a layer of high retentivity where it was frozen by diurnal chilling, forming an ice layer. This layer grew to a thickness of 2.5 inches in three days.

The development of this ice layer probably duplicates the development of ice layers in depth. Thus, the requisites for the formation of

31 Philipp, H., "Geologische Untersuchungen über den Mechanismus der Gletscherbewegung und die Entstehung der Gletschertextur", New. Jahrb. für Min., 1920, pp. 502-508;
Drygalski,E., "Über die Struktur des grönländischen Inlandeises und ihre Bedeutung für die Theorie der Gletscherbewegung", Dies. Jahrb., 1900, p.76.

32 Sverdrup, H.U., "Scientific Results of the Norwegian-Swedish Spitsbergen Expedition in 1934", Geogr. Ann., Vol.17, 1935, pp. 78-80.

33 Moss, R., "The Physics of an Ice-Cap", Geogr. Jour., Vol.92, 1938,p.219.

34 Perutz, M.F. and G. Seligman, "A Crystallographic Investigation of Glacier Structure and the Mechanism of Glacier Flow", Proc. of the Roy. Soc. of London, Vol. 172, 1937, p. 346.

an ice layer in depth appear to be a firn horizon of high retentivity for water, below-freezing temperatures, and a supply of downward percolating melt-water.

As already discussed, transmitted radiation disarticulated ice layers within three feet of the firn surface. When the ice layers reached the crust-forming zone they were nearly completely disintegrated. This prevented an increase in thickness of ice layers in the crustal zones, because water passed on through the layers. In pit walls on mornings following the formation of a crust, ice layers were observed to have grown at the expense of the overlying firn layer where the wall was completely shaded. These ice layers were wedge-shaped, thinning into the wall. Direct radiation during the morning prevented the refreezing of melt-water on the upper surfaces of other ice layers, rendering them even more permeable than the contiguous firn layers.

Theoretically, ice layers may form in the autumn during the incidence of the winter cold wave, in the winter during the periods of thawing, and in the spring during the dissipation of the winter cold wave. However, in the autumn the greater part of the melt-water should have time to percolate away before the temperature of the firn falls below freezing.[35]

Ahlmann[36] states that the most continuous and thickest ice layers on Isachsen's Plateau correspond to crusts frozen in the autumn at the end of the ablation season. This was true on the Juneau Ice Field in the instance of the top of the 1948 layer, the only annual dirty horizon identified. At the end of the 1948 ablation season the firn must have been suncupped, because the base of the overlying annual ice layer was scalloped similarly to the 1949 firn surface. The horizontal base surfaces of other ice layers probably represented former wind-packed surfaces or the tops of other denser layers.

Icification increased progressively with depth in the 1948-49 accumulation layer despite the presumably greater negative firn temperatures near the surface.[37] This was largely because of the increased retentivity and greater specific heat in depth, and the longer time available for growth of new ice layers and thickening of all ice layers. The same ice layer may, of course, continue to thicken at its upper surface as long as it remains within the depth of penetration of the winter cold wave.

[35] Sverdrup, op. cit., p.88
[36] Ahlmann, H. W:son, "Results of the Norwegian-Swedish Spitsbergen Expedition in 1934", Geogr. Ann., Vol. 17, 1935, p. 36.
[37] Sverdrup, op. cit., pp. 69-71.

Meteorological records from the U.S. Weather Bureau in Juneau suggest that surface melting occurred on the ice field during the spring of 1949. Such melting tends to increase the number of ice layers with depth. Alternating accumulation and melting during the spring would afford the 1948-49 accumulation layer greater opportunity to form new ice layers.

(b) Ice Columns:

Introduction. No extensive description of ice columns appears in the literature. Ahlmann[38] first christened these forms "ice glands". Subsequently, Moss[39] and Glen[40] referred to them as columns of ice and pipes, respectively. Of these designations, ice column is more apt and will be used here.

Description. Where exposed by ablation, ice columns were readily recognized by their characteristic protrusions above the firn surface as small rounded knobs of coarse frosted ice crystals, either disjointed or "loose in their sockets". The knobs ranged from one to six inches in diameter. Their relief was never over three inches and was produced by differential melting, which in turn was dependent upon the weather. As a general rule the greater the rate of ablation, the greater the difference in melting between the firn and ice knobs. On sunny days, their frosted appearance blended in with the general firn surface. On rainy days they were more conspicuous; not only was their relief accentuated, but their crystalline character was compacted and less frosted.

Though regularly distributed on a broad scale, ice columns were unevenly distributed on a smaller scale, often occurring in groups on the flats. On slopes they were linearly aligned with the inclination of the slope. From a distance they appeared as parallel sinuous dotted-lines. The knobs also showed a linear trend over concealed crevasses. Thus, the traces of underlying crevasses could be accurately determined.

The knobs made their appearance above the surface progressively later at successively higher elevations. As the summer progressed, ablation exposed an increasing number within a given area. On August 14 in the vicinity of Camp 10, the number counted averaged one per three square feet over concealed crevasses and one per ten square feet elsewhere on the flat. By August 31 the count in this same area had increased to one per two square feet over concealed crevasses and one per six square feet elsewhere.

38 Ahlmann, op. cit., p. 35.
39 Moss, op. cit., p. 219.
40 Glen, A.R., "A Sub-Arctic Glacier Cap: The West Ice of North East Land", Geogr. Jour., Vol. 98, 1941, p. 143.

A vertical pit wall has a much better chance of cutting a horizontal ice layer than a vertical ice column. Nevertheless, square pits 10 feet on a side and up to 23 feet deep revealed blue ice columns at all levels.

On flats, the vertical, roughly cylindrical ice columns formed the core of a system of lateral projecting ice layers. Several such systems were in some instances connected, forming a network of horizontal ice layers and vertical ice columns. Where ice columns were absent, the horizontal ice layers were also usually lacking or at least poorly developed.

Ice columns require three-dimensional analysis. Surface exposures and pit walls supply clues, but it is only by excavation that the three-dimensional nature of these features can be studied. This was accomplished by digging around the ice columns with a small shovel. The boundaries of the ice columns were so sharp below the disarticulated level that the remaining firn could be scraped away with a knife. Even so, the firn in contact with the dense columns was slightly coarser than more distant firn.

Ice columns were one to six inches in diameter and from one to seven feet in length. Most terminated downward at an ice lens; others extended downward from an ice lens, or connected one lens to another. Columns and lenses commonly formed inverted pedestals and sometimes pedestals and I bars. Ice layers formed lateral offshoots from the columns and resembled irregular ribs extending out from a backbone. These offshoots were thickest at their juncture with the ice columns. A few columns were offset by several feet at ice lenses, the lower part usually extending downward from the tapered or blunt end of the lens.

Though generally vertical and roughly cylindrical many deviations in size and shape were observed. Columns commonly pinched and swelled, or formed nodular outgrowths. Many bulges in the columns attained 16 inches in diameter. Some columns bifurcated and formed inverted Y's. Gnarled, twisted forms mentioned by Ahlmann[41] were not observed by the writer. On slopes were all gradations between laterally-connected chains of vertical columns and ice structures of dike-like form. All of these were concentrated in great numbers at the bottom of slopes.

Ice columns are essentially of the same crystalline character and density as ice layers described in the previous section. Special

41 Ahlmann, op. cit., p.35.

characteristics of ice columns are the inward coarsening of the larger columns, and the arrangement of air bubbles in crude rings about the vertical axes of some columns.

Experiments with dyed melt-water established ice columns in the zone of transmitted radiation as more rapid transmitters of melt-water than firn (Fig. 14). Ice columns were disarticulated to a depth of at least 50 inches, or 10 inches below the maximum disarticulated depth of ice layers. The rapid rate of melt-water flow in the columns must have promoted the transmission of some heat below the general disarticulated level. However, below 50 inches ice columns proved impermeable to dyed melt-water.

Dyed melt-water also brought out in minute detail the horizontal stratification of ice columns inherited from the firn, and the slight arching of firn laminae directly above some ice columns.

Origin. The literature contains few references to the genesis of ice columns. Ahlmann[42] implied that ice columns formed through the vertical coalescence of ice layers. Moss[43] pictured the following mode of growth: "If such water layers can percolate downward in an irregular way owing to relatively small irregularities in the intervening wind crusts, they may reach a temperature level where they become immobilized before they have time to spread out in level sheets again". Glen[44] stated "....it is only when the firn above an impermeable layer becomes consistently sodden that an upward extension (meaning ice column) of the ice band can occur".

In as much as ice columns were interconnected with ice layers and contained the same fabric as the ice layers, it seems safe to assume that they formed in an analogous manner, that is, by the refreezing of downward percolating melt-water. The formation of incipient ice columns was not observed as was the formation of ice layers. Therefore, the evolution of melt-water freezing into vertical columns must be deduced from analogy and from the following field facts:

1. Ice columns did not develop during the summer when the firn was isothermal at 0°C.
2. There was concentration of melt-water during the summer in the centers of suncup depressions.

42 Ahlmann, op. cit., p.35.
43 Moss, op. cit., p. 219.
44 Glen, op. cit., p. 143.

3. Ice columns did not appear above the surface near the Camp 10B site until late summer.
4. Columns showed a linear trend over some concealed crevasses and down slopes.
5. Most columns were associated with horizontal ice layers.
6. Stratification of the firn was preserved in the ice columns.
7. Some columns were at least seven feet in length.
8. The centers of the columns were more coarsely crystalline than the sides, and air bubbles were often arranged concentrically about the vertical axes of the columns.
9. Ice columns usually developed lateral rib-like projections.

Considering each of the above points in order the following evolution of ice columns is envisaged:

Ice columns formed when the winter cold wave was present in the firn. Melt-water generated at the surface was concentrated in surface irregularities. The top foot or two of the winter accumulation layer was probably already isothermal when this melt-water was produced. Thus, no melt-water, even though it may have concentrated in vertical channels, refroze in this upper section.

A lower, denser firn stratum caused some of the melt-water to spread laterally until it found a permeable passageway downward. These passageways were sometimes controlled by the slumping of firn over crevasses or by uneven settling in the firn. The melt-water in percolating downward through the openings moved slowly, preserving the stratification of the snow or firn. It ultimately moved into the winter cold zone. Despite the negative temperatures the melt-water descended some distance before it gave up its latent heat and was immobilized. The columns of water froze slowly in the firn from the outside inward. It is believed that water-rich columns and water-rich layers in firn of equal negative temperature and depth froze as a unit during the same time interval. Had this not been true, a later supply of melt-water would have flowed along the many rib-like projections extending from the ice columns and over their edges, forming additional vertical columns and a more thoroughly interconnected plumbing system than was observed.

As the firn temperature rose, additional melt-water passed to greater depths. Other relatively dense strata impounded the channelized melt-water until it was able to permeate them. The alternation of permeable and less permeable firn and a fluctuating supply of melt-water was probably responsible for the development of lateral offshoots from the columns.

It is difficult to visualize subsequent enlargement of ice columns unless melt-water spread along an impermeable ice lens and descended vertically along the sides of an ice column which extended downward from

the termination of the lens. The freezing of this melt-water would call for a second transgression of the winter cold wave, and therefore, is not likely.

5. The Summer Melt-water Cycle.

The ablation season begins when the curve of ablation crosses the curve of accumulation on a time-quantity graph.[45] This occurs during May on the Juneau Ice Field when the warm winds from the ocean replace the cold winds from the continent. In some cases alternating above - and below-freezing air temperatures may cause a firn layer of negative temperature to overlie a firn layer at the melting point.[46]

The first substantial amounts of melt-water are utilized to dissipate the winter cold wave. When this melt-water percolates downward in the snow it refreezes in the form of ice layers or ice columns upon reaching the depth where the snow temperature is sub-freezing. In refreezing, water releases its latent heat which raises the temperature nearby. Owing to this refreezing and to continuous compaction-settling the snow evolves to firn, and with continued ablation and frequent rains the whole firn mass can soon become isothermal at 0°C.

It is now possible for melt-water to percolate downward to glacier ice and accumulate there, but only after many interruptions by and lateral flow along impermeable ice layers in the firn. As the days grow longer and warmer, increasing amounts of melt-water reach glacier ice. Movement of this melt-water down-glacier is similar to the movement of ground water. The melt-water is eventually concentrated in englacial and subglacial channels and passages. In some instances these drainage channels are obstructed, causing ponding of melt-water in crevasses and flow of melt-water upon the surface.

Melt-water production ceases with the oncoming of the winter cold wave. The surface crust now lasts from day to day and is extended downward by conduction from sub-freezing air temperatures. Ultimately, it is buried beneath snowfalls. Melt-water derived from these first snowfalls may penetrate to the top of the old firn surface and where temperatures are sub-freezing refreeze to form an annual ice layer. An annual ice layer is not so likely to form if the first autumn snows fall upon a summer surface that is at the melting point.

[45] Sharp, R.P., personal communication.
[46] Ahlmann, H.W:son, "Vatnajökull, Scientific Results of the Swedish-Icelandic Investigations", Geogr. Ann., Vol. 20, 1938, pp. 42-55.

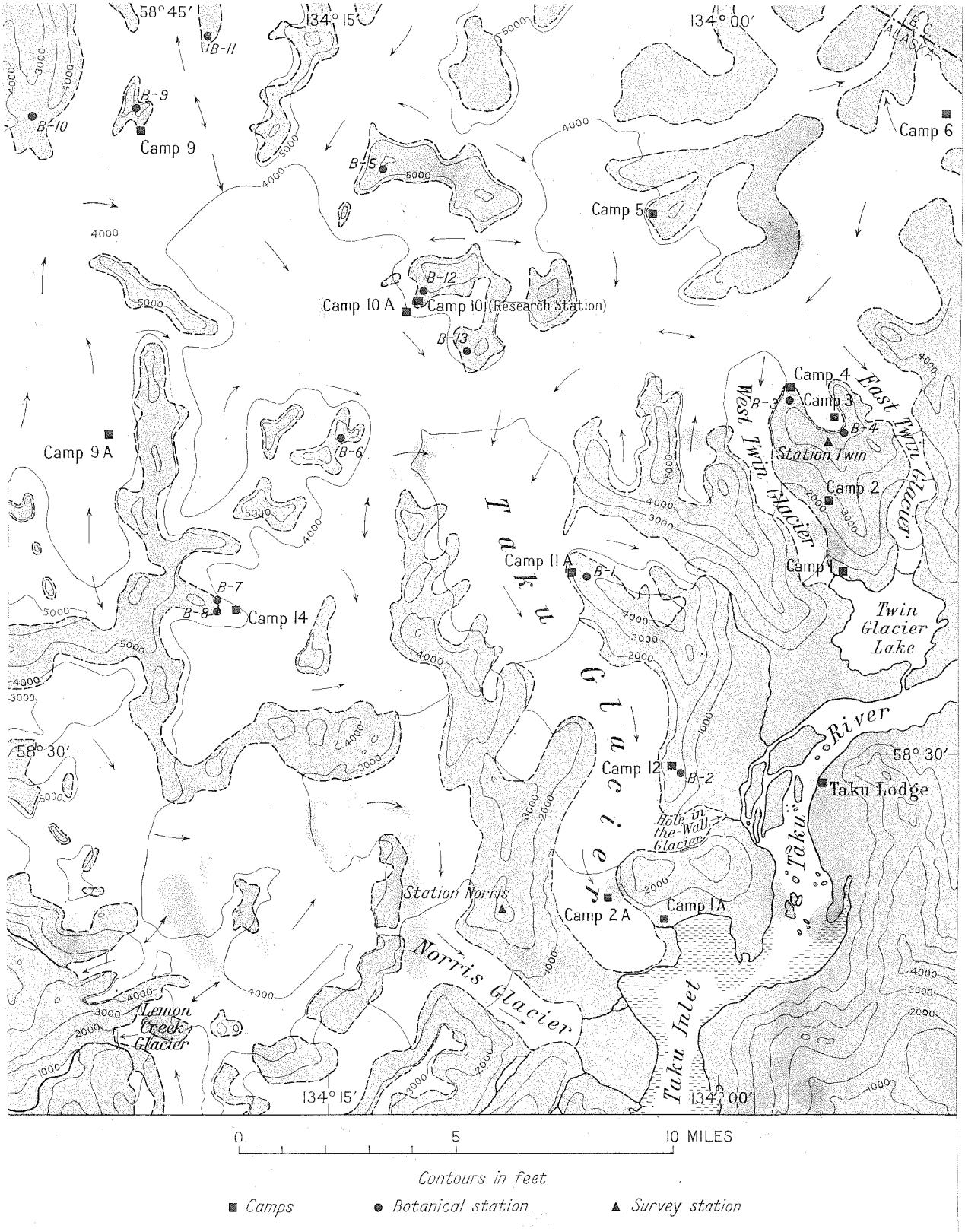

Fig. 3. Map of a portion of the Juneau Ice Field showing the scene of operations of the Juneau Ice Field Research Project, 1949. The map west of 134° 00′ longitude is based on the U.S.G.S. topographic sheet "Juneau, Alaska-Canada", Edition of 1951, Scale 1:250,000 with modifications determined by field investigations. The remainder of the map has been compiled from unpublished sources. No contour intervals have been included in the northeast section.

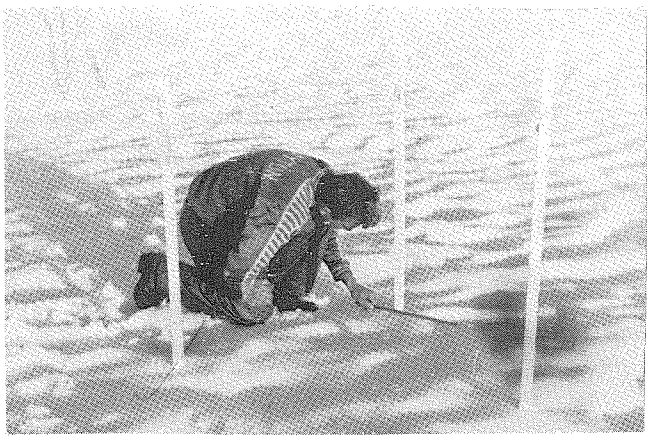

Fig. 11. Obtaining daytime record of ablation from stakes on upper Taku Glacier. Stakes were reset each morning and evening and were painted white to reduce loosening by excessive absorption of the sun's heat.

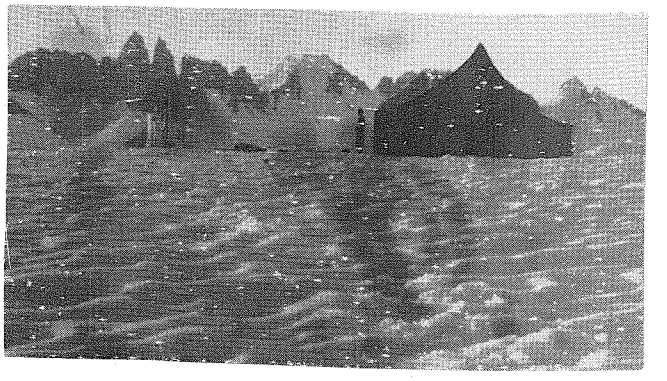

Fig. 12. Suncupped surface near Camp 10A.

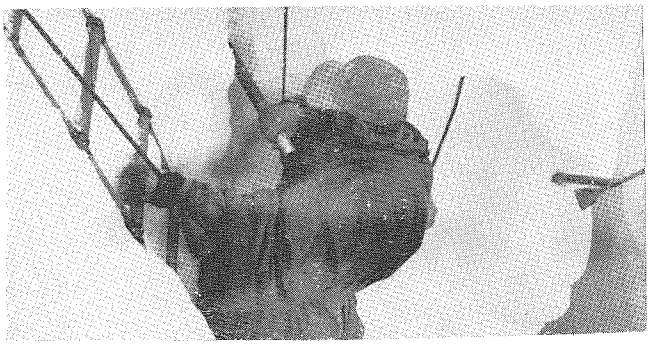

Fig. 13. Samples of névé being obtained in toothed pipe corer inserted into wall of pit on upper Taku Glacier. From such samples density determinations and free water content analyses were made.

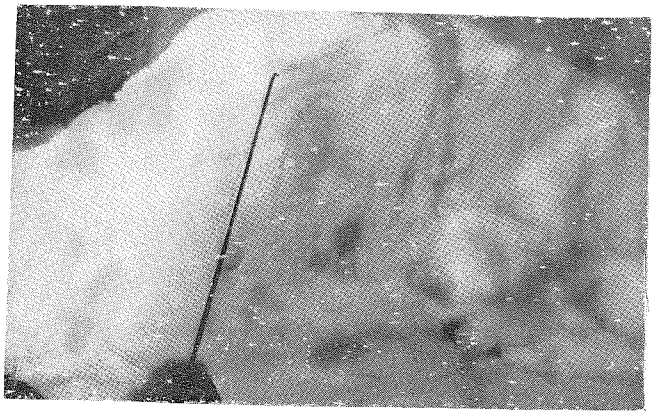

Fig. 14. Section of ice column 3-4 inches in diameter. Dyed melt-water generated at the surface has penetrated the column to the base of the rule (26 inches), but only half this distance in the adjacent firn.

Fig. 15. Nighttime measurement of melt-water.

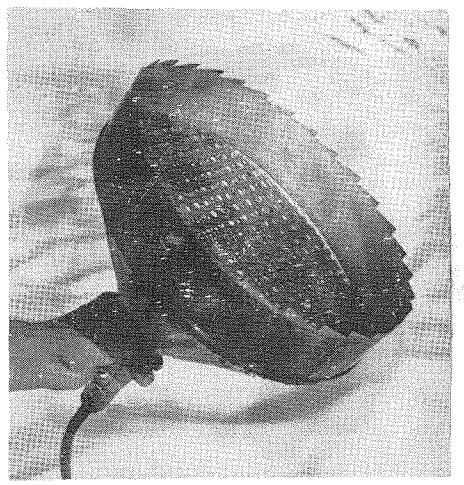

Fig. 16. Funnel-type pan. Pan was turned upward into roof of tunnel until firn touched the screen.

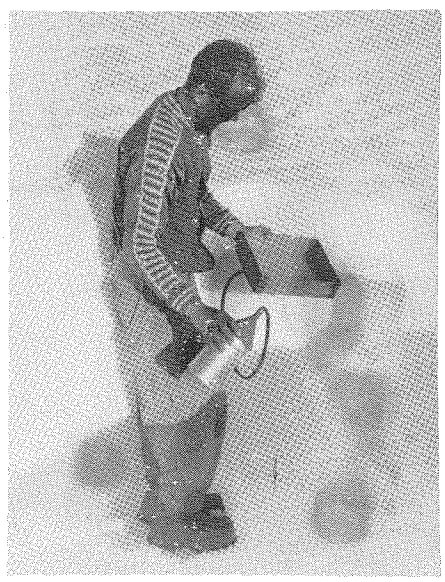

Fig. 17. Open box-type metal pan. Melt-water received by pan drains through rubber tube to receptacle.

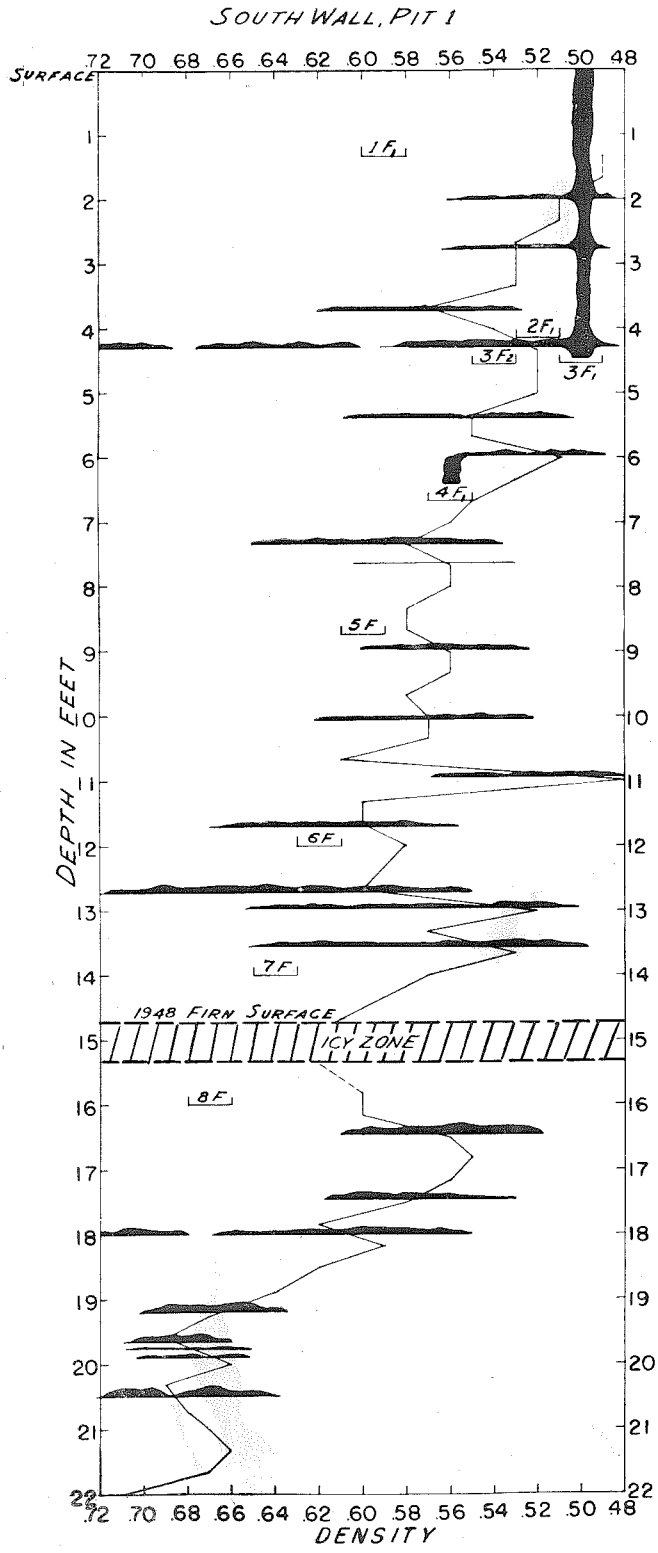

Fig. 24. Position of melt-water pans in the south wall of pit 1, at Camp 10A, and their relationship to ice structures (in solid black) and the density curve of firn. Density of ice structures is not to be inferred from the density curve of firn.

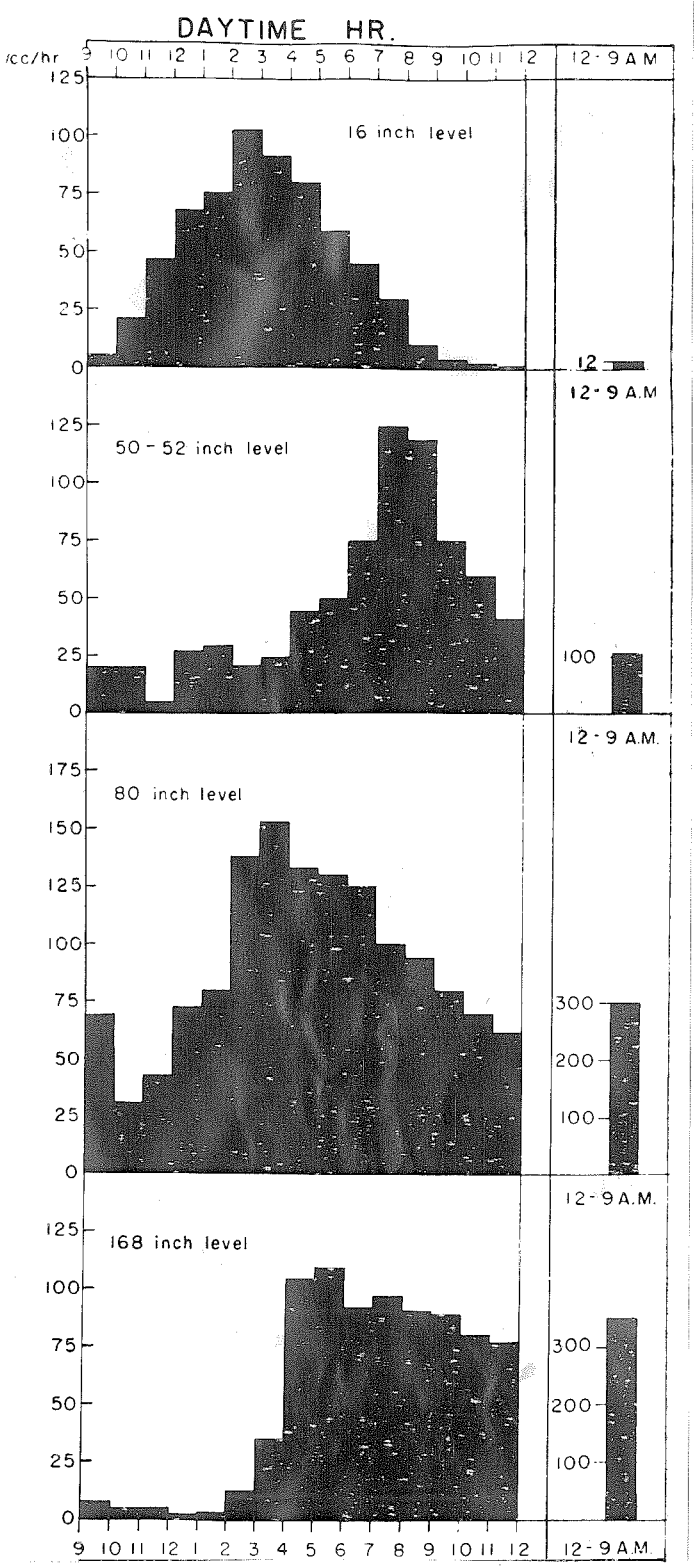

Fig. 25. Average hourly melt-water collections for several pans at 4 different levels during the daytime and the average total melt-water received at night (12-9 a.m.). Period of observation was Aug. 15-Sept. 1.

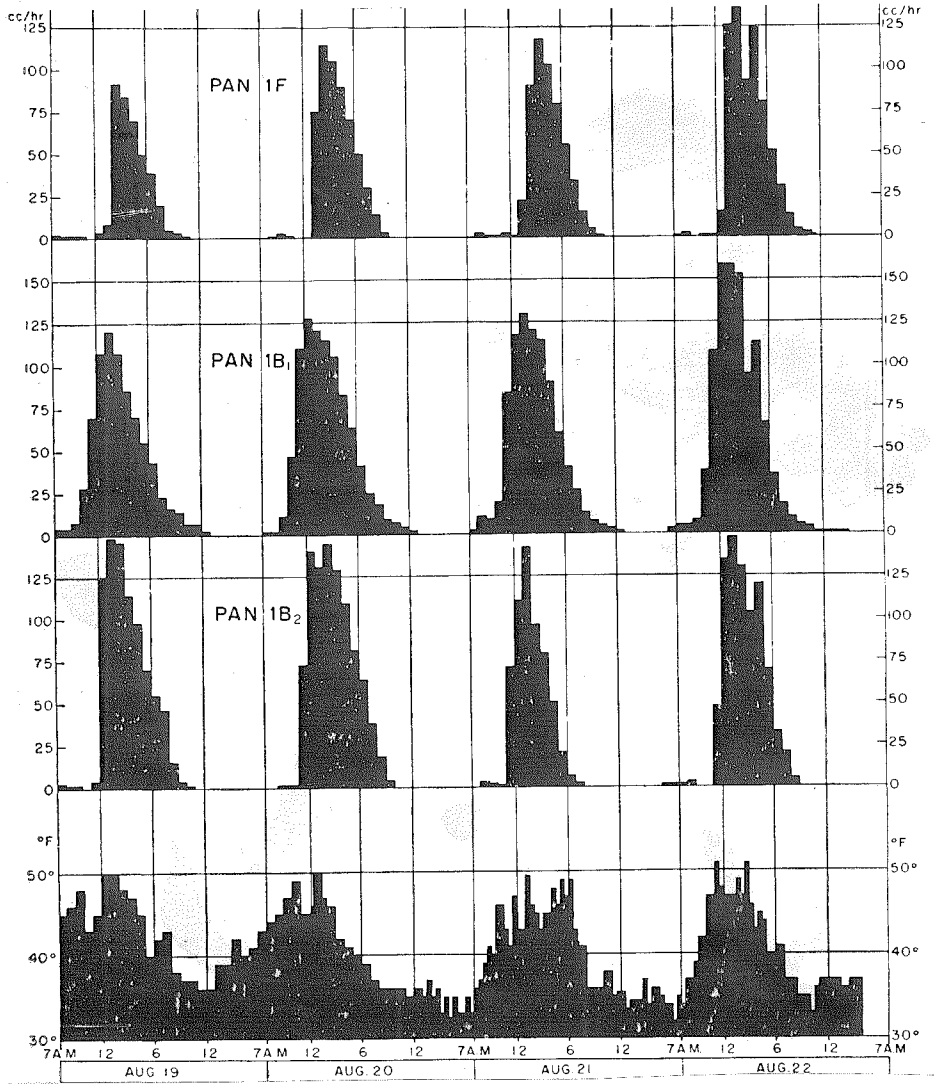

Fig. 26. Melt-water received hourly by three pans in pit 1 (Camp 10A), 1F, $1B_1$, and $1B_2$, at the 16 inch level with hourly temperatures for comparison. Melt-water measurements were made hourly between 6 a.m. and midnight and at least once every two hours between midnight and 6 a.m. from August 19 to 21.

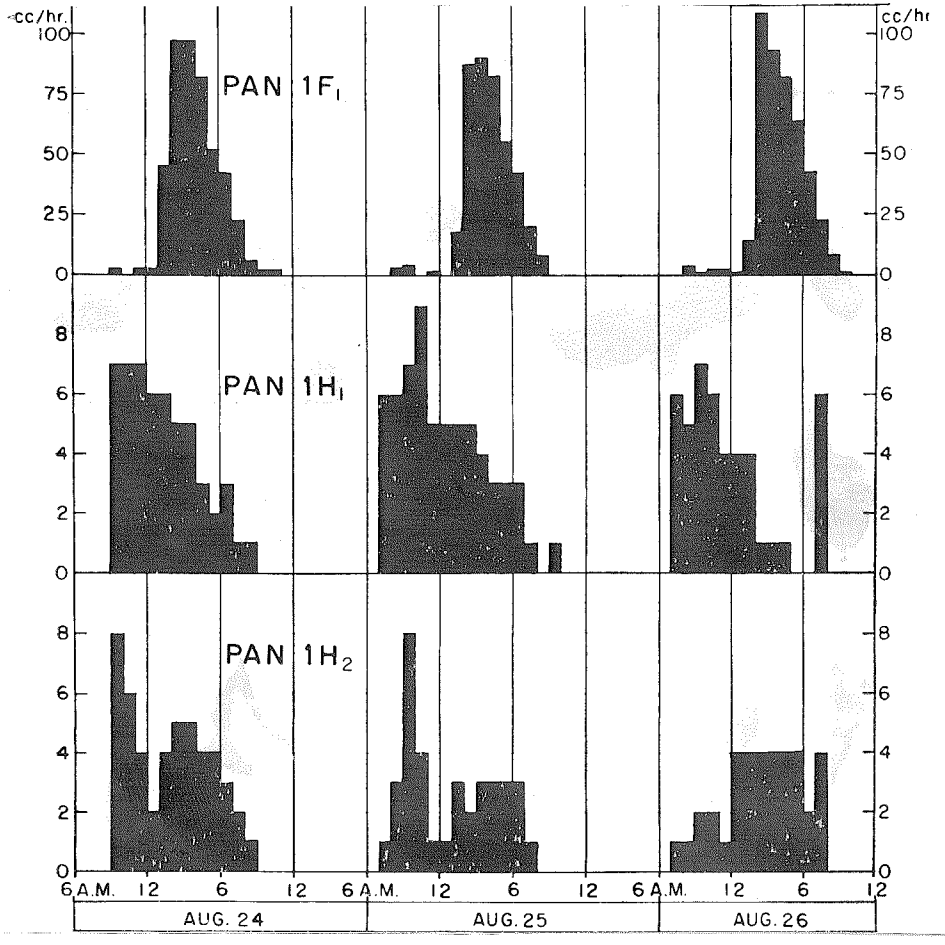

Fig. 27. Comparison of the horizontal component of flow (pans $1H_1$ and $1H_2$) with the vertical component (pan $1F_1$) at the 16 inch level. Vertical scales of diagrams differ.

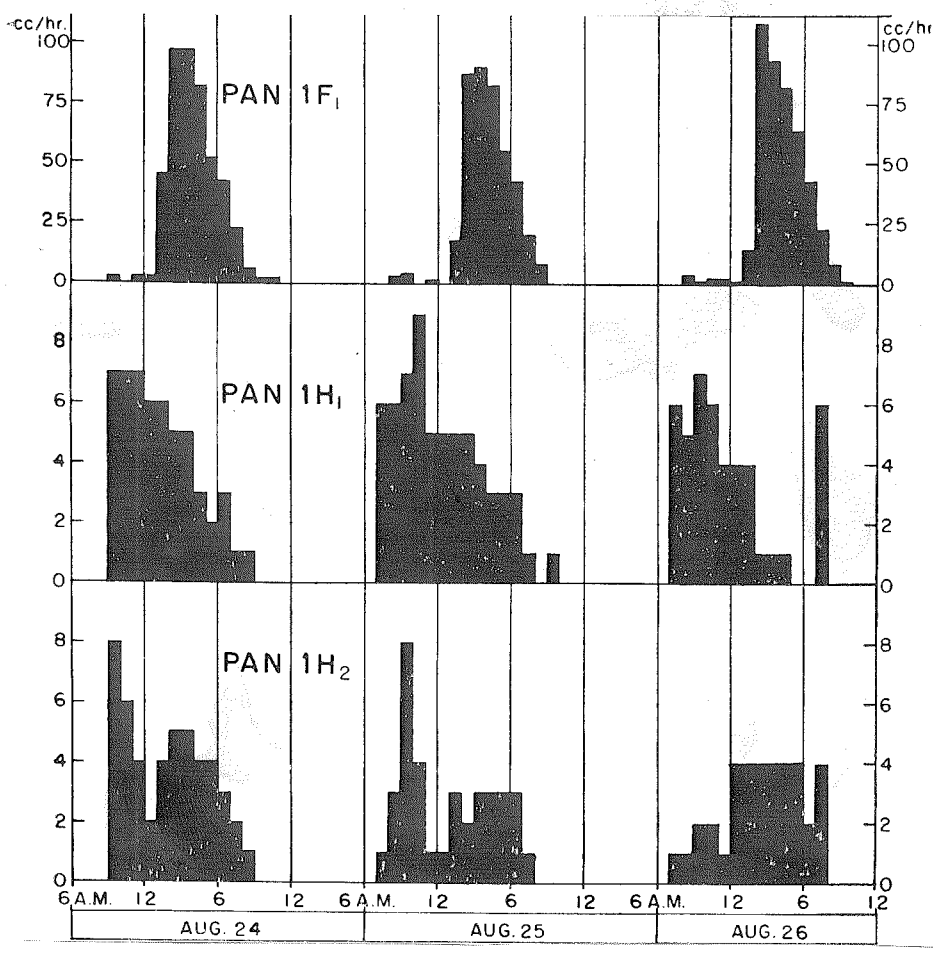

Fig. 26. Melt-water received hourly by three pans in pit 1 (Camp 10A), 1F, $1B_1$, and $1B_2$, at the 16 inch level with hourly temperatures for comparison. Melt-water measurements were made hourly between 6 a.m. and midnight and at least once every two hours between midnight and 6 a.m. from August 19 to 21.

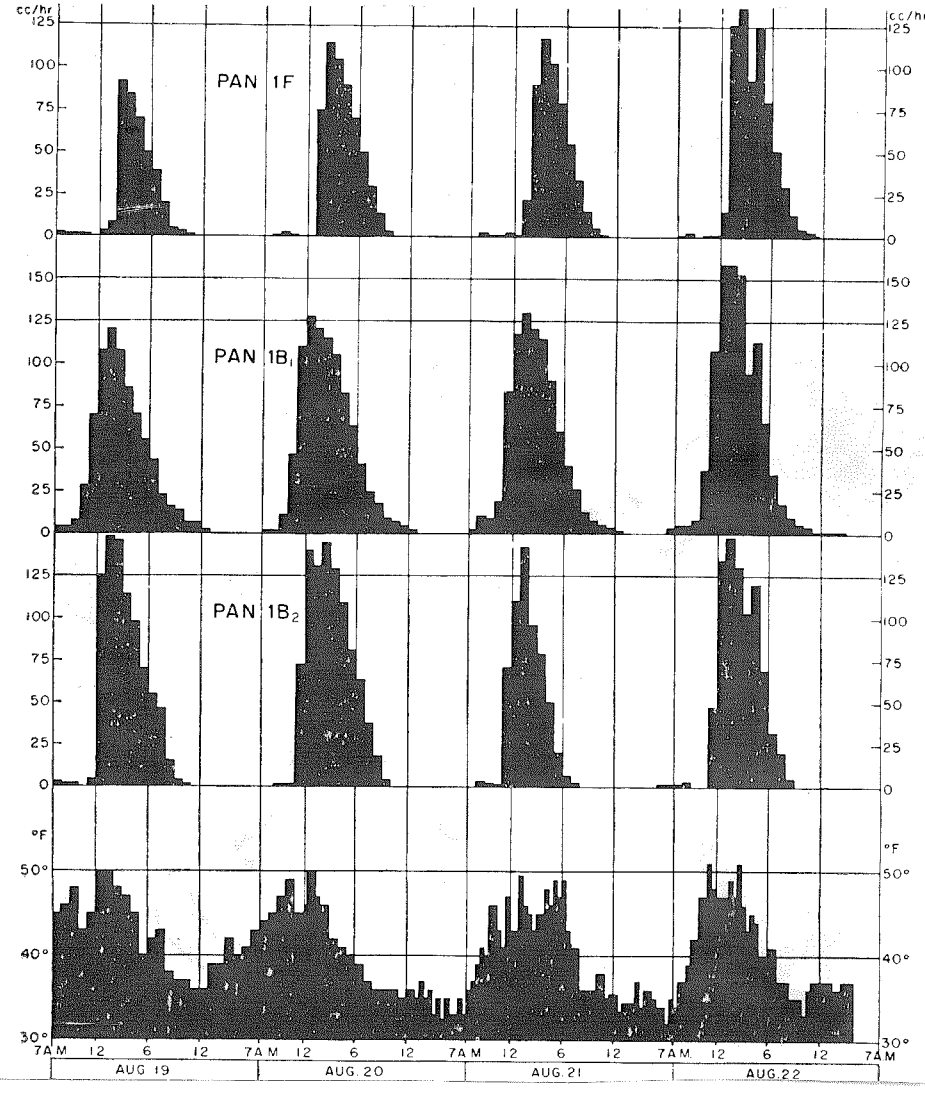

Fig. 27. Comparison of the horizontal component of flow (pans $1H_1$ and $1H_2$) with the vertical component (pan $1F_1$) at the 16 inch level. Vertical scales of diagrams differ.

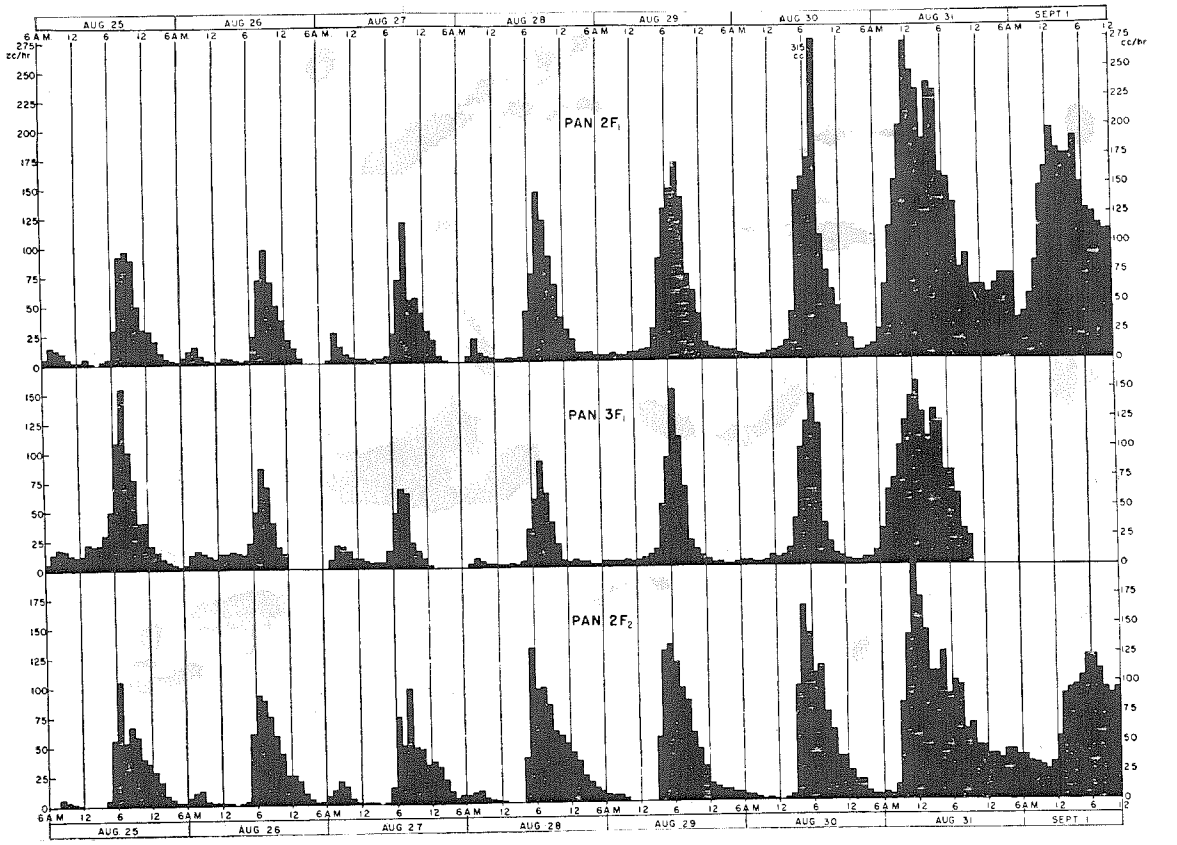

Fig. 28. Results of hourly melt-water collection at the 50 and 53 inch levels. Melt-water measurements were made hourly between 6 a.m. and midnight and at least three times between midnight and 6 a.m. from August 25 to 27 and on August 29. Pans $2F_1$ and $2F_2$ were at the 50 inch level; pan $3F_1$ at the 53 inch level.

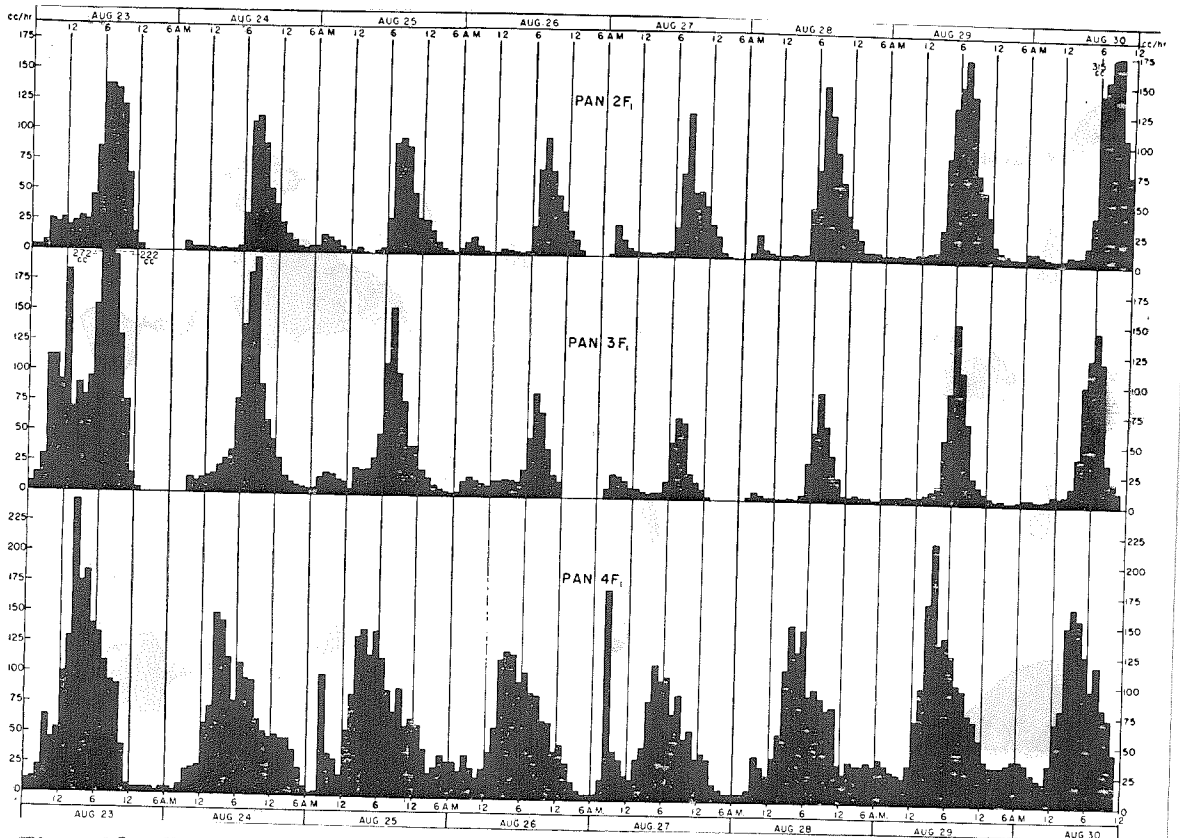

Fig. 29. Hour to hour melt-water collected from pans $2F_1$, $3F_1$, and $4F_1$ at the 50, 53, and 80, inch levels, respectively, from August 23 to 30. Melt-water measurements were made hourly between 6 a.m. and midnight and at least three times between midnight and 6 a.m. from August 25 to 27 and on August 29.

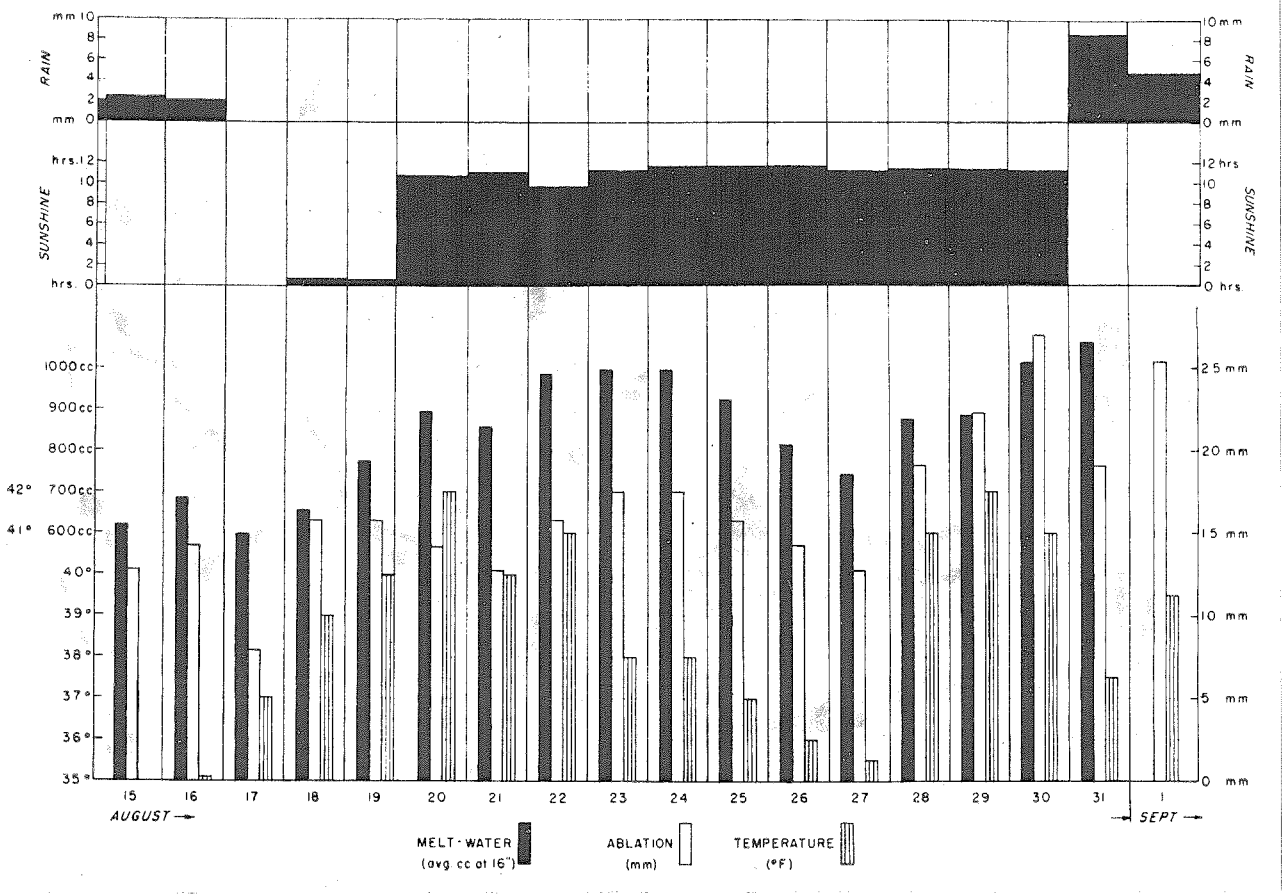

Fig. 30. Meteorological data compared with surface ablation data and the average daily melt-water received at the 16 inch level, Camp 10A, upper Taku Glacier.